Regeneration of Neuronal Diversity in the Axolotl Brain

A dissertation presented

by

Ryoji Amamoto

to

The Division of Medical Sciences

in partial fulfillment of the requirements

for the degree of

Doctor of Philosophy

in the subject of

Developmental and Regenerative Biology

Harvard University

Cambridge, Massachusetts

April 2017

Dissertation Advisor: Professor Paola Arlotta Ryoji Amamoto

Regeneration of Neuronal Diversity in the Axolotl Brain

Abstract

The axolotl can regenerate multiple organs, including the brain. It remains, however, unclear whether neuronal diversity, tissue architecture, and axonal connectivity can be regenerated; yet, this is critical for functional recovery and a central aim of cell replacement strategies in the mammalian central nervous system. Here, we demonstrate that, upon injury to the adult pallium, axolotls regenerate specific neuronal populations present before injury. Notably, regenerated neurons acquire functional electrophysiological traits and respond appropriately to afferent inputs. Despite the ability to regenerate molecularly-defined neuronal subtypes, we also uncovered previously unappreciated limitations by showing that newborn neurons organize within altered tissue architecture and fail to re-establish long-distance axonal tracts and circuit physiology present before injury. The data provide a direct demonstration that neuronal diversity can be regenerated in axolotls, while challenging prior assumptions of functional brain repair in regenerative species.

The molecular mechanism underlying the process of brain regeneration in regenerative organisms is poorly understood. Previous work in zebrafish and newt have identified factors that are critical for regeneration. To elucidate the molecular players involved in axolotl brain regeneration, we performed whole-genome RNA-sequencing at 1, 2, and 4 weeks post-injury. We found that transcripts associated with cell cycle regulation, immune activation, and retinoic acid signaling pathway are enriched among the differentially expressed genes during brain regeneration. Additionally, we found that genes upregulated in the blastema during limb regeneration are also expressed in the regenerating brain. These results identify, for the first time,

key genes that may contribute to axolotl brain regeneration and suggest that some regeneration-specific genes may be shared among different organs.

To understand the molecular mechanisms of processes such as regeneration or disease, it is critical to capture the transcriptional profile of specific cell types as opposed to profiling the whole tissue. This is difficult in organisms such as the axolotl where genetic labeling of specific cell types is challenging. Here, we developed a novel technology to quantify gene expression of specific cell types from unlabeled brain samples. This approach will, in the future, facilitate identification of cell type-specific mechanisms responsible for the regenerative process in the axolotl brain.

Table of Contents

Acknowledgments

I cannot think of a better scientific mentor and colleague for a budding graduate student than Paola Arlotta. I want to thank her for allowing me to take on a risky and unique project, working with a species that neither one of us had ever seen before, and encouraging me through the whole way. Over the last 6 years, I've learned how to ask the right questions, how to formulate a hypothesis, meticulously go over every detail, and present data in a clear manner, mostly by emulating Paola's approach to science. She has assembled a great team of scientists over the years (going from ~6 people to 20+ in the last 6 years!), and I believe the collaborative spirit in the lab certainly stems from her willingness to work with others. Everyday has been a joy to work in this wonderful lab.

I want to thank my lab mates for making lab an interesting place to work every day. My fellow graduate students, Aurora, James, Mo, and Dean have been brilliant sources of conversation, scientifically and most often, non-scientifically. I wish to continue the often-nonsensical debates in the lunchroom (lunch crew!), our bay, and conference room wherever I go next. I've had the opportunity to learn a lot from the postdoctoral fellows in the lab, past and current, especially from The Italians – Simo, Giulio, Giorgia, and Ema (and I think May is included here as an honorary member). I certainly need to thank all the technical staff over the years, Zak, Helen, Nathan, Edward, Natalie, and Andrea, for making the lab run smoothly. I would not have been able to grow as a scientist if it weren't for the interactions with all the great people in the lab.

I want to thank my scientific collaborators, for which this work would not have been possible. Zhanyan Fu and Violeta Gisselle Lopez Huerta were critical for the electrophysiology experiments when we needed it most. The MRI and DTI imaging would not have been possible if it weren't for Emi Takahashi and Aaron Grant. I think it was everybody's first time working with axolotls, and we may have been the first people in the world to stick an axolotl into an MRI machine. The human nuclear sorting could not have happened if Nathan Curry did not graciously

offer time out of his busy (busy!) day with a smile. My DAC committee, and outside advisors, Dr. Connie Cepko, Dr. Cliff Tabin, Dr. John Rinn, Dr. Doug Melton, and Dr. Jessica Whited, were instrumental in my progress as a scientist, and I hope to continue our fruitful interactions for years to come. I would not have come this far without the help from my axolotl crew, in particular Dennis Sun, Stephanie Tsai, and Salman Bhai, with whom we shared joys and griefs over working with these creatures. I've learned over the years that science is truly a collaborative venture, and it takes a village to produce a scientific finding.

I've had a chance to teach in 10 courses over the last 6 years, and I want to thank the professors, Professor Bill Anderson, Professor Kevin Eggan, Professor Steve Hyman, and Paola for teaching me how to engage and captivate students. I hope the skills learned as a teacher will transfer to my skills as a scientific presenter, and in the future, I hope to be teaching as a professor one day.

I want to thank from the bottom of my heart, my fellow Ph.D. student, then-girlfriend, now-wife, soon-to-be-Dr. Liz Lane, for being my best friend and encouraging me throughout our graduate work. It seems like a long time ago when we first met as first year graduate students, unsure of what will unfold in the next 6 years. All my friends from DMS pushed each other to strive for success in and out of lab, and we've stuck together through thick and thin. My parents have always wanted the best for me, and they sometimes pushed me to strive when I needed it most. I will certainly not be here if it weren't for their support and encouragements.

Chapter 1

Introduction

I. Strategies for Mammalian Brain Regeneration

The adult human brain is an organ of unparalleled complexity. It is composed of a vast diversity of cell types, which are further divided into specific subtypes (Darmanis et al., 2015; Hawrylycz et al., 2012; Kang et al., 2011; Lake et al., 2016). Among the different cell types of the human brain, the connection and interaction between distinct neuronal subtypes are considered to play a major role in conferring humans with unique abilities such as creative thinking, planning, and scientific reasoning. Given the importance of such cognitive functions for day-to-day living, damage to the brain, in disease or injury, is utterly debilitating. For example, traumatic brain injury (TBI) and stroke remain two of the leading causes of disability in the world (Rubiano et al., 2015). In the United States alone, approximately 5.3 million people suffer from disability caused by TBI (Coronado et al., 2011). Additionally, stroke affects 800,000 people annually in the United States, and these numbers are only increasing each year (Ovbiagele and Nguyen-Huynh, 2011). These injuries lead to loss of various cell types of the brain, including neurons. While many cell types regenerate after injury, repopulation of new neurons is scarce and does not occur in specific areas such as the neocortex, the part of the mammalian brain required for executive functions (Huttner et al., 2014). Therefore, a novel strategy is needed to replace lost neurons, and more importantly, to replace specific neuronal subtypes, in the human neocortex upon injury.

The adult mammalian brain is severely limited in its ability to generate new neurons. In the uninjured mouse brain, neurogenesis is restricted to two niches. Neural stem cells of the subventricular zone (SVZ) give rise to interneurons of the olfactory bulb while those in the subgranular zone (SGZ) differentiate into granule cells of the dentate gyrus (Bond et al., 2015). In both cases, these newborn neurons integrate into pre-existing, mature circuits, indicating that, even in the mammalian brain, adult neural circuits could incorporate new neurons (Song et al., 2012). During homeostasis, it is believed that other regions of the mouse brain do not generate new neurons.

Upon focal ischemia in a mouse model, limited regeneration of different cell types is observed in the striatum and the neocortex. Neural stem cells (NSC) of the SVZ exhibit increased rate of proliferation, and some neuroblasts, normally destined to the olfactory bulb, migrate towards other regions of the brain, including the striatum and neocortex (Arvidsson et al., 2002; Gu et al., 2000; Jiang et al., 2001; Jin et al., 2006; Kernie and Parent, 2010; Kreuzberg et al., 2010; Leker et al., 2007; Liu et al., 2009; Magnusson et al., 2014; Ohira et al., 2010). Newly generated medium spiny neurons in the striatum survive long-term and form synapses with neighboring neurons (Ernst et al., 2014; Hou et al., 2008; Jin et al., 2003). In contrast, most newborn neurons in the mouse neocortex fail to survive and integrate into the circuitry in focal ischemia models, although targeted, cell type-specific ablation of mouse cortical neurons leads to neurogenesis of the correct neuronal subtype (Chen et al., 2004; Magavi et al., 2000). In ischemia models, the surviving cells from the SVZ that have migrated into the neocortex differentiate into astrocytes, and there is no evidence that the neuronal diversity of the neocortex is ever remade (Carlén et al., 2009; Faiz et al., 2015). In accordance, carbon dating of human cortical neurons from postmortem stroke-affected tissue revealed that the human neocortex does not contain new neurons upon ischemia (Huttner et al., 2014). In murine models of traumatic brain injury to the neocortex, NSCs of the SVZ also display increased rate of proliferation (Chang et al., 2016; Chirumamilla et al., 2002; Goings et al., 2004; Goodus et al., 2014; Ramaswamy et al., 2005; Saha et al., 2013). Much like in ischemia models, some neuroblasts from the SVZ migrate towards the injury site after TBI (Goings et al., 2004; Saha et al., 2013). In the neocortex, most progenitors differentiate into glia, and it remains controversial whether mature neurons are generated in the neocortex (Saha et al., 2012).

Three broad approaches to regenerate new neurons in the mammalian neocortex include 1) generating specific neuronal subtypes from stem cells *in vitro* and transplanting into the brain, 2) directly reprogramming abundant cell types into new neurons, and 3) inducing endogenous neural stem cells of the adult brain to generate specific neurons. Rapid advances in human stem

cell biology have enabled the generation of human embryonic stem cells (ESC) and induced pluripotent stem cells (iPSC), which could theoretically differentiate into every cell type of the human body (Takahashi et al., 2007; Thomson et al., 1998). Recent work has identified media conditions and factors to directly differentiate pluripotent stem cells into cortical neurons *in vitro* (Chambers et al., 2009; Eiraku et al., 2008; Espuny-Camacho et al., 2013; Kmet et al., 2013; Maroof et al., 2013; Shi et al., 2012). Encouragingly, these induced neurons express markers of endogenous adult cortical neurons such as BCL11B and SATB2 and display mature electrophysiological properties (Eiraku et al., 2008; Maroof et al., 2013). When transplanted into the mouse neocortex, some of the neurons project their axons to correct, subcortical long-distance targets (Espuny-Camacho et al., 2013). However, the extent to which these transplanted cortical neurons integrate into the local circuit and project to the correct brain regions remains poorly understood. Furthermore, it is not known whether transplantation of *in vitro* generated cortical neurons could restore lost function in the same way that other induced cell types (e.g. β-cells) restores function in non-neural tissues (Pagliuca et al., 2014; Rezania et al., 2014). Further research is warranted before transplantation of stem cell-derived cortical neurons is used to treat TBI or stroke.

More recently, specific neuronal subtypes have been generated by directly reprogramming non-neuronal cells by overexpressing defined factors (Amamoto and Arlotta, 2014). *In vitro*, this approach has been shown to be considerably faster and more efficient than directed differentiation (Vierbuchen et al., 2010). However, the need to transplant into the brain still exists. The major advantage of direct reprogramming over directed differentiation is the ability to generate the specific cell types *in vivo* (Buffo et al., 2005; De la Rossa et al., 2013; Montana et al., 2013; Niu et al., 2013; Rouaux and Arlotta, 2013; Torper et al., 2013). Given that direct reprogramming does not undergo an intermediate pluripotent state (Son et al., 2011), it is possible to reprogram cells into specific neuronal subtypes within the brain. In mice, relatively abundant cell types such as astrocytes have been reprogrammed into neurons (Niu et al., 2013; Torper et

al., 2013). Alternatively, one neuronal subtype could be reprogrammed into another neuronal subtype. For example, overexpression of a transcription factor, Fezf2, in callosal projection neurons of early postnatal mouse brain reprograms them into corticofugal projection neurons (Rouaux and Arlotta, 2013). The resulting corticofugal neurons acquire class-specific electrophysiological properties and transcriptional profile (Ye et al., 2015). Using this approach, it is feasible to replace specific neuronal subtypes by converting nearby cells; thus, overcoming the need to transplant into the brain parenchyma. Despite the acquisition of the correct molecular profile, it is still unclear whether axonal projection and local circuitry can be reprogrammed in the adult brain. These two factors are likely crucial for restoring function to a damaged brain.

Another approach to regenerate new cortical neurons is to manipulate the endogenous NSCs in the mammalian brain. In mice and human, NSCs proliferate and differentiate into functional neurons, even as adults. Unfortunately, generation of new neurons is restricted to the olfactory bulb and the hippocampus in mice (Bond et al., 2015) and perhaps also the striatum in humans (Ernst et al., 2014). Nonetheless, these NSCs in the adult brain represent an endogenous cellular source for new neurons in the case of injury. Moreover, homeostatic neurogenesis in select regions of the brain indicates that the adult human brain retains the capacity to incorporate new neurons. To restore cortical function upon injury, endogenous NSCs need to be manipulated to 1) respond to injury by proliferating, 2) migrate to the neocortex, 3) differentiate into specific neuronal subtypes, and 4) integrate into both local and long-distance circuitry. However, to apply this approach for therapy, it is critical to identify the key factors that are necessary to induce each of these cellular processes in endogenous NSCs. One plausible method is to elucidate the molecular mechanisms underlying neurogenesis in the olfactory bulb and hippocampus, which are the two neurogenic regions during homeostasis. For example, Ezh2, a subunit of the polycomb repressive complex 2, has been shown to regulate NSC self-renewal in the SGZ through the Pten pathway (Zhang et al., 2014). By identifying the key molecular players underlying NSC proliferation, migration, differentiation, and integration in the mouse, it might be possible to

find a combination of factors to coerce endogenous NSCs to restore function to the damaged neocortex in human patients.

II. Brain Regeneration in Non-Mammalian Vertebrates

A complementary approach to identifying key factors for mammalian brain regeneration is to study the mechanism of brain regeneration in organisms that are naturally endowed with superior regenerative capacities such as salamanders and zebrafish. These organisms have been studied for centuries for their capacity to regenerate various organs including the limb, heart, and spinal cord (Butler and Ward, 1967; Cano-Martínez et al., 2010; Kikuchi et al., 2010; Kragl et al., 2009; Lo et al., 1993; Piatt, 1955a; Poss et al., 2002). The brain has also been extensively studied for regeneration studies. Resection of the middle one-third of one hemisphere, but not the whole hemisphere, in the axolotl telencephalon results in reconstruction of the injured hemisphere to a similar length as the contralateral, uninjured side (Kirsche and Kirsche, 1964a). Similarly, after mechanical excision of the newt optic tectum, new tissue fills the space produced by injury (Okamoto et al., 2007). Interestingly, in the newt, selective chemical ablation of dopaminergic neurons within a largely intact midbrain triggers regeneration of the ablated pool of neurons (Parish et al., 2007). In zebrafish, a stab wound in the dorsal telencephalon leads to increased proliferation of NSCs and subsequent neurogenesis in the injured region (Ayari et al., 2010; Baumgart et al., 2012; Kishimoto et al., 2012; Kroehne et al., 2011; März et al., 2011). Similarly, after chemical ablation of cells in the telencephalon using Quinolinic Acid, neurons regenerate in the injured region and adopt multiple neuronal subtype identities (Skaggs et al., 2014). Owing to the genetic tools available to the zebrafish as a model system, some key genes involved in the regenerative process such as *gata3* and *cysltr1* have been identified (Kizil et al., 2012c; Kyritsis et al., 2012). These studies highlight the unique ability for non-mammalian vertebrates to respond

to brain injury and generate new neurons at the injury site, leading to a perfect morphological regeneration.

The urodele pallium is a one-layer structure, with an undefined neuronal population near the ventricle and ependymoglia cells lining the ventricles. Under physiological conditions, ependymoglia cells of the axolotl telencephalon uptake and retain BrdU, indicating that these cells are slowly cycling (Maden et al., 2013). In the newt brain, two types of ependymoglia cells have been identified based on combination of molecular markers. Type 1 ependymoglia cells ($MCM2^+/GS^+/GFAP^+$) are label-retaining cells that display the self-renewal capacity of a stem cell population. Type 2 ependymoglia cells ($MCM2^+/GS^-/GFAP^+$) are sensitive to AraC treatment and does not retain BrdU, indicating that these cells represent a transit amplifying cell type (Kirkham et al., 2014). Such heterogeneity of dividing cells is also present within the zebrafish radial glia (RG) population. Quiescent Type 1 RG, active Type 2 RG, and non-RG Type 3 progenitors are dispersed in different proportions between dorsal, lateral, and medial pallium of the zebrafish telencephalon (Dray et al., 2015). It is still unknown whether further subdivisions of NSCs exist and whether different progenitor pools differentiate into specific subpopulations of neurons.

Upon injury, the rate of ependymoglia cell proliferation dramatically increases near the injury site. For example, upon dopaminergic neuron ablation in the newt, the number of $BrdU^+$ cells increase in the midbrain within a matter of days (Parish et al., 2007). Live imaging of fluorescent RG in the zebrafish telencephalon revealed that stab injury induces recruitment of quiescent RGs and symmetric cell division, leading to the depletion of the RG population (Barbosa et al., 2015). In contrast, symmetric cell division is rarely seen without injury. In the newt and zebrafish, two studies have converged upon the Notch signaling pathway as a key regulator for NSC exit from quiescence (Alunni et al., 2013; Kirkham et al., 2014). Further transcriptional analysis in the injured zebrafish telencephalon identified *id1* as a regulator of stem cell quiescence (Rodriguez Viales et al., 2015). Notch signaling pathway and *id1* are key components of the mammalian NSCs (Nam and Benezra, 2009; Pierfelice et al., 2011), suggesting that some

molecular mechanisms for cell cycle quiescence and exit may be shared between mammalian and non-mammalian vertebrates.

Upon cell cycle exit, NSCs differentiate into putative neurons. Lineage tracing of RGs in the zebrafish pallium has indicated that this population of NSCs give rise to newborn HuC/D^{+} neurons at the injury site (Kroehne et al., 2011; Skaggs et al., 2014). Regenerated neurons acquire subtype-specific molecular markers, including NeuroD, PV, and Prox1 although whether neuronal subtypes regenerate in same numbers and with fidelity is not known (Kroehne et al., 2011). Newborn neurons at the injury site survive long-term, suggesting that they have integrated into the pre-existing circuitry (Kroehne et al., 2011; Skaggs et al., 2014). Despite progress, the input and output of these newborn neurons remains unresolved; therefore, the function of the regenerated zebrafish pallium is undetermined. In contrast, the regenerated dopaminergic neurons of the newt midbrain have been shown to possess re-acquired functionality when assessed for behavior. Upon 6-OHDA chemical ablation of dopaminergic neurons, newts were injected with amphetamine, which induces dopamine release and thus increases locomotion. Ablated animals exhibited significantly reduced locomotion, but after 30 days, locomotion recovered back to baseline (Parish et al., 2007). Importantly, this recovery was blocked by AraC treatment, a proliferation inhibitor, suggesting that behavioral recovery is mediated by generation of new dopaminergic neurons as opposed to synaptic or structural plasticity.

Another essential process in brain regeneration is immune activation. In the newt, ablation of dopaminergic neurons recruits microglia around the site of injury, and within days, they start proliferating (Kirkham et al., 2011). Similarly, in the zebrafish brain, stab wound injury leads to microglia recruitment and activation (Baumgart et al., 2012; Kyritsis et al., 2012; März et al., 2011). However, in these two species, microglia exhibit divergent roles. In the newt, administration of dexamethasone, an immune suppressor, during dopaminergic regeneration inhibits apoptosis and an increase in the number of newborn dopaminergic neurons is observed (Kirkham et al., 2011). In contrast, in the zebrafish, dexamethasone treatment upon stab wound injury decreases

RG proliferation and subsequently, fewer newborn neurons repopulate the injured region, indicating that the immune response is necessary for initiation of regeneration (Kyritsis et al., 2012). In accordance, knockdown of *cxcr5,* a chemokine receptor, expressed in RGs upon injury leads to decreased proliferation and neurogenesis (Kizil et al., 2012a). These studies highlight the importance of immune activation during brain regeneration in non-mammalian vertebrates. During mammalian brain development, microglia plays a critical role in synaptic remodeling. For example, during retinogeniculate pruning in early postnatal mice, the presynaptic inputs from the retinal ganglion cells are engulfed by microglia in an activity-dependent manner (Schafer et al., 2012). While previous studies in regenerative organisms pinpointed the role of the immune response during the proliferative phase, immune cells such as microglia may also play a role in reestablishing proper circuitry upon regeneration of new neurons in the adult.

III. Necessary Components of Brain Regeneration

The mammalian CNS is incredibly complex, and its ability to compute high-level functions, like those of the human neocortex, relies on the presence of a great diversity of neuronal subtypes integrated in specific long-distance and local circuits and working within a defined tissue architecture. Disruption of brain structure, connectivity, and neuronal composition is often associated with behavioral deficits, as observed in models of neurodevelopmental, neuropsychiatric, and neurodegenerative disease. It is therefore likely that functional regeneration of higher-order CNS structures will entail the regeneration of a great diversity of neuronal subtypes, the rebuilding of original connectivity, and the synaptic integration of newborn neurons in the pre-existing tissue. It is not known to what extent even regenerative species can accomplish these complex tasks, beyond their broad ability to generate new neurons and to rebuild gross brain morphology. It remains therefore debated whether any vertebrates are capable of true functional brain regeneration.

I have decided to use the adult axolotl pallium as the model system, to investigate whether a diverse array of neuronal subtypes and their tissue-level organization can regenerate after mechanical injury. In contrast to the zebrafish pallium, the everted nature of which makes linking distinct regions to their mammalian counterparts difficult (Northcutt, 2008), the gross neuroanatomy of the axolotl pallium, organized around two ventricles, shows clear similarities to that of the mammalian telencephalon. During mammalian embryonic development, the dorsal telencephalon gives rise to a six-layered cerebral cortex, the region of the mammalian brain with the most extreme diversity of neurons and complex tissue architecture. The evolutionary origin of the mammalian cerebral cortex remains a topic of controversy (Molnár, 2011); however, recent studies in sauropsids suggest that cortical neurons might be present in non-mammalian amniotes (Chen et al., 2013; Dugas-Ford et al., 2012; Jarvis et al., 2013; Suzuki et al., 2012). Therefore, I have reasoned that the axolotl pallium might contain a basic representation of several cortical neuronal subtypes and thus be a good model for investigating regeneration of neuronal heterogeneity.

Upon migration into the injured region, neuroblasts differentiate into different cell types including neurons. However, the extent to which different neuronal subtypes are regenerated is poorly understood. Selective chemical ablation of dopaminergic neurons in the newt regenerate neurons with region-specific, cell type-specific neuronal identity (Parish et al., 2007), suggesting that there is a feedback mechanism in place to sense which cell types are lost and must be regenerated. In this system, dopamine has been shown to be a key player in the feedback mechanism. Administration of L-DOPA, a precursor of dopamine, in the newt midbrain inhibits ependymoglia cell proliferation upon ablation. Conversely, Haloperidol, a dopamine receptor antagonist, is sufficient to induce ependymoglia proliferation (Berg et al., 2011). However, neurons in other brain regions share the neurotransmitter identity and divided into subpopulations based on molecular markers; therefore, there must be additional mechanisms to instruct NSCs to regenerate specific cell types damaged by injury. For regenerative studies, particularly in the

brain, where cellular complexity is unrivaled, it is critical to understand whether specific cell types regenerates with fidelity.

While molecular markers of various cell types have been used to assay for neuronal maturity, it remains unclear to what extent regenerated neurons acquire functional properties. The maturity of neurons generated by directed differentiation of pluripotent stem cells and direct reprogramming *in vitro* have been assessed by electrophysiology (Berninger et al., 2007; Caiazzo et al., 2011; Heinrich et al., 2010; Maroof et al., 2013; Shi et al., 2012). Similarly, integration of newly generated striatal medium spiny neurons upon cerebral ischemia was assayed by electrophysiological recordings *in vivo* (Hou et al., 2008). Despite the availability of tools in regenerative organisms (Fleisch et al., 2011), electrophysiological recordings have yet to shed light on the maturation properties of newborn neurons in the regenerated brain.

In addition to receiving afferent inputs from the neighboring neurons, the regenerated neurons must also project axons to the correct targets, which are long-distance for some neuronal subtypes. During mammalian brain development, growth cones at the end of axons find their targets based on the interaction of specific receptors and chemoattractive and chemorepellant cues in the environment (Chilton, 2006). In the adult, the expression of these guidance cues persists; however, the distribution is altered, a speculative reason why most regenerating axons in mice are misdirected (Harel and Strittmatter, 2006). When GFP^+ hESC-derived cortical neurons are transplanted into the neonatal mouse cerebral cortex, sparse axons reach target subcortical regions such as the thalamus and spinal cord (Espuny-Camacho et al., 2013). However, the ability of neurons generated *in vitro* to project to correct targets once transplanted in the adult brain is unknown. Despite the shortcoming, this remains a hopeful strategy for regenerative medicine, and it is necessary to determine whether regenerative organisms are capable of regrowing axons through the pre-existing brain to the right targets. Previous studies have qualitatively tracked the GFP-labeled axons originating from newborn neurons in the zebrafish telencephalon (Skaggs et al., 2014). While GFP^+ axons can be found in distant regions from the injury site, it is difficult to

determine whether the targets are correct and whether only a small subpopulation of newborn neurons extend their axons distally. More importantly, it is not known if the regenerated neurons are able to functionally activate the postsynaptic neurons, a requirement for any functional brain regeneration.

IV. Molecular Mechanisms of Brain Regeneration

A handful of factors that are necessary for brain regeneration has been isolated in the zebrafish. For example, whole-telencephalon transcriptional analysis has identified an upregulation of *gata3* expression in the injured telencephalon (Kizil et al., 2012c). It is highly expressed in the RG and newborn neurons upon injury although it is not expressed during embryonic brain development. Knockdown of *gata3* significantly reduces the number of proliferating RGs and newborn neurons indicating that it plays a role during the initial phase of brain regeneration. In parallel, an *in situ* hybridization screen showed that *cxcr5* is upregulated in RGs after stab injury in the zebrafish telencephalon (Kizil et al., 2012a). Like *gata3,* knockdown of *cxcr5* leads to decreased neurogenesis. In the newt midbrain, transcriptional analysis of microdissected ventricular cells has identified the Sonic Hedgehog signaling pathway as a key regulator of ependymoglia cell proliferation (Berg et al., 2010). Chemical inhibition of the Sonic Hedgehog pathway by cyclopamine reduces the number of regenerated dopaminergic neurons. These molecular studies highlight the value of using regenerative organisms to identify key regulators of certain aspects of brain regeneration.

To-date, no molecular mechanisms have been identified for axolotl brain regeneration. In contrast, transcriptome and proteome data during axolotl limb regeneration are readily accessible (Bryant et al., 2017; Campbell et al., 2011; Gorsic et al., 2008; Habermann et al., 2004; Holman et al., 2012; Monaghan et al., 2012; Rao et al., 2009; Stewart et al., 2013; Wu et al., 2013), and a comprehensive transcriptome that covers 88% of the axolotl transcriptome is available (Bryant

et al., 2017). Therefore, tissue-level transcriptional analysis of the brain before and after injury is a possibility, and such study could reveal important signaling pathways and genes that play a role during axolotl brain regeneration.

However, the cellular heterogeneity in the central nervous system is unrivaled. For example, the mouse neocortex contains various cell types, and among them are the numerous classes of neurons that have been defined by their molecular, electrophysiological, morphological, and topographical traits. The diversity of neuronal subtypes most likely contributes to the complex functionality of the mammalian brain. However, it was not until recently that different cell types have begun to be defined at the molecular level. Transcriptional profiling at the population and single-cell level has begun to elucidate the signature genes that combinatorially identify each class of neurons. Deep understanding of the molecular players within specific cell types has promoted the elucidation of mechanisms in brain development and disease.

Despite these efforts, quantitative transcriptional analysis of specific cell types remains a challenge in organisms that are not genetically tractable such as the axolotl. Even for non-mammalian vertebrates, the telencephalon contains multitude of cell types (Brox et al., 2003, 2004; Ganz et al., 2012; Ganz et al., 2014; Moreno et al., 2004; Moreno and González, 2007; Puelles et al., 2000). If a regenerative response is induced in only one cell type of the brain upon injury, the signal will be significantly reduced if the whole tissue is sampled for transcriptional analysis. Therefore, a cell type-specific RNA sequencing technology is necessary to obtain high cellular resolution.

To overcome this obstacle, I have adopted a recently-developed technique (Hrvatin et al., 2014; Molyneaux et al., 2015; Pan et al., 2011; Pechhold et al., 2009; Yamada et al., 2010) to enable transcriptional profiling of specific neuronal subtypes from non-genetically tractable model systems. Using the unlabeled mouse and human brain tissues as a proof-of-concept, I show that neuronal subtype-specific purification and transcriptional profiling is possible. With this

method, it is possible to profile the transcriptional changes during axolotl brain regeneration at the resolution of specific cell types.

IV. Thesis Overview

In Chapter 2, I sought to determine whether brain regeneration of the axolotl pallium extends beyond morphological regeneration. In particular, I assayed the ability to 1) regenerate specific neuronal populations, 2) acquire mature electrophysiological properties, 3) remake tissue architecture, and 4) regenerate long-distance connectivity and circuit physiology. I created a novel injury paradigm in which a microknife removes a specific region of the dorsal pallium and its constituent neuronal populations. Combination of histology and *in vivo* imaging revealed a reproducible time course of regeneration, which starts with wound closure, then proliferation of the ependymoglia cell pool, and finally, differentiation into mature neuronal subtypes.

To determine whether specific neuronal subtypes regenerate, I mapped the distinct neuronal populations within the pallium via *in situ* hybridization. I found that, upon regeneration, the exact populations that were damaged were replaced in comparable numbers to sham-injured controls, even after metamorphosis. Beyond molecular markers, electrophysiological recording of newborn neurons showed that the neurons acquired mature electrophysiological properties and were integrated within the local circuitry. These results indicate that adult axolotls are capable of regenerating specific neuronal populations, and this system could be used to model neuronal regeneration.

Regenerating the brain requires more than remaking the individual neurons. The regenerated tissue needs to recreate the original architecture and the neurons must connect locally and distally to regain functionality. Surprisingly, I found that the neuronal topography is disorganized and that the tissue architecture is not remade, contrary to the assumption that the regenerative capacity of the axolotl brain is perfect. Furthermore, long-distance connections from

the dorsal pallium to the olfactory bulb are significantly reduced in number, indicating that some neurons are unable to find their targets upon regeneration. These results highlight the inability of the adult vertebrate brain to accommodate new connections and tissues, even in a regenerative organism like the axolotl.

In Chapter 3, I identified genes induced by the injury in the axolotl brain by whole-tissue RNA sequencing. Despite the heterogeneity of the cells sampled, I generated a list of genes that were differentially expressed between injured and uninjured hemispheres. Groups of genes involved in cellular proliferation, immune activation, and retinoic acid signaling were identified, suggesting that these signaling pathways, known to be important in vertebrate regeneration, play major roles in the axolotl brain during regeneration. Furthermore, I found that axolotl limb blastema markers were highly and specifically expressed in the injured region during the first four weeks of brain regeneration. Together, these results generated a set of genes and signaling pathways that may play a role during this initial regeneration stage.

In the Appendix, I developed a new technology to overcome the issue of cellular heterogeneity in RNA-seq samples. In any tissue sample, especially the brain, sampling a mixed population could drown out signal from small subpopulations. Therefore, it's necessary to isolate specific cell types prior to transcriptional analysis. Here, I combined two techniques to isolate specific neuronal populations from unlabled brain samples for downstream RNA sequencing. This technique will allow for simple, fast cell type-specific transcriptional profiling from any organism including the axolotl and human.

Taken together, the results from this dissertation expand upon our knowledge regarding the extent of brain regeneration in the axolotl. I found that the neuronal diversity of the axolotl pallium regenerates with fidelity, and they mature into electrophysiological functional neurons. However, the tissue architecture and long-distance connectivity remain impaired, questioning the functionality of brain regeneration in vertebrates. I also identify a set of genes that may play a role in the regenerative process. Finally, I developed a new technology to isolate specific neuronal

subtypes from brain tissue for downstream transcriptional profiling. Future work is necessary to determine whether brain regeneration is behaviorally functional and what molecular players instruct the birth of neuronal diversity in the axolotl for potential translation into human patients with severe brain damage.

Chapter 2

Regeneration of Neuronal Diversity in the Axolotl

Publication

The work in this chapter was published previously as:

Amamoto, R., Huerta, V.G., Takahashi, E., Dai, G., Grant, A.K., Fu, Z., and Arlotta, P. (2016). Adult axolotls can regenerate original neuronal diversity in response to brain injury. eLife *5*.

Introduction

Under physiological conditions, the neurogenic capacity of the adult mammalian brain is largely restricted to two neurogenic niches, the subventricular zone of the lateral ventricle, which gives rise to interneurons of the olfactory bulb and the subgranular zone of the dentate gyrus, which generates granule cells of the hippocampus (Ming and Song, 2011). Neurons in other brain regions are only generated during embryonic development and are not replaced postnatally.

In contrast to mammals, other vertebrates are endowed with superior capacity to regenerate multiple organs, including parts of the central nervous system (CNS). Among these, urodele amphibians like the axolotl (*Ambystoma mexicanum)* are endowed with the capacity to add new neurons to the brain throughout life (Maden et al., 2013) and can regenerate the spinal cord and parts of the brain after chemical or mechanical injury (Burr, 1916; Butler and Ward, 1967; Kirsche and Kirsche, 1964b; Piatt, 1955b). Resection of the middle one-third of one hemisphere, but not the whole hemisphere, in the axolotl telencephalon results in reconstruction of the injured hemisphere to a similar length as the contralateral, uninjured side (Kirsche and Kirsche, 1964a, b; Winkelmann and Winkelmann, 1970). Similarly, after mechanical excision of the newt optic tectum, new tissue fills the space produced by injury (Okamoto et al., 2007). Interestingly, in the newt, selective chemical ablation of dopaminergic neurons within a largely intact midbrain triggers regeneration of the ablated pool of neurons (Berg et al., 2010; Parish et al., 2007). In addition to urodeles, teleost fish have also been extensively studied for their capacity to regenerate the CNS and have led to the identification of some of the molecular signals involved in the regenerative process (Kizil et al., 2012b). These studies highlight the value of regenerative organisms as models to understand the mechanisms that govern brain regeneration for possible application to the mammalian brain.

However, the mammalian CNS is notoriously complex, and its ability to compute high-level functions, like those of the mammalian cerebral cortex, relies on the presence of a great diversity of neuronal subtypes integrated in specific long-distance and local circuits and working

within a defined tissue architecture. Disruption of brain structure, connectivity, and neuronal composition is often associated with behavioral deficits, as observed in models of neurodevelopmental, neuropsychiatric, and neurodegenerative disease. It is therefore likely that functional regeneration of higher-order CNS structures will entail the regeneration of a great diversity of neuronal subtypes, the rebuilding of original connectivity, and the synaptic integration of newborn neurons in the pre-existing tissue. It is not known to what extent even regenerative species can accomplish these complex tasks, beyond their broad ability to generate new neurons and to rebuild gross brain morphology. It remains therefore debated whether any vertebrates are capable of true functional brain regeneration.

Using the adult axolotl pallium as the model system, we have investigated whether a diverse array of neuronal subtypes can regenerate and whether their tissue-level organization, connectivity, and functional properties can also regenerate after mechanical injury.

In contrast to the teleostean pallium, the everted nature of which makes linking distinct regions to their mammalian counterparts difficult (Northcutt, 2008), the gross neuroanatomy of the axolotl pallium, organized around two ventricles, shows clear similarities to that of the mammalian telencephalon. In addition, while the evolutionary origin of the mammalian cerebral cortex remains controversial (Molnár, 2011), it is likely that the axolotl pallium contains a basic representation of several of the neuronal subtypes found in the mammalian cerebral cortex and thus may serve as a good model for investigating regeneration of neuronal heterogeneity and complex circuit function.

Here, we demonstrate that both pre- and post-metamorphosis adult axolotls are able to regenerate a diversity of neurons upon localized injury to the dorsal pallium. This process occurs through specific regenerative steps that we defined in live animals using non-invasive magnetic resonance imaging (MRI). Strikingly, newborn neurons can acquire mature electrophysiological properties and respond to local afferent inputs. However, they unexpectedly fail to rebuild long-distance circuit and the original tissue architecture.

The data provide the first proof for the precision with which axolotls regenerate a diverse set of neurons, which in turn become electrophysiologically active and receive local afferent inputs. Notably, however, our results also challenge prior assumptions of functional brain regeneration in salamanders by uncovering unappreciated limitations in the capacity of adult axolotls to fully rebuild original long-distance connectivity and tissue organization, a finding that redefines expectations for brain regeneration in mammals.

Results

The axolotl pallium contains molecularly diverse neuronal populations

In order to investigate whether axolotls can reconstruct neuronal diversity, we have started by building a molecular map of the neuronal populations present in the axolotl pallium.

The neuronal composition of the axolotl pallium is largely unknown, with the urodele pallium being classically divided into medial pallium (MP), dorsal pallium (DP), and lateral pallium (LP) based on the size and location of cell nuclei, as well as rudimentary connectivity (Herrick, 1948; Kokoros and Northcutt, 1977; Westhoff and Roth, 2002) **(Figure 2.1a)**. We first used Nissl staining of serial sections to build an anatomical atlas of the pallium, which we have subsequently used to precisely match the rostro-caudal location of sections among all animals compared in this study **(Figure 2.2).**

Next, we built a molecular map of neurons present in the pallium. We selected 19 genes that, in the mouse, are known to mark specific subtypes of either excitatory pyramidal neurons or inhibitory interneurons of the cerebral cortex **(Figure 2.1b)** and performed *in situ* hybridization on coronal sections of the adult axolotl brain, using riboprobes designed on axolotl cDNA sequences. Among all markers tested, expression of nine genes could be detected reliably in the axolotl pallium: *ctip2, satb2, tle4, rorb, er81, fezf2, gad2, sst,* and *calb2*. In the mouse neocortex, *Fezf2* and *Ctip2* are specifically expressed by subcerebral projection neurons (ScPNs) in layer Vb at high levels and by corticothalamic projection neurons (CThPNs) in layer VI at low levels (Arlotta

Figure 2.1: The axolotl pallium contains molecularly diverse neuronal subpopulations. (a) Schematic representation of the axolotl pallium showing ependymoglia cells (red) lining the ventricle, neurons (black) positioned in the dorsal pallium close to the ventricle, and fiber tracts (green) occupying the region closer to the pia. (b) Schematic representation of cortical neuronal subtypes in the mouse neocortex. Major classes of murine cortical projection neuron subtypes as well as selected classes of cortical interneurons are depicted. (c) *in situ* hybridization and immunohistochemistry for selected cortical projection neuron and interneuron markers on coronal sections of the adult axolotl pallium. Insets, high-magnification images of regions of marker expression in the dorsal pallium (top panels) and the medial/lateral pallium (bottom panels). (d) Schematic map of the localization of molecularly distinct neuronal subtypes within the adult axolotl pallium. (e) $Satb2^{HI}$ regions in the dorso-lateral pallium are distinctly separate from regions of $Ctip2^{HI}$ and $Tle4^{HI}$ expression, showing a molecular boundary. (f) $Satb2^{HI}$ cells largely coexpress Calb2. A, Anterior; P, Posterior; D, Dorsal; V, Ventral; MP, Medial Pallium; DP, Dorsal Pallium; LP, Lateral Pallium; S, Septum; Str, Striatum; Ctx, Cortex; IN, cortical Interneurons; PN, cortical Projection Neurons; SCPN, Subcerebral Projection Neurons; CThPN, CorticoThalamic Projection Neurons; CPN, Callosal Projection Neurons; L4N, Layer 4 Neurons; SST, Somatostatin; V, Ventricle. Scale bars; 500 μm (c, top panels), 200 μm (c, insets; e and f, left panels), 100 μm (e and f, right panels).

Figure 2.1 (Continued)

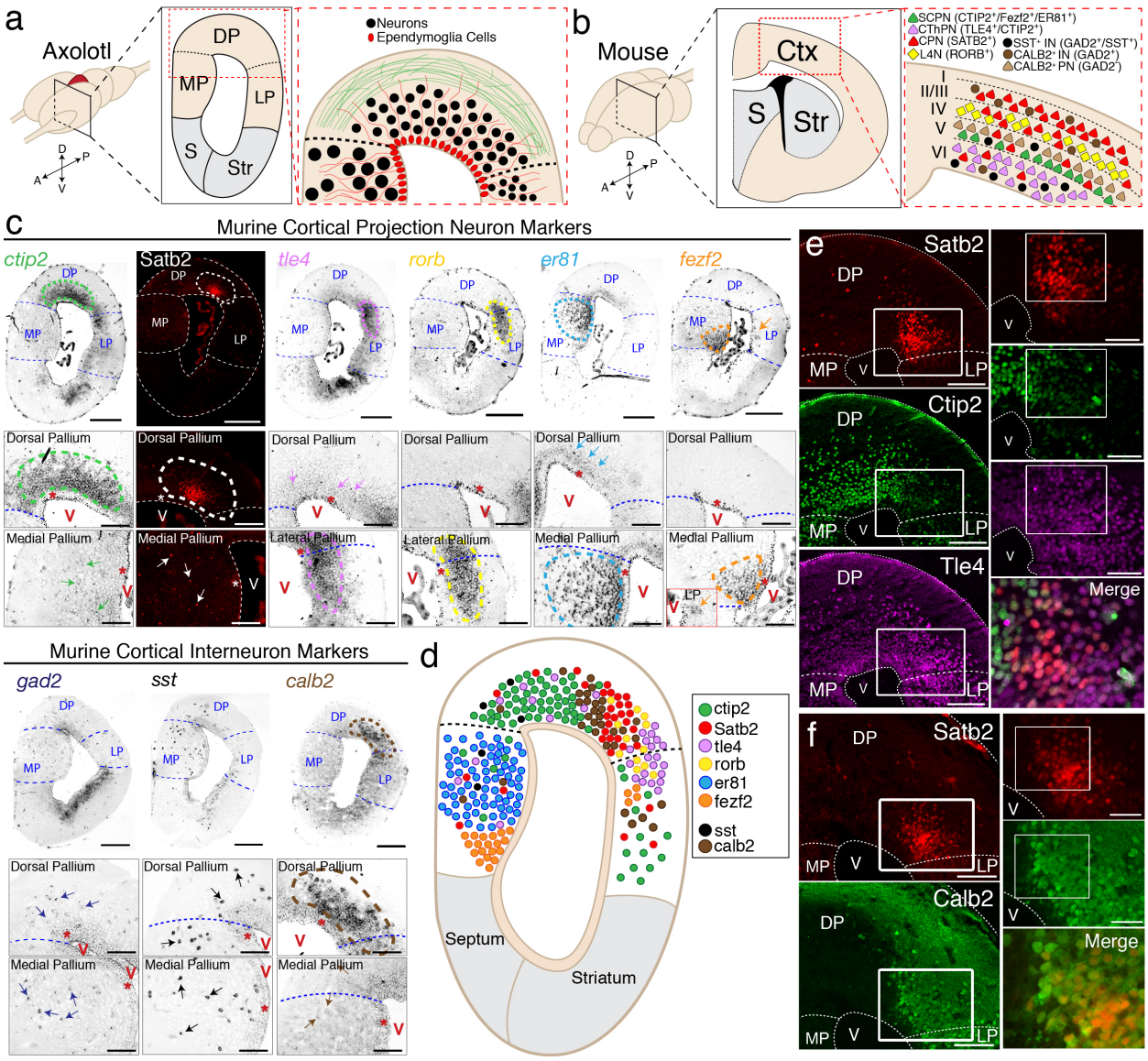

Figure 2.2: Anatomical map of the axolotl pallium.

(a) Top view of the axolotl brain, with an indication of the section numbering system in the pallium. Inset: Whole-body image of a representative axolotl used in the study. (b) Nissl staining of representative coronal sections spaced at 300 μm. (c) Immunohistochemistry for NeuN or Hu-C/D and neuronal subtype markers, Ctip2, Satb2, Tle4, and Calb2 shows that the majority of neuronal subtype markers colocalize with either NeuN or Hu-C/D. Tle4 is also expressed at low levels in $NeuN^-$ ependymoglia cells. Th, Thalamus; OT, Optic Tectum; SC, Spinal Cord. Scale Bars, 500 μm (b), 50 μm (c).

Figure 2.2 (Continued)

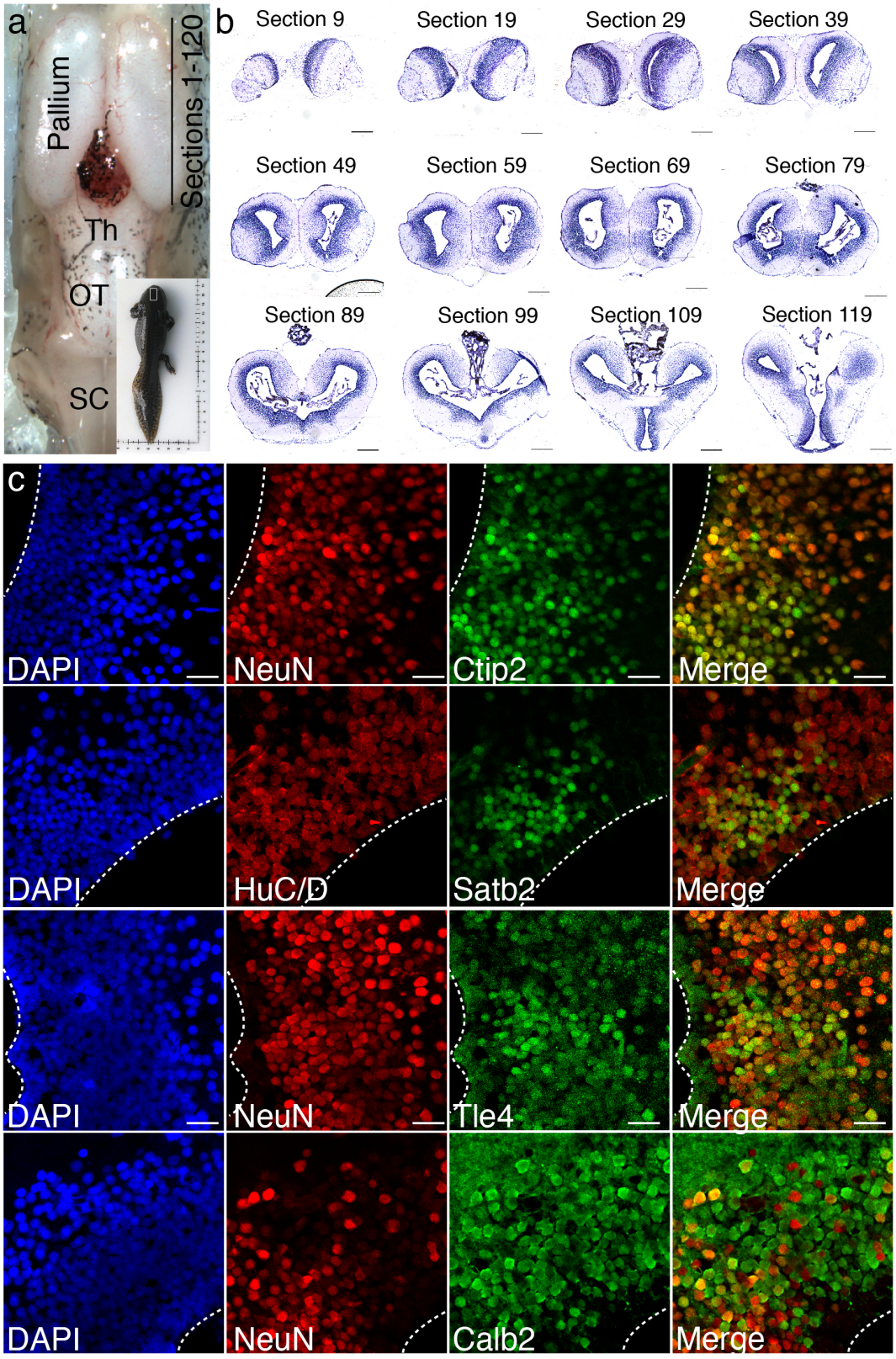

et al., 2005; Chen et al., 2005a; Chen et al., 2005b; Molyneaux et al., 2005). Within these two neuronal populations, *Er81* labels ScPNs (Yoneshima et al., 2006), but not CThPNs, which selectively express *Tle4* (Molyneaux et al., 2007). Callosal projection neurons (CPNs) across all layers distinctly express *Satb2* and are negative for *Ctip2, Fezf2,* and *Tle4* (Alcamo et al., 2008; Britanova et al., 2008). Finally, *Rorb* labels locally connected excitatory interneurons of layer IV (Jabaudon et al., 2012). Among *Gad2*$^{+}$ cortical GABAergic interneurons, *Sst* and *Calb2* mark specific subtypes (Bartolini et al., 2013), although *Calb2* has been shown to also be transiently expressed in pyramidal neurons residing in layer Va (Liu et al., 2014).

We found that, similarly to the mouse brain, these markers labeled specific regions of the axolotl pallium. *Ctip2* was highly expressed in DP with lower expression in MP and LP; Satb2, detected by immunohistochemistry, was expressed in a restricted region of DP and in scattered cells within MP; *tle4* marked a domain at the border of the dorso-lateral pallium and was expressed at lower levels across DP and MP; *rorb* was expressed in a distinct domain in the dorso-lateral pallium; *er81* was expressed in MP at high levels and in DP at lower levels; *fezf2* was expressed mostly in the ventral MP and in scattered cells within LP **(Figure 2.1c).** Among the murine cortical interneuron markers, *gad2* was expressed in scattered cells within the dorso-medial pallium and MP, *sst* was expressed in scattered cells across DP and MP, and *calb2* defined a circumscribed domain in DP, as well as sparse cells in MP **(Figure 2.1c)**.

While all genes tested showed unique distributions, the data indicated that markers of subpopulations of mouse pyramidal neurons, which are normally grouped into defined neocortical layers, cluster within distinct domains in the axolotl pallium **(Figure 2.1d)**.

In order to have reliable molecular reference points after regeneration, we selected, for further analysis, four of the nine genes tested - *ctip2, satb2, tle4,* and *calb2* - because of their highly circumscribed and robust profiles of expression within defined regions of the dorsal and dorso-lateral pallium. We used immunohistochemistry to define, at the single cell level, the colocalization of these markers. We found that the dorso-lateral pallium contains Satb2^{HI}, Ctip2^{LO},

Tle4^{HI} cells and Satb2^{LO}, Ctip2^{HI}, Tle4^{HI} cells **(Figure 2.1e).** Additionally, Satb2^{HI} cells in the dorso-lateral pallium also express Calb2 **(Figure 2.1f)**. Cells labeled with these markers also colocalized with NeuN or Hu-C/D, indicating that they are neurons **(Figure 2.2).**

Together, the data provide the first map of molecularly distinct populations of neurons within the adult axolotl pallium to enable injury of defined neuronal groups with fidelity.

In vivo MRI reveals tissue-level dynamics of regeneration in the axolotl pallium

We established a stereotactic injury model to remove a reproducible portion of the dorsal pallium such that the *ctip2, satb2, tle4,* and *calb2* domains were ablated **(Figure 2.3a)**. To define the time course of regeneration, we first investigated the overall pallial morphology of fixed whole brain preparations from adult axolotls sacrificed at 1, 2, 4, and 11 weeks post injury (wpi). We found that the wound closes by 4wpi, and is largely undetectable by 11wpi **(Figure 2.3b)**.

The tissue dynamics that accompany brain regeneration *in vivo* have never been investigated. To gain information on the tissue-level morphological changes that take place over the course of the regenerative process in individual animals and to account for animal-to-animal variability, we performed *in vivo* MRI of live axolotls undergoing pallial regeneration. This method demonstrated that the wound closure process occurs rapidly, between 2 and 4wpi **(Figure 2.3c-e)**. Notably, the lateral pallium formed a stump, which subsequently thinned out before protruding towards the medial pallium and closing the gap generated by the injury **(Figure 2.3d)**. This indicates that wound healing occurs largely by dynamic tissue remodeling that occurs before cellular proliferation starts.

To assess the cellular dynamics of the first eleven weeks post-injury and to map the time course of neurogenesis, animals were pulsed with Bromodeoxyuridine (BrdU; see Materials and methods). At 4wpi, a large number of BrdU^{+}/NeuN^{-} cells populated the injured hemisphere, indicating that accumulation of proliferative cells precedes neuronal differentiation **(Figure 2.3g)**. Of note, BrdU^{+} cells expressed Sox2 and Gfap, two ependymoglia cell markers (Kirkham et al.,

Figure 2.3: Temporal dynamics of successful pallial regeneration after acute mechanical injury.

(a) Location of the injury site in the dorsal pallium, left hemisphere. (b) Representative stereoscope photographs of injured brains at 1, 2, 4, and 11wpi. (c) 3D renderings of *in vivo* MRI images (top panels) and MRI coronal cross-sections within the injury site (bottom panels) of a representative axolotl brain during a 28-day time course post-injury. (d) Enlarged insets (from the red boxes in c) show three distinct stages of wound closure: stump formation, protrusion (red arrow), and closure. Red dotted lines outline the tissue. (e) The sizes of the injury site (in mm^3, see Online Methods) remain unchanged for the first 14 days, but decrease rapidly within a subsequent four-day period (n=3). (f) Schematic of *in vivo* BrdU labeling in the early post-injury phase. (g) Time course of BrdU and NeuN immunohistochemistry on coronal sections at 1, 2, and 4wpi shows limited cell proliferation within the first 2 weeks and increased proliferation by 4 wpi. Insets, magnified images at 4wpi (panel g'). (h) Schematic of *in vivo* BrdU labeling at mid post-injury phases. (i) Immunohistochemistry for BrdU and NeuN on coronal sections at 11wpi shows that a large subset of $BrdU^+$ cells is composed of $NeuN^+$ postmitotic neurons. Insets, magnified images at 11wpi (panel i'). (j) Model of the regenerative process during the first 11 weeks after acute mechanical injury. Wound closure proceeds in 3 distinct stages during the first 4 wpi: stump generation, stump protrusion, and wound closure. Only subsequently, newly proliferated $BrdU^+$ cells populate, in large number, the injured region. By 11wpi, newborn neurons are generated. OB, Olfactory Bulb; Th, Thalamus; OT, Optic Tectum; wpi, weeks post injury; D, Day; LP, Lateral Pallium; MP, Medial Pallium; Str, Striatum; S, Septum. Scale bars; 500 μm (g and i), 100 μm (g' and i').

Figure 2.3 (Continued)

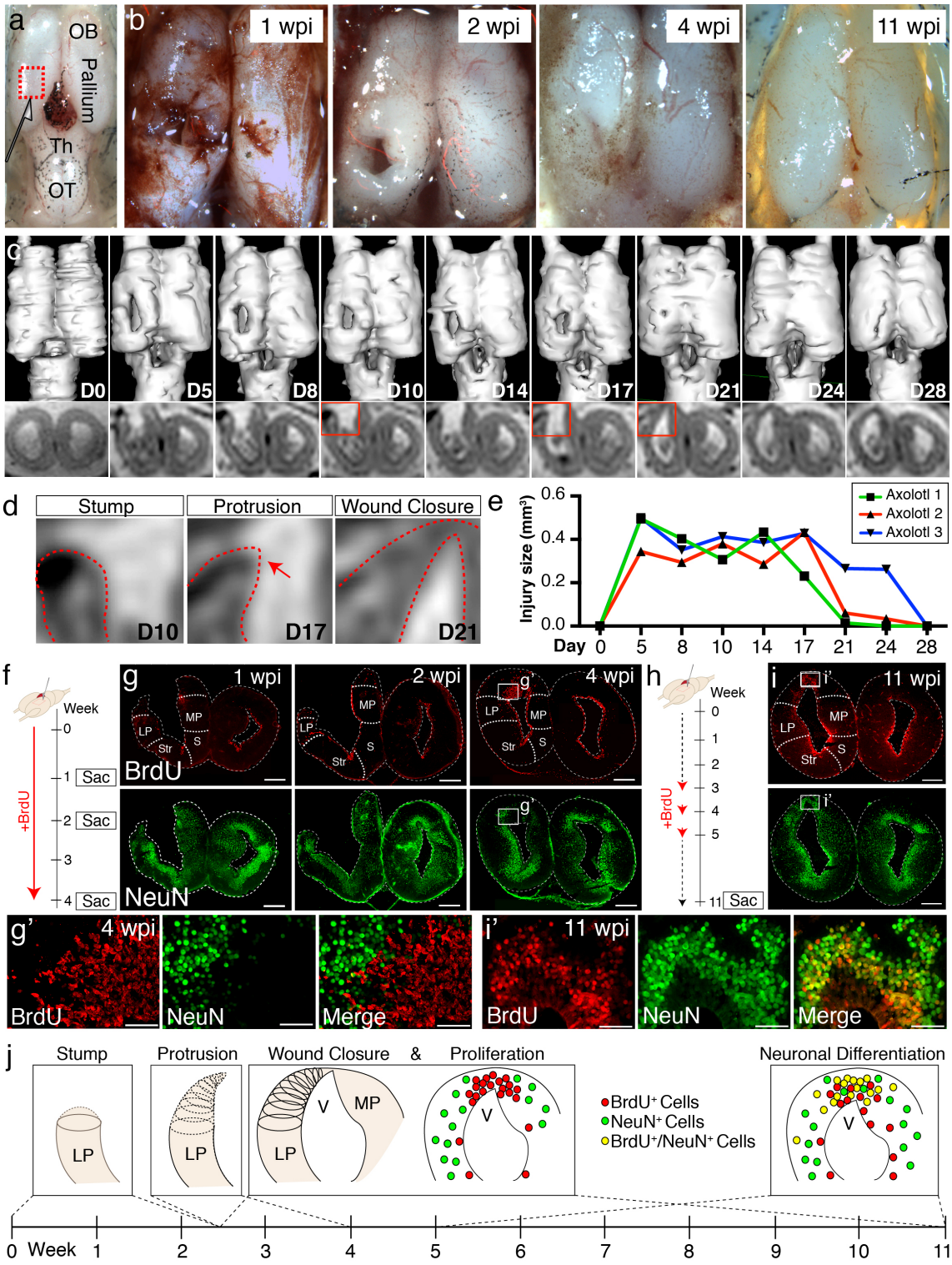

2014) and could represent the proliferative cells found around the ventricles during homeostasis **(Figure 2.4** and **Figure 2.5)**. By 11wpi, the majority of $BrdU^+$ cells expressed NeuN (69.5%, n=6 animals) **(Figure 2.3i)** indicating that neuronal differentiation occurs between 4 and 11wpi.

Interestingly, we observed an increased number of $BrdU^+$ and $PH3^+$ proliferative cells in regions rostral to the injury site, at the level of the rostral telencephalon, despite the fact that this region was not injured **(Figure 2.6).** In accordance, we also found an increased number of $BrdU^+$ cells in the pallium of the contralateral hemisphere upon injury **(Figure 2.7)**. To determine whether this distal proliferative response leads to regeneration of new neurons, we quantified the number of $BrdU^+/NeuN^+$ cells in the rostral telencephalon at 11wpi in injured and sham controls, in which the skin and skull were opened but the brain was not injured. Quantification revealed that there were significantly more $BrdU^+/NeuN^+$ nuclei in the rostral telencephalon of injured animals compared to sham animals, indicating that an injury to the pallium leads to generation of newborn neurons distally **(Figure 2.6)**.

Taken together, these data demonstrate that regeneration of the pallium initiates with distinct morphological changes to the injury edge (stump), which thins out and closes the wound. This process precedes rapid proliferation of progenitors and neurogenesis **(Figure 2.3j)**. In addition, the progenitor proliferative response induced by injury is not restricted to the region immediately adjacent to the injury site but induces a more global response in distal uninjured regions.

Molecular diversity of neuronal subtypes regenerates upon injury to the pallium of both pre- and post-metamorphosis axolotls

To assess the axolotl's ability to regenerate distinct neuronal populations in distinct regions of the pallium, we quantified the number of $NeuN^+$, $Ctip2^+$, $Satb2^+$, $Tle4^+$, and $Calb2^+$ neurons at 11wpi in the dorsal pallium of contralateral, injured, and sham hemispheres. Cells were counted in four consecutive sections, sampled every 300 μm, over a total rostral-caudal

Figure 2.4: 4wpi proliferative cells express markers of ependymoglia cells.

(a-h) Immunohistochemistry against Sox2 (a and c), BrdU (b, d, f, and h), and Gfap (e and g) on representative coronal sections of 4wpi pre-metamorphosis animals. This analysis shows that the majority of the $BrdU^+$ nuclei in the injured hemisphere are $Sox2^+$ and $Gfap^+$. (i-l) Immunohistochemistry against Gfap (i), BrdU (j and l), and Sox2 (k) on representative coronal sections of 4wpi post-metamorphosis animals. $BrdU^+$ nuclei in the injured hemisphere are $Sox2^+$ and $Gfap^+$ even after metamorphosis. V, Ventricle. Scale Bars, 500 μm (whole brain images) 200 μm (insets).

Figure 2.4 (Continued)

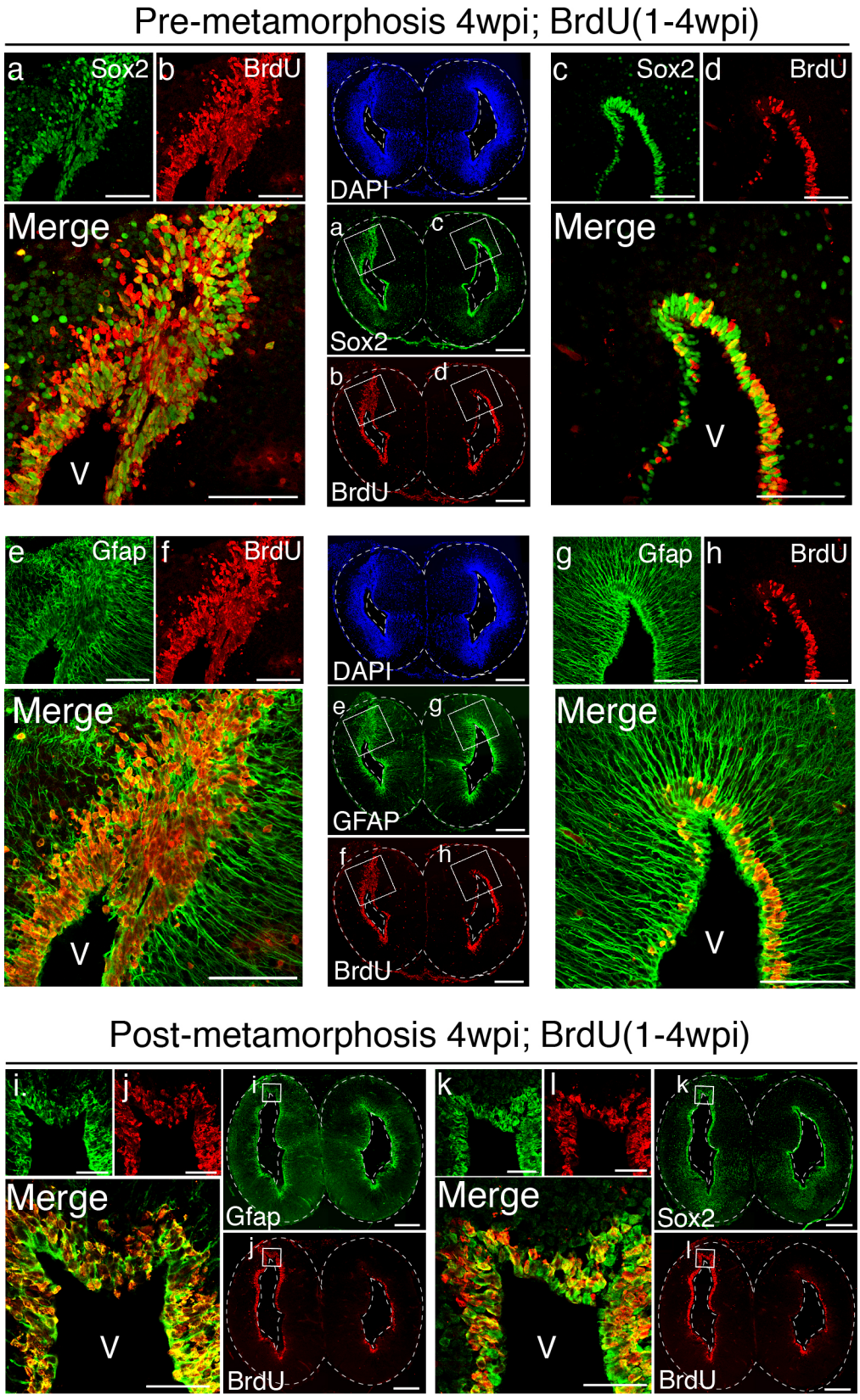

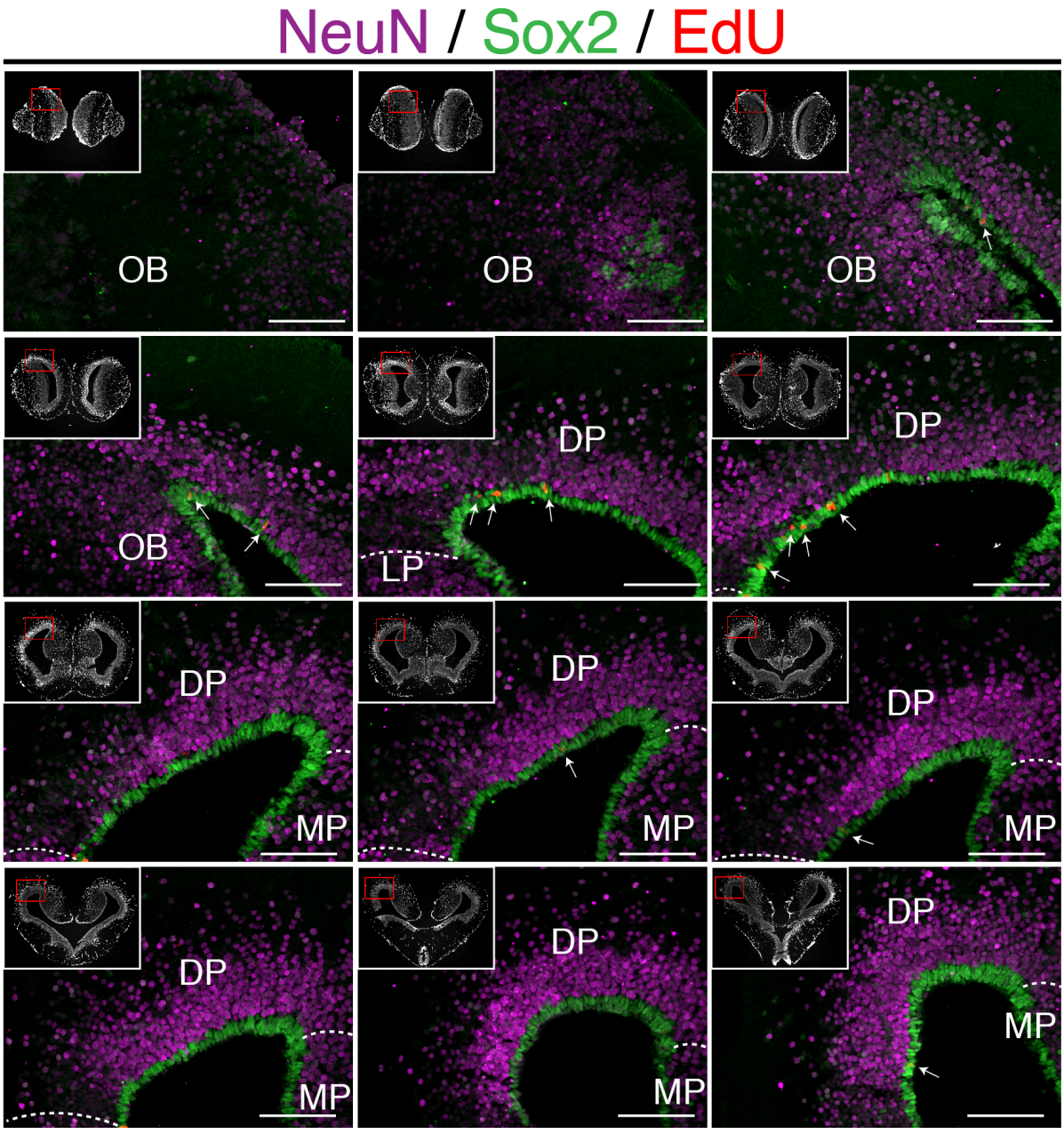

Figure 2.5: Ependymoglia cells proliferate at a low rate during homeostasis.

Immunohistochemistry against Sox2, EdU, and NeuN on representative coronal sections without injury. Arrows indicate $EdU^{+}/Sox2^{+}$ cells. OB, Olfactory Bulb; LP, Lateral Pallium; DP, Dorsal Pallium; MP, Medial Pallium. Scale Bars, 200 μm.

Figure 2.6: Newborn neurons populate distant, uninjured regions of the brain.

(a-b) An increase in the numbers of BrdU-labeled cells and $PH3^+$ mitotic cells is observed upon injury both at the injury site (dorsal pallium, a) and in regions distal to the injury (rostral telencephalon, b). Upper panels, schematics of the telencephalic regions analyzed in 4wpi injured and sham axolotls (pallium in a, rostral telencephalon in b). Middle panels, representative images used for cell counting. Lower panels, quantification of $BrdU^+$ nuclei and $PH3^+$ nuclei in rostral-caudal matched coronal sections of injured (n=7) and sham (n=5) animals. (c-d) Regeneration of $BrdU^+/NeuN^+$ newborn neurons upon injury at both the injury site (dorsal pallium, c) and in regions away from the injury (rostral telencephalon, d) at 11wpi. Upper panels, schematics of the telencephalic regions analyzed in 11wpi injured and sham axolotls (pallium in c, rostral telencephalon in d). Middle panels, representative immunohistochemistry images used for cell counting. Lower panels, quantification of $BrdU^+/NeuN^+$ newborn neurons in the injured pallium (c) and rostral telencephalon (d) (n=6) compared to the sham (n=4). V, Ventricle. Scale Bars; 500 μm (a-b, left panels), 50 μm (a-b, right panels, c-d). All results are expressed as the mean ± SEM. * $p<0.05$, ** $p<0.01$, unpaired, two-tailed Student's t-test.

Figure 2.6 (Continued)

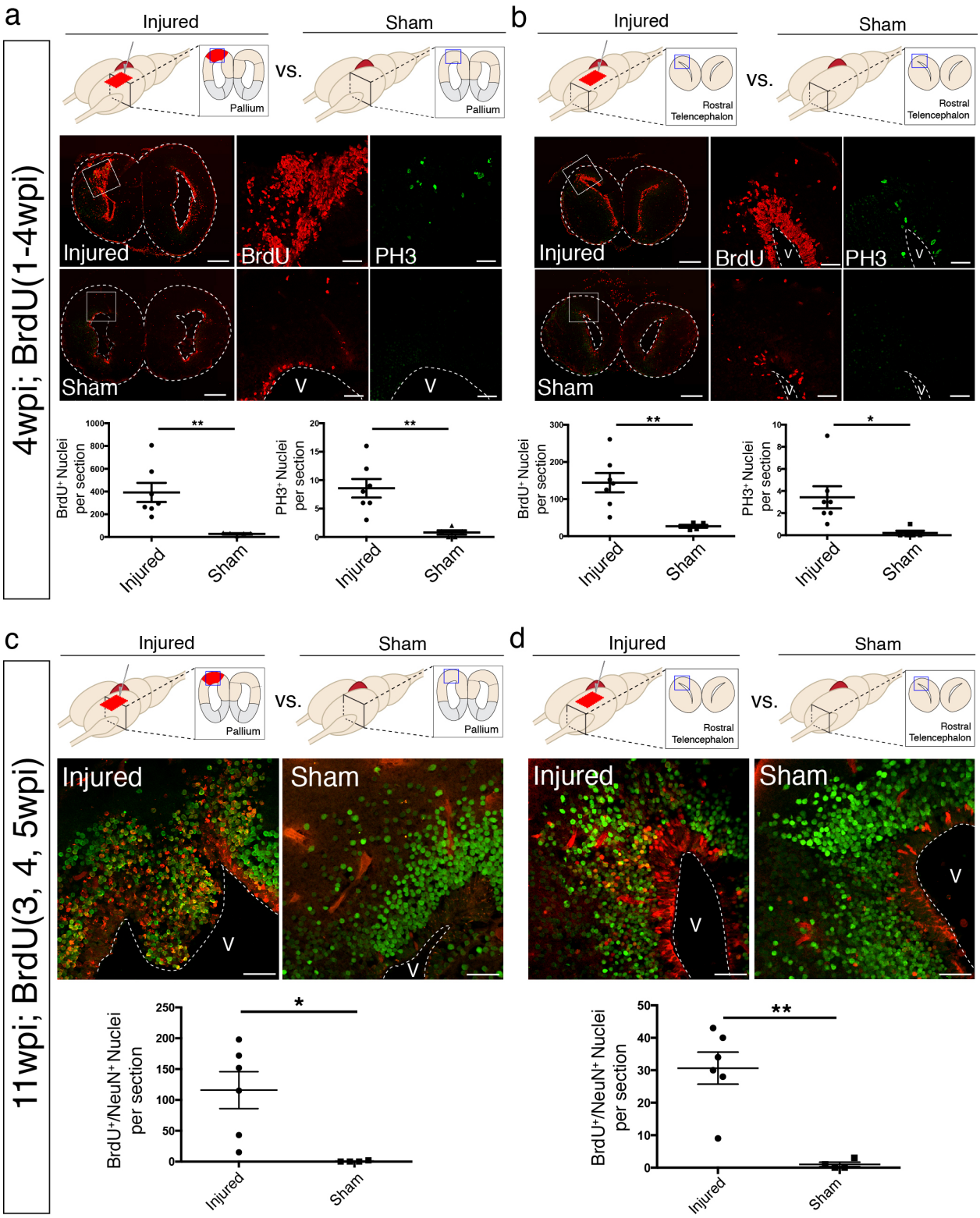

Figure 2.7: Increased proliferation in the uninjured, contralateral pallium.

(a) A schematic of a horizontal section of an axolotl brain. The red shaded region represents the ventricle, which connects the two hemispheres. (b) Upper panels, schematics of the telencephalic regions analyzed in 4wpi injured and sham axolotls. Middle panels, representative images used for cell counting. Lower panels, quantification of $BrdU^+$ nuclei in rostral-caudal matched coronal sections of injured (n=7) and sham (n=5) animals. OB, Olfactory Bulb; Th, Thalamus; V, Ventricle. Scale Bars; 500 μm (b, middle panels), 50 μm (b, insets). All results are expressed as the mean ± SEM. * $p<0.05$, unpaired, two-tailed Student's t-test.

Figure 2.7 (Continued)

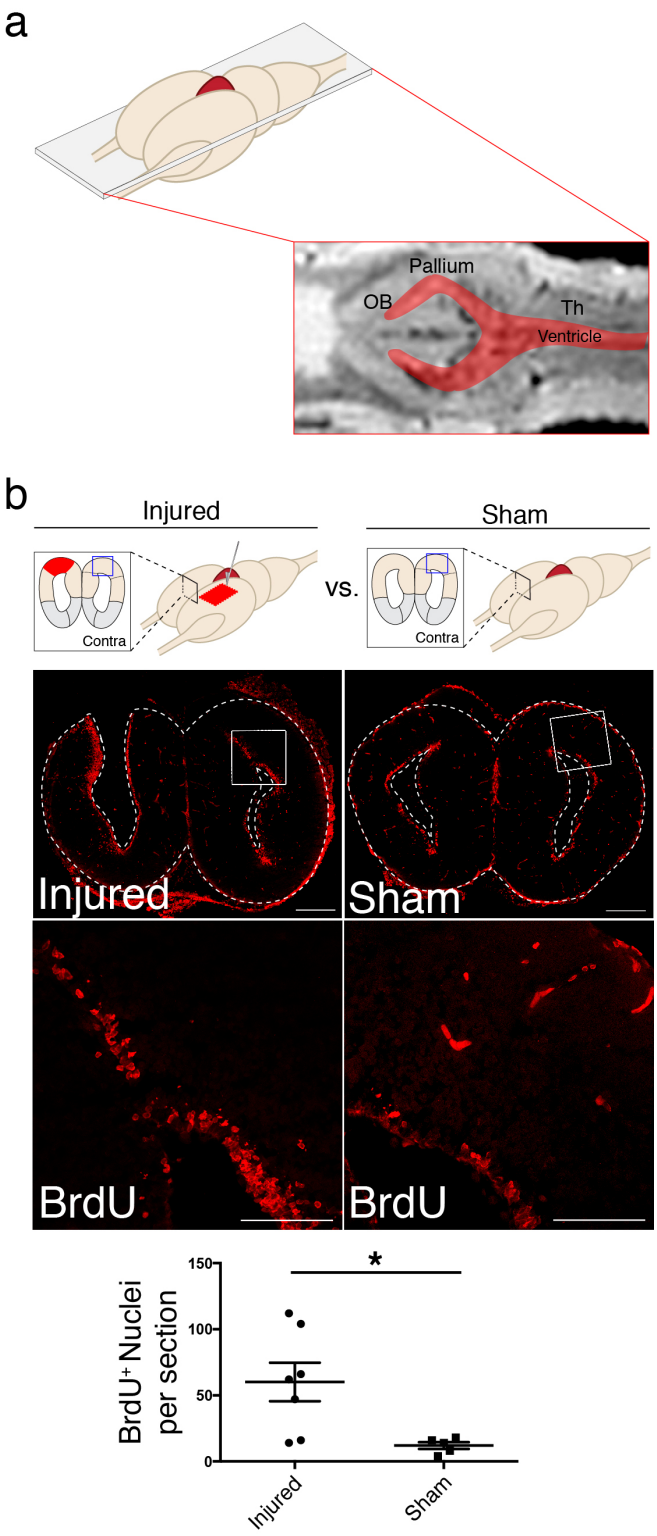

length of 900 μm spanning the injury site. The sum of all cells counted in all sections was taken for each sample **(Figure 2.8a)**. From this analysis, we found no significant differences between the number of cells present in the contralateral, injured (regenerated), and sham hemispheres for any of the markers quantified **(Figure 2.8b-f)**. The data indicate that the regenerated pallium contains each neuronal population in numbers comparable to control (contralateral and sham) pallium.

To determine whether there was an increase in the number of newborn neuronal subtypes in the injured pallium compared to controls, we quantified the number of cells that showed colocalization of each neuronal subtype-specific marker with BrdU at 11wpi. This analysis showed that the injury significantly increases the number of newborn neurons within each molecularly defined neuronal subpopulation, compared to controls (n=6 contralateral; n=6 injured; n=4 sham) **(Figure 2.8g-k)**, indicating that distinct neuronal populations are regenerated upon injury.

These numbers likely underestimate the number of neurons within each population that are newly born due to the difficulty of labeling by BrdU the entirety of the dividing cell pool. It is therefore not possible to conclude whether some of the neurons in the regenerate are newborn (yet not labeled by BrdU) or are endogenous neurons that have migrated from neighboring territories. If migration of neurons into the injured region were a major contributor to the regenerative process, this could cause a decrease in the number of certain neuronal subtypes in regions adjacent to the injury site. We thus quantified the number of neuronal subtypes in MP and LP. We found no significant differences between contralateral, injured, and sham hemispheres for any of the neuronal subtype markers tested **(Figure 2.9)**, suggesting, albeit not fully excluding, the possibility that no major waves of migration of endogenous neurons reconstitute neuronal diversity in the regenerated dorsal pallium.

It has been previously reported that the brain regeneration capability of the axolotl decreases upon metamorphosis (Kirsche et al., 1965). To address this issue directly, we induced metamorphosis in adult, sexually mature axolotls by administration of L-thyroxine exogenously

Figure 2.8: Molecularly diverse neuronal subtypes regenerate in the axolotl pallium.

(a) Schematic of the sections used for quantification (panels b-f and k). Images from 4 consecutive coronal sections, 300 µm apart, and spanning the injury site from contralateral, injured, and sham hemispheres were used for cell counting. (b-f) Quantification of $NeuN^+$, $Ctip2^+$, $Satb2^+$, $Tle4^+$, and $Calb2^+$ nuclei in the region of interest shows no significant differences among contralateral, injured, and sham hemispheres. (g-j) Newborn $BrdU^+$ cells in injured coronal sections co-express Ctip2, Satb2, Tle4, and Calb2, showing that neuronal subtype diversity is replenished upon regeneration; insets, high-resolution confocal images of co-labeled nuclei. (k) Quantification of $BrdU^+$/neuronal subtype-$marker^+$ nuclei in the dorsal pallium of contralateral, injured, and sham hemispheres. LP, Lateral Pallium; DP, Dorsal Pallium; MP, Medial Pallium; V, Ventricle. Scale Bars; 200 µm (g-j, top panels), 20 µm (g-j, bottom panels).

All results are expressed as the mean ± SEM. ** $p<0.01$, *** $p<0.001$, **** $p<0.0001$; one-way ANOVA with post-hoc Tukey's multiple comparison test.

Figure 2.8 (Continued)

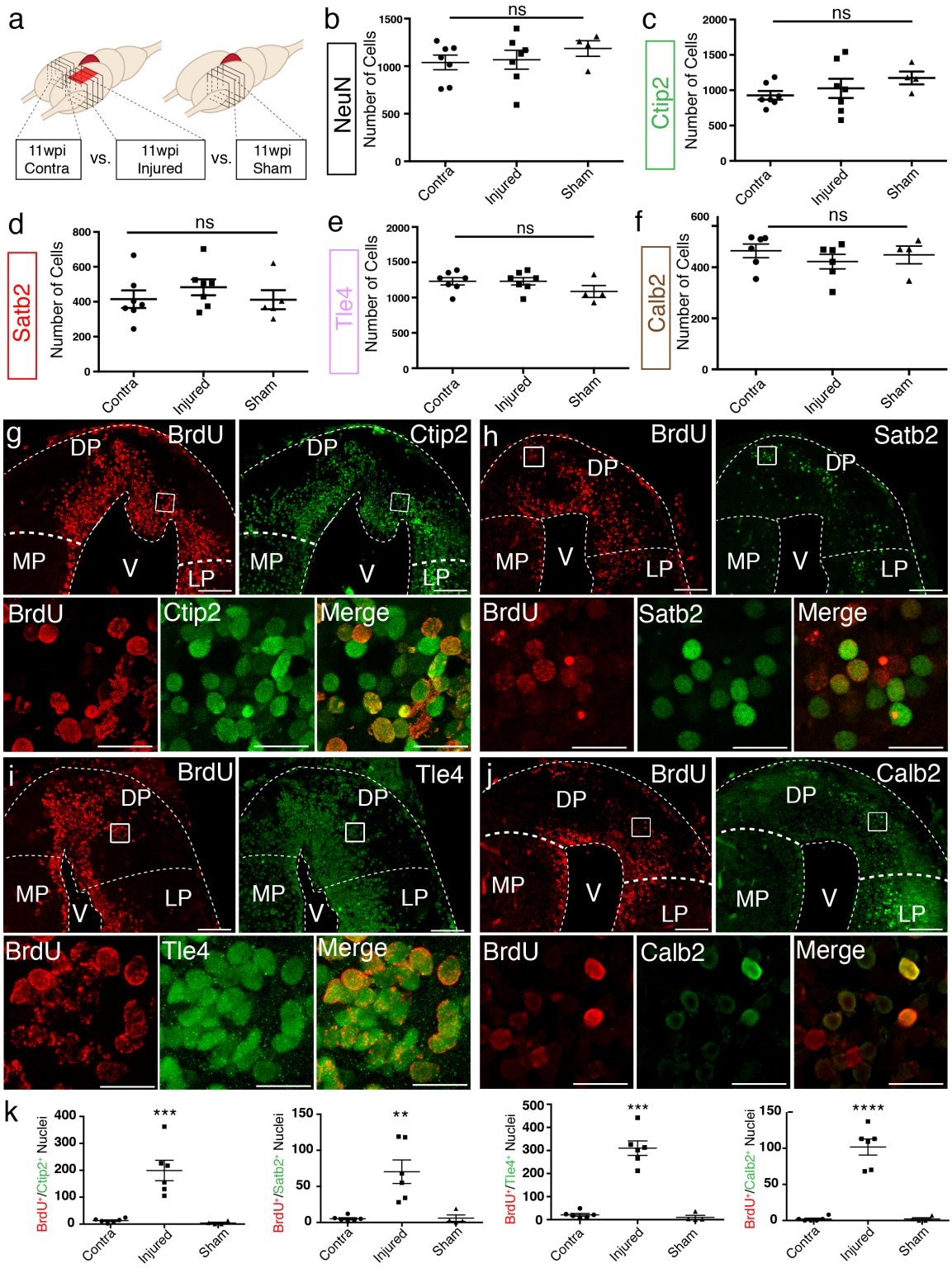

Figure 2.9: Neuronal subtypes in uninjured regions of the pallium remain unchanged in number at 11wpi.

(a-b) Immunohistochemistry against Ctip2, Satb2, Tle4, Calb2, and NeuN on representative coronal pallium sections of injured 11wpi axolotls, showing the medial pallium (a, left panels) and the lateral pallium (b, left panels). Quantification of $Ctip2^+$-, $Satb2^+$-, $Tle4^+$-, $Calb2^+$-, and $NeuN^+$-nuclei numbers from four sections spaced at 300 µm in the medial pallium (a, left panels) and the lateral pallium (b, right panels). Scale Bars, 50 µm.

All results are expressed as the mean ± SEM. One-way ANOVA.

Figure 2.9 (Continued)

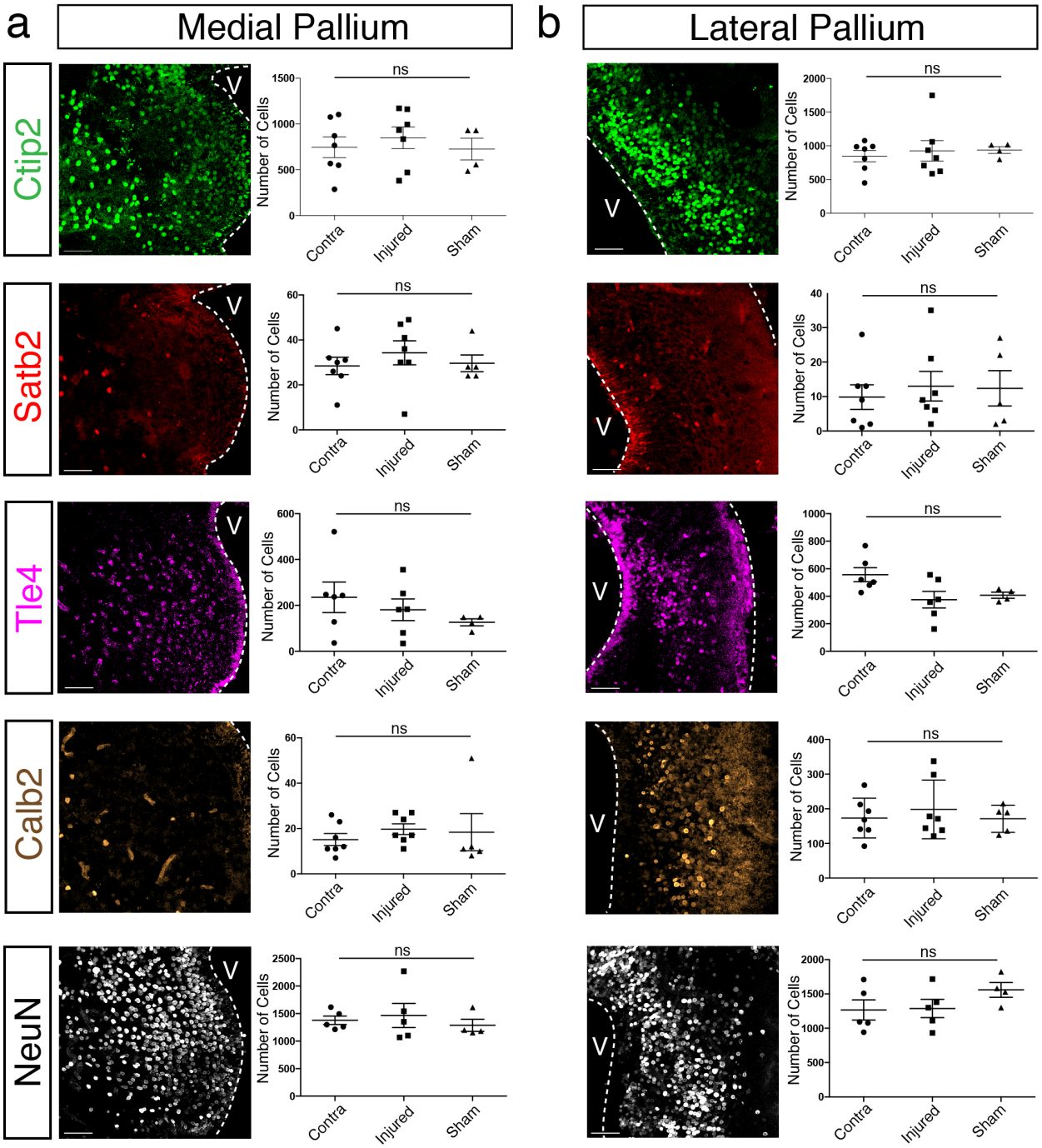

via immersion (Page and Voss, 2009) **(Figure 2.10)**. Upon metamorphosis, we injured the dorsal pallium of post-metamorphosis axolotls and found that morphological regeneration takes place within a similar time frame as the pre-metamorphosis axolotls **(Figure 2.10).** At 11wpi, we found that the post-metamorphic injured pallium contains $BrdU^+/NeuN^+$, $BrdU^+/Ctip2^+$, $BrdU^+/Satb2^+$, $BrdU^+/Tle4^+$**,** and $BrdU^+/Calb2^+$ nuclei **(Figure 2.10)**. Together, these data show that adult pre- and post-metamorphosis axolotls are able to regenerate neuronal subtypes within the dorsal pallium.

Regenerated neurons in the injured pallium are electrophysiologically active and receive afferent local input

To determine whether the regenerated neurons in the injured pallium mature into functional neurons, we sought to characterize their electrophysiological properties by using whole-cell patch clamp recordings **(Figure 2.11a).** We compared neurons identified as EdU^+ by *post hoc* staining in the dorsal pallium of injured animals (11-15wpi; n=14 neurons) and neurons at matched locations in uninjured control animals (n=9 neurons) **(Figure 2.11b)**. Injected, depolarizing current steps evoked action potentials in all cells recorded in the regenerated pallium **(Figure 2.11c-d).** We found that regenerated neurons exhibited passive and active membrane properties that were comparable to those of control neurons **(Figure 2.11e)**. However, in some cases (2/14 neurons), when compared with uninjured neurons, newly regenerated neurons displayed passive and active membrane properties indicative of a slightly immature state, such as a larger R_m, a smaller C_m, more depolarized resting membrane potential, and broader and shorter action potentials **(Figure 2.12).** These results indicate that the regenerated pallium contained neurons of varying maturity, but a large number of regenerated neurons were able to acquire mature electrophysiological traits comparable to endogenous control neurons.

To determine whether the regenerated neurons received synaptic input, we recorded spontaneous postsynaptic currents (sPCSs). We found that all EdU^+, regenerated neurons in the

Figure 2.10: Neuronal diversity in the dorsal pallium is regenerated in post-metamorphic axolotl brain.

(a) Representative images of adult axolotls before and after L-thyroxine-induced metamorphosis. Left, pre-metamorphosis axolotl, inset shows the presence of a tail fin (left panel). Right, post-metamorphosis axolotl, inset shows the lack of a tail fin. Post-metamorphosis axolotls also lack external gills (red arrowhead). (b) Stereoscope images showing the injury sites of the post-metamorphosis axolotls (left hemisphere, red dotted rectangle) at 4wpi and 11wpi. (c) Representative immunohistochemistry images of coronal section show similar localization pattern of $BrdU^{+}/PH3^{+}/NeuN^{-}$ proliferating cells to that of the pre-metamorphosis axolotl in the dorsal pallium. (d) Regenerated cells labeled with BrdU colocalize with neuronal markers NeuN, Ctip2, Satb2, Tle4, and Calb2 as shown in representative injured coronal sections; insets, magnification of co-labeled nuclei (arrowheads). LP, Lateral Pallium; DP, Dorsal Pallium; MP, Medial Pallium; V, Ventricle. Scale Bars; 500 μm (c, top panels), 200 μm (c, bottom panels, d, top panels), 20 μm (d, bottom panels).

Figure 2.10 (Continued)

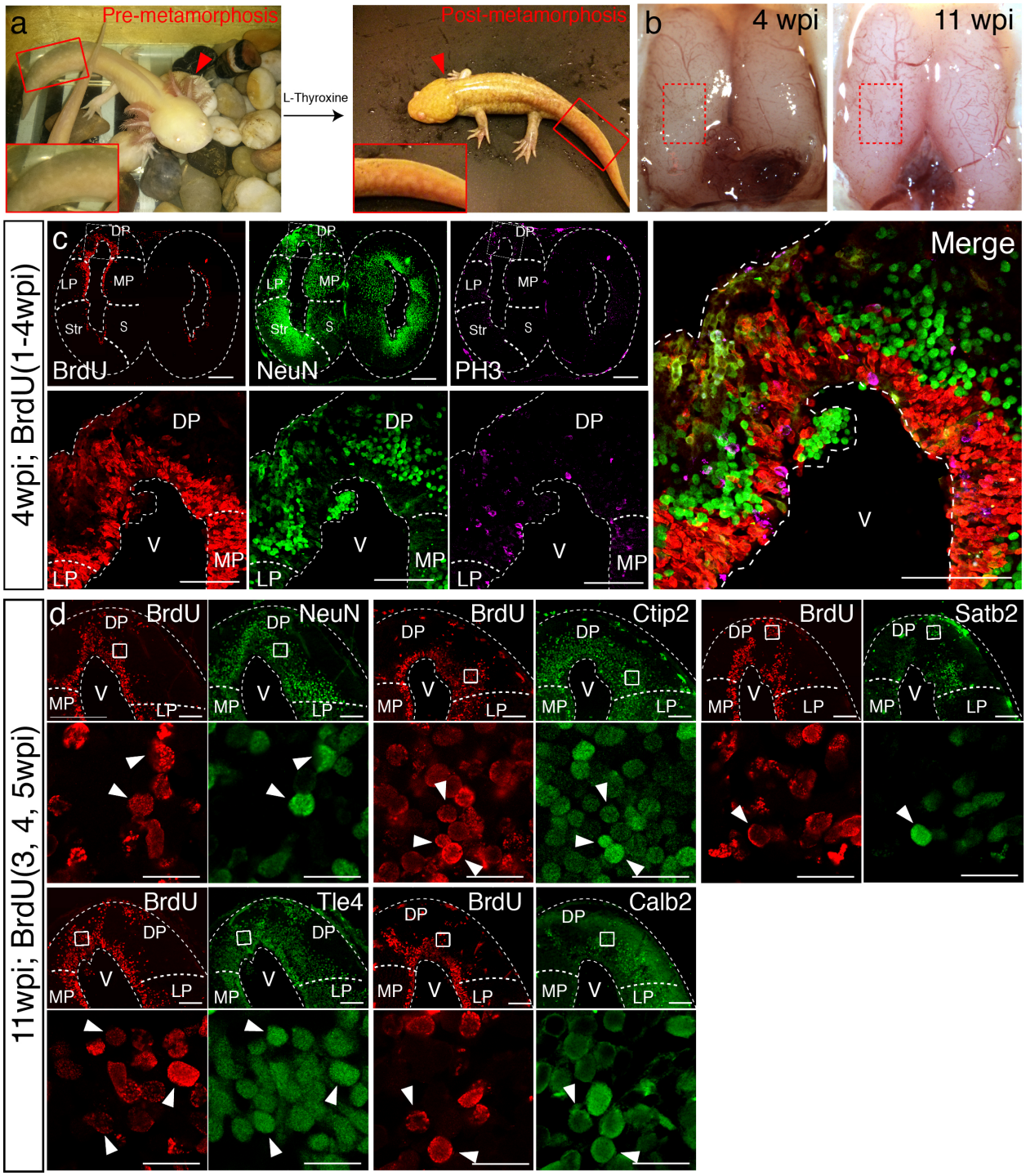

Figure 2.11. Regenerated neurons show electrophysiological features similar to uninjured pallium neurons and receive afferent input.

(a) Schematic representation of whole-cell patch clamp recording and subsequent biocytin filling. (b) Representative images of EdU^+/$Biocytin^+$ neurons in the injured pallium. (c) Representative traces of the membrane voltage changes in response to depolarizing and hyperpolarizing current steps injections of neurons from uninjured and injured animals. (d) Zoom-in of single action potential evoked by a depolarizing current step recorded in neurons of dorsal pallium. (e) Summary of passive and active electrophysiological properties: membrane capacitance (C_m), membrane resistance (R_m), resting membrane potential (RMP), action potential (AP) threshold, AP height and AP half width. (f) Sample traces of spontaneous postsynaptic currents (sPSCs) recorded under voltage clamp (Vh = −70 mV). (g) Summary of sPSCs features in neurons from uninjured and injured animals.

All results are expressed as the mean ± SD. * $p<0.05$; unpaired, two-tailed Student's t-test.

Figure 2.11 (Continued)

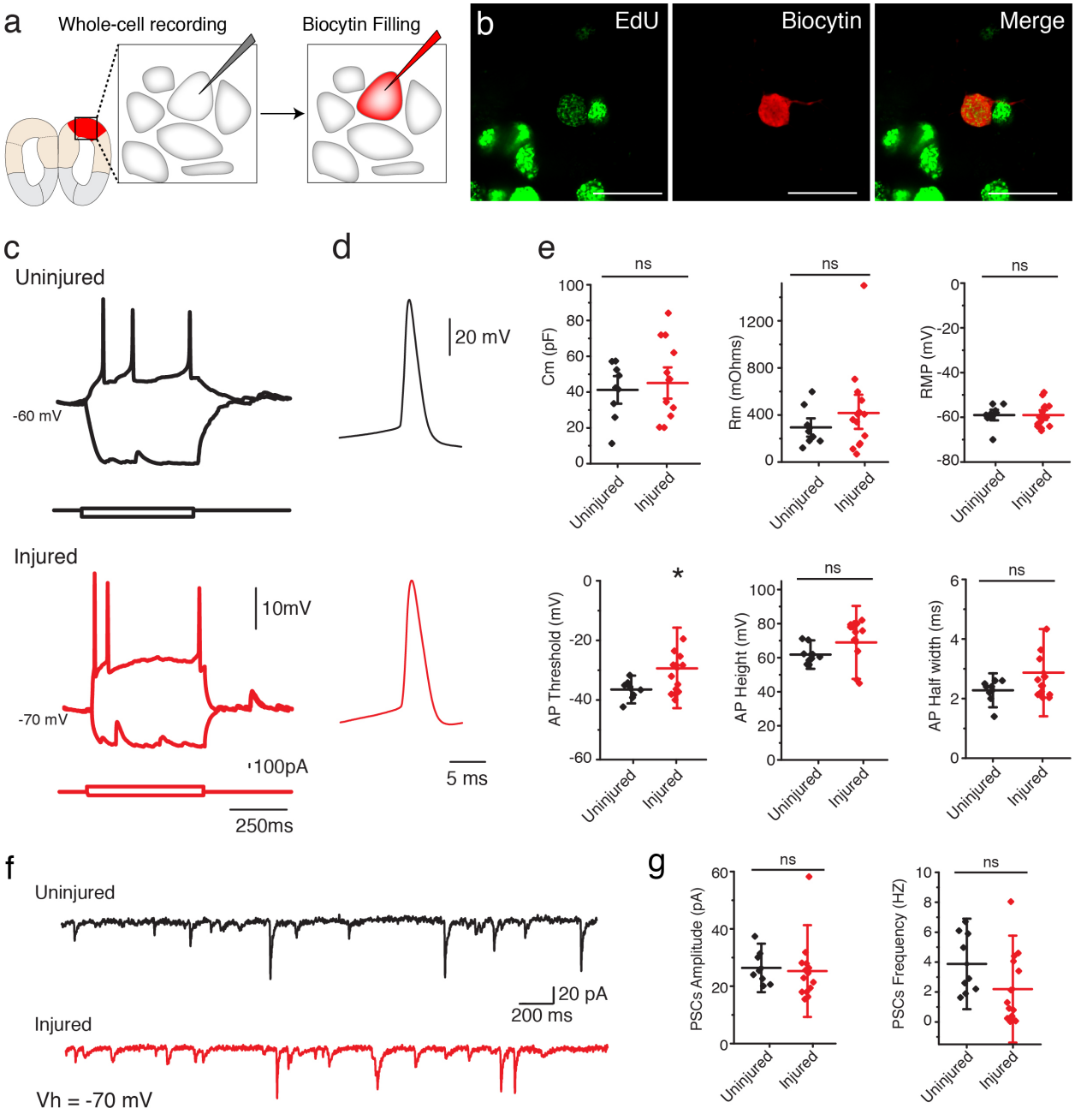

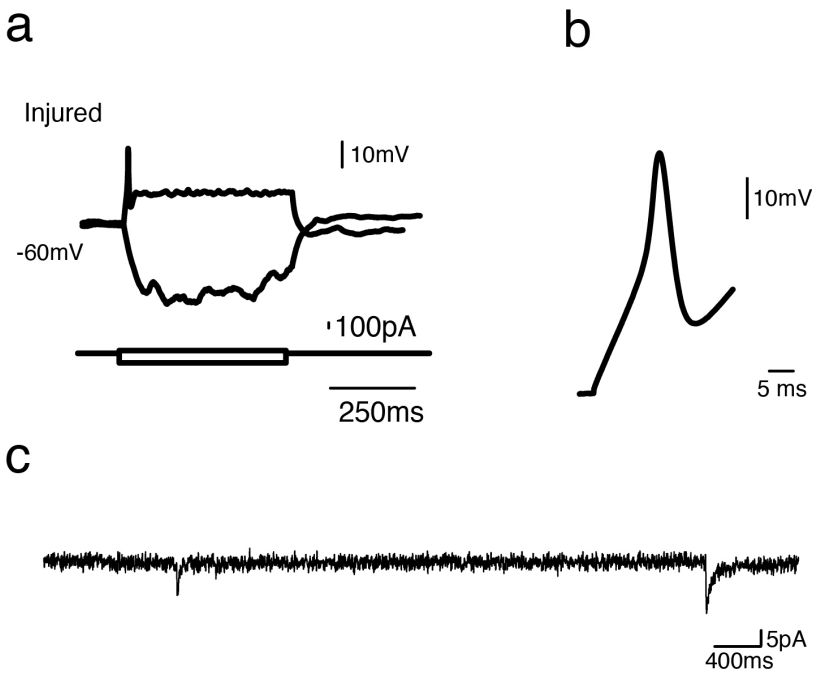

Figure 2.12: EdU$^+$ neurons in the injured pallium show immature electrophysiological properties.

(a) Changes of the membrane voltage in response to depolarizing and hyperpolarizing current steps injections from an EdU$^+$ neuron recorded in the injured pallium. (b) Zoom-in of single action potential evoked by a depolarizing current step. Broad and short action potential is typical of immature neurons. (c) Sample trace of spontaneous postsynaptic currents (sPSCs) recorded under voltage clamp (Vh=−70 mV).

injured pallium received postsynaptic currents **(Figure 2.11f)** and displayed no differences in postsynaptic response compared to control neurons in the uninjured pallium **(Figure 2.11g)**. Most of the spontaneous currents were blocked by the AMPA receptor antagonist, NBQX, suggesting that AMPA receptors were involved in the synaptic transmission **(Figure 2.13)**.

To understand the kinetics of large-scale neuronal activity, we performed *ex vivo* calcium imaging with single-cell resolution **(Figure 2.14)**. Measuring the key characteristics of spontaneously generated calcium transients, including the peak amplitude, rise time, and fall time, we detected no significant differences between uninjured (n=5 animals) and injured (11-15wpi; n=4 animals) dorsal pallium neurons **(Figure 2.14)**.

Together, these results indicate that the regenerated neurons are able to mature into electrophysiologically functional neurons and to receive and respond locally to afferent inputs from other neurons.

Original tissue architecture cannot be regenerated in the axolotl pallium

It is unclear whether, beyond generating the diversity of neuronal constituents, the original topography of neurons and fiber tracts in the pallium are also rebuilt upon injury, yet this may be required for proper pallial function.

To quantify the radial organization of neurons in regenerated pallium, we radially subdivided the dorsal pallium into three equally sized bins and quantified the number of $NeuN^+$ neurons in bin 3 (closest to pia) normalized to the area of each individual bin (disorganization index; DI). The sum of DI from four consecutive sections spanning the injury site was taken for each group. In uninjured animals, bin 3 is mostly populated by neuronal processes and does not contain cell bodies. In agreement, we found that virtually no $NeuN^+$ neurons are present within this bin in the contralateral and sham hemispheres. However, in the regenerated pallium at 11wpi, we consistently found neurons in bin 3 (Contra n=7 DI 19.46±3.272; Injured n=7 DI 212.4±65.85; Sham n=5 DI 22.95±8.508), indicating that the radial organization of neurons in the dorsal pallium

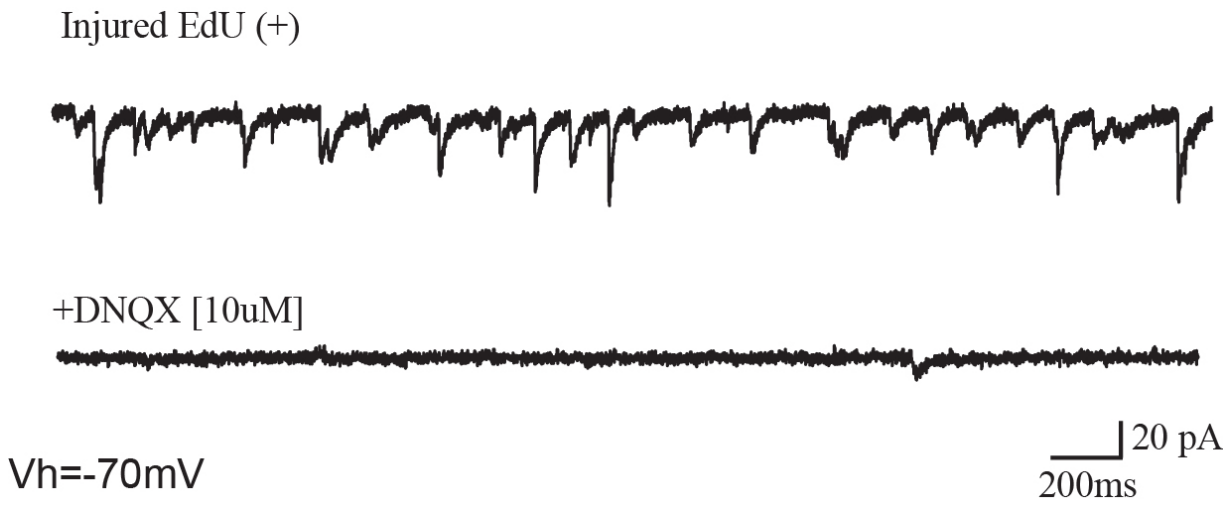

Figure 2.13: Most sPSCs are abolished by administration of AMPA receptor blocker.

(a) Sample trace of spontaneous postsynaptic currents (sPSCs) recorded under voltage clamp (Vh=−70 mV). (b) Sample trace of the same neuron after application of AMPA receptor blocker, NBQX [10μM], which abolishes most sPSCs.

Figure 2.14: Spontaneous calcium transients in neurons do not differ between injured and control dorsal pallium.

(a) Schematic of *ex vivo* calcium imaging. (b) Representative image of Fluo-4 staining in the dorsal pallium after dye loading (left panel). Region of interest (ROI) segmentation for individual neurons (middle panel) and merge (right panel). (c) Representative traces of spontaneously generated calcium transients in labeled neurons within dorsal pallium. (d) Raster plot of peaks in traces from panel c. (e) Quantification of the peak amplitude (left panel), rise time (middle panel), and fall time (right panel) in individual neurons shows no significant difference between injured and control dorsal pallium. V, ventricle.

All results are expressed as the mean ± SEM. Unpaired, two-tailed Student's t-test.

Figure 2.14 (Continued)

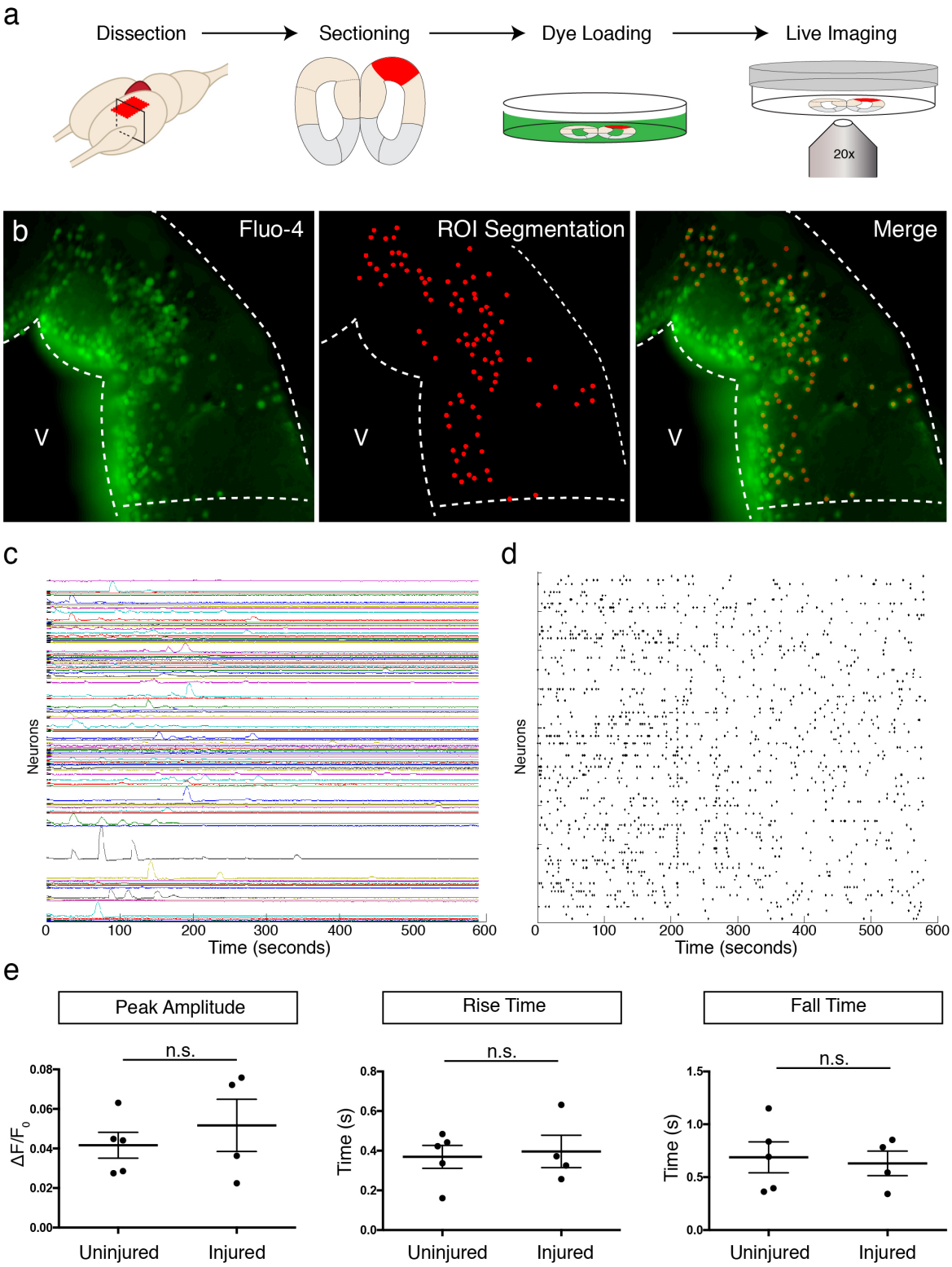

at 11wpi is disrupted compared to controls **(Figure 2.15a-b).** To confirm that the observed radial disorganization is not temporary, we performed the same analysis at 20wpi. Similar to the 11wpi time point, neurons were consistently positioned in bin 3 in the injured hemisphere, but not in the control (Contra n=5 DI 40.87±9.746; Injured n=5 DI 548.6±104.1) **(Figure 2.15a-b)**, indicating that neuronal disorganization remains present at 20wpi and is a stable feature of the regenerated pallium.

The data prompted the question of whether the topography of neuronal subtypes is disorganized in the regenerate. We thus performed immunohistochemistry for Ctip2, Satb2, Tle4, and Calb2 at 20wpi. We found that, while the uninjured contralateral hemisphere showed stereotyped organization, in which neuronal subtypes cluster within distinct domains **(Figure 2.15c, top panels)**, the dorsal pallium of the injured hemisphere contained neuronal subtypes localized outside of their stereotyped domains **(Figure 2.15c, bottom panels)**.

In agreement, immunohistochemistry for Tubb3 in the dorsal pallium of 11wpi contralateral, injured, and sham hemispheres showed that the injured pallium contained scattered neuronal processes that lacked the stereotypical, circumscribed organization along the pia seen in the uninjured pallium **(Figure 2.15d)**.

Taken together, these results indicate that the molecular diversity of neuronal subtypes is rebuilt within an altered pallial architecture.

Long-distance projections from the dorsal pallium to the olfactory bulb are reduced in the regenerated brain

Given the abnormal tissue architecture of the regenerated pallium, we sought to determine whether regenerated neurons are able to remake long-distance axonal projections to original targets. In amphibians, tracing studies have shown that neurons in the dorsal pallium project to the medial pallium (MP), lateral pallium (LP), and olfactory bulb (OB) (Neary, 1990; Northcutt and Kicliter, 1980; Westhoff and Roth, 2002). We selected OB-projecting neurons for further analysis

Figure 2.15: Tissue architecture is disrupted in the regenerated pallium

(a) The radial distribution of $NeuN^+$ cells within the dorsal pallium is altered after regeneration. Representative immunohistochemistry images of coronal sections of contralateral, injured, and sham hemispheres at 11wpi (left) and 20wpi (right). $NeuN^+$ neurons populate the bin closest to the pia (bin 3) in the injured hemispheres at both time points, in contrast to controls. (b) Quantification of the disorganization index in four consecutive sections of contralateral (11wpi and 20wpi), injured (11wpi and 20wpi), and sham (11wpi) hemispheres. (c) The topography of neuronal subtypes is altered upon regeneration. Representative immunohistochemistry images of coronal sections of contralateral (top panels) and injured (bottom panels) hemispheres at 20wpi. (d) Immunohistochemistry for Tubb3 shows atypical organization of neuronal processes in the 11wpi injured pallium compared to uninjured contralateral and sham controls. LP, Lateral Pallium; MP, Medial Pallium; V, Ventricle. Scale Bars; 400 μm (a), 50 μm (c-d).

All results are expressed as the mean ± SEM. * $p<0.05$, ** $p<0.01$; one-way ANOVA with post-hoc Tukey's multiple comparison test.

Figure 2.15 (Continued)

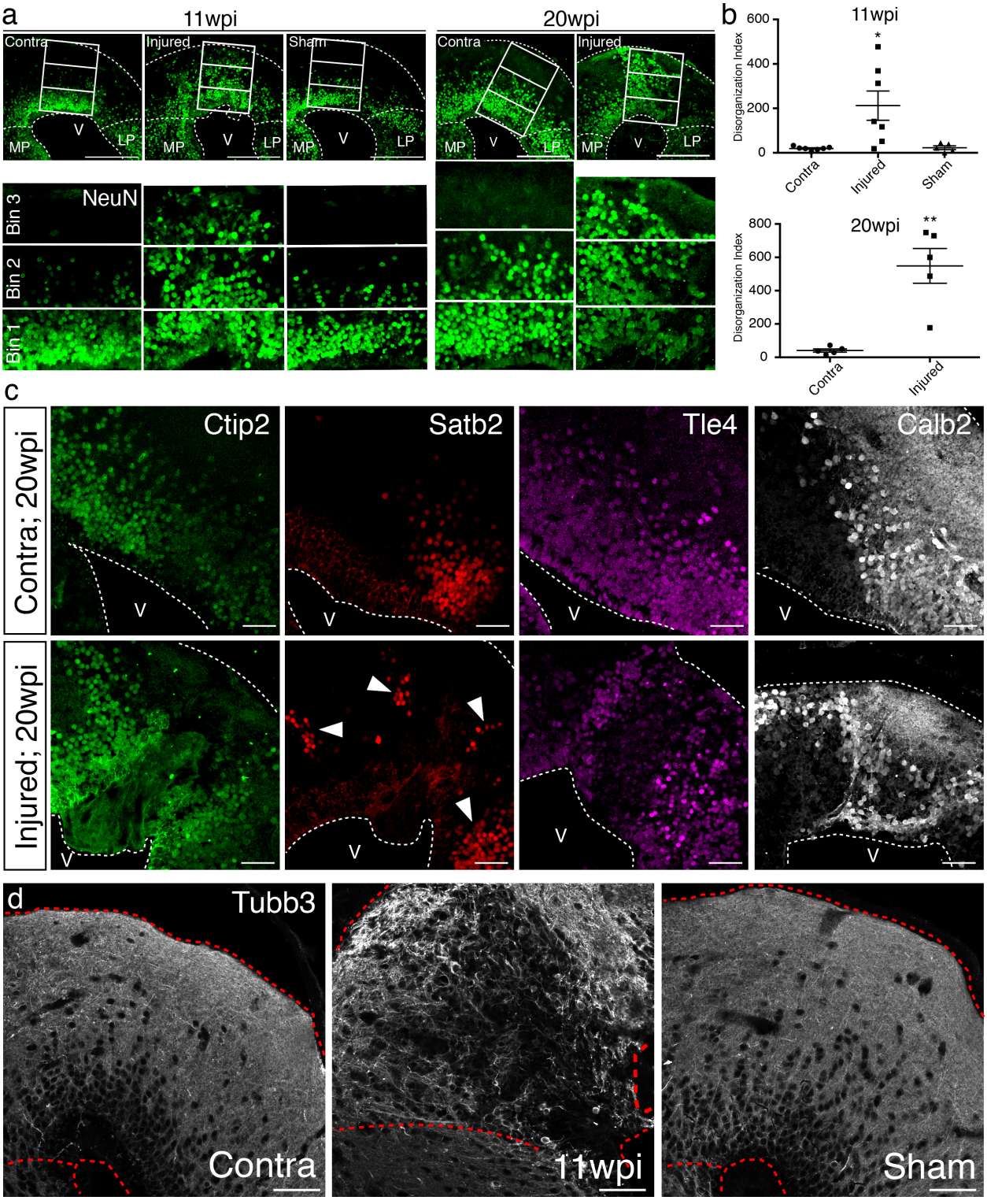

because their cell bodies (in DP) are distinctly separated from their axon targets (in OB). We injected red fluorescent microspheres (Retrobeads) in the OB of control, uninjured (n=5) and regenerated axolotls at both 11wpi (n=6) and 42wpi (n=3). All animals were sacrificed one week post-injection. In each sample, we quantified the total number of Retrobead$^+$ neurons present in the dorsal pallium, across four consecutive sections spanning the injury site. We found that a reduced number of neurons were retrogradely traced from the OB in the regenerated versus control axolotls (Uninjured n=5 81.60±13.90 neurons; 11wpi n=6 24.83±5.326 neurons; 42wpi n=3 19.33±2.603 neurons) **(Figure 2.16a-b)**. In agreement, anterograde tracing using lipophilic DiI revealed a reduction in the number of projections from labeled neurons in the dorsal pallium **(Figure 2.17)**.

Notably, regenerated BrdU$^+$/Retrobead$^+$ neurons accounted for only 10.2% and 6.6% of the total number of OB-projecting neurons located in the DP at 11wpi and 42wpi, respectively, suggesting that the majority of the axons extending from the regenerated pallium to the OB originate from pre-existing BrdU$^-$ neurons that were spared by the injury **(Figure 2.16c, arrowheads)**. Given that the number of Retrobead$^+$ neurons remains significantly reduced at 42wpi, it is unlikely that this is a matter of neuronal maturity or low speed of axon growth. Interestingly, we also found a reduction in the number of Retrobead$^+$ neurons in the lateral pallium, despite the fact that this region was not mechanically injured (Uninjured n=5 118.2±38.96 neurons; 11wpi n=6 21.83±4.629 neurons; 42wpi n=3 29.67±10.35 neurons) **(Figure 2.16a-b)**. However, this was not accompanied by disorganization of the lateral pallium at 11wpi, as detected by NeuN, Tle4, and *rorb* labeling **(Figure 2.18)**. Potential severance of the tract that connects the lateral pallium to the olfactory bulb during the dorsal pallium injury may account for this reduction. As expected, we found no significant difference between groups in the retrogradely labeled neurons that project to the olfactory bulb from the medial pallium **(Figure 2.16a** and **data not shown).**

Figure 2.16: Long-distance projections from the regenerated dorsal pallium are significantly reduced.

(a) Retrograde tracing from the olfactory bulb shows reduced number of labeled cells in the dorsal pallium and lateral pallium at 11wpi (middle panels) and 42wpi (right panels) compared to uninjured control (left panels). Insets, high-magnification images of DAPI (green) and Retrobeads (red). (b) Quantification of the number of $Retrobead^{+}$ cells in the dorsal and lateral pallium at different time points after injury. (c) Representative immunohistochemistry images of $BrdU^{+}$/$Retrobead^{+}$ cells in the regenerated dorsal pallium at 11wpi (left panel) and 42wpi (right panel). (d) *ex vivo* DTI of 11wpi brains show disruption of fiber tracts (arrowheads) in the injured hemisphere. White dotted lines (left panels) represent regions of interest in injured and contralateral hemispheres. OB, Olfactory Bulb; CP, Choroid Plexus; Th, Thalamus; V, Ventricle; DP, Dorsal Pallium; MP, Medial Pallium; LP, Lateral Pallium. Scale Bars; 50 μm (a), 20 μm (b).

All results are expressed as the mean ± SEM. * $p<0.05$, ** $p<0.01$; one-way ANOVA with post-hoc Tukey's multiple comparison test.

Figure 2.16 (Continued)

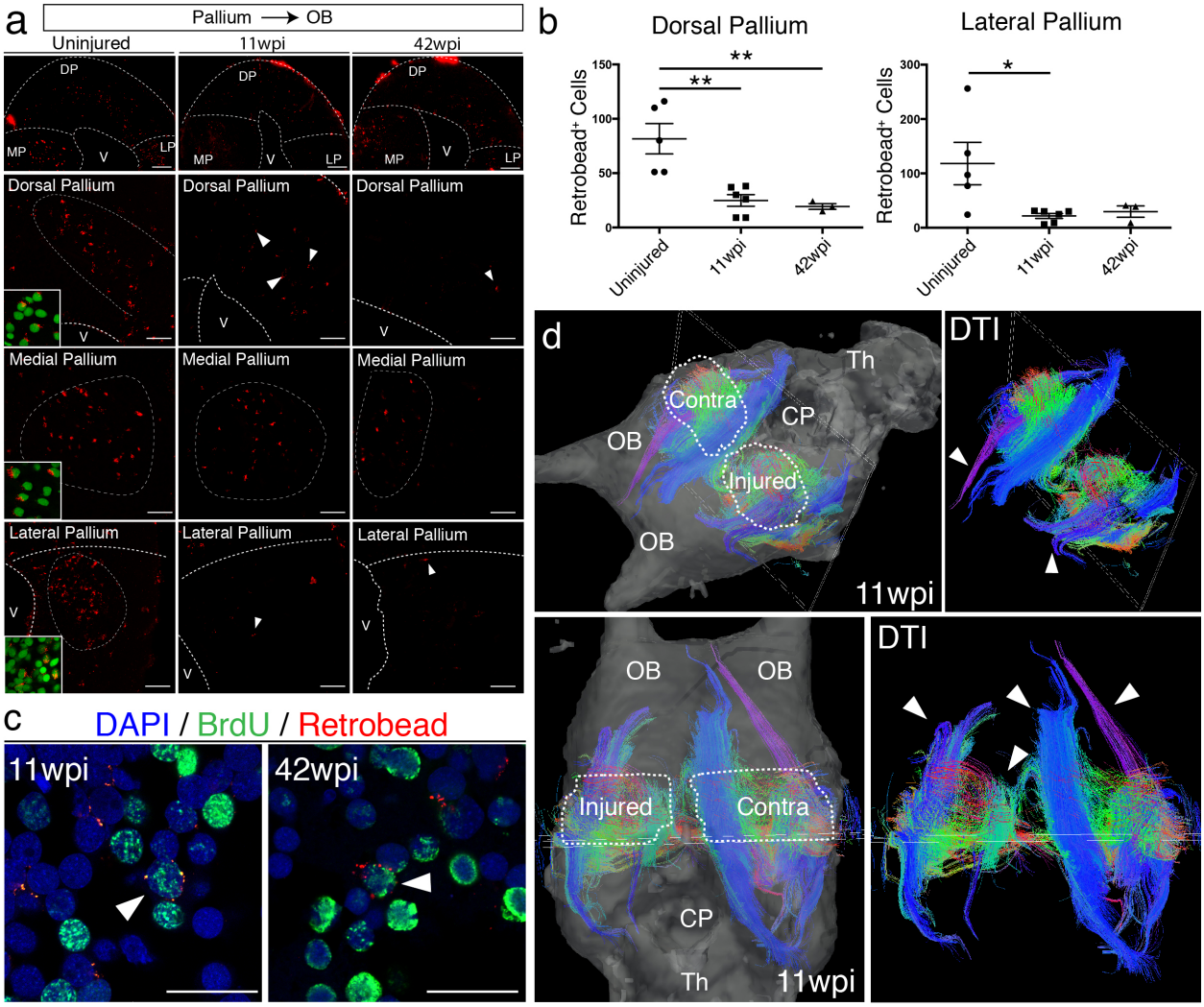

Figure 2.17: Neurons in the regenerated pallium do not extend axons to the olfactory bulb.

(a) Before and after images of the whole brain from the top with DiI crystal embedded into the left pallium. The left images are brightfield and the right images are fluorescence. (b) Schematic of the section in c. (c) The majority of the DiI signal is from the embedding site, which is the dorsal pallium. Insets: Higher magnification images show labeled projections in the olfactory bulb of the uninjured hemisphere, but not in the 20wpi hemisphere, indicating that the neurons in the dorsal pallium at 20wpi do not project their axons to the olfactory bulb. Scale bars; 500 μm (c, d, top panels), 20 μm (c, d, bottom panels).

Figure 2.17 (Continued)

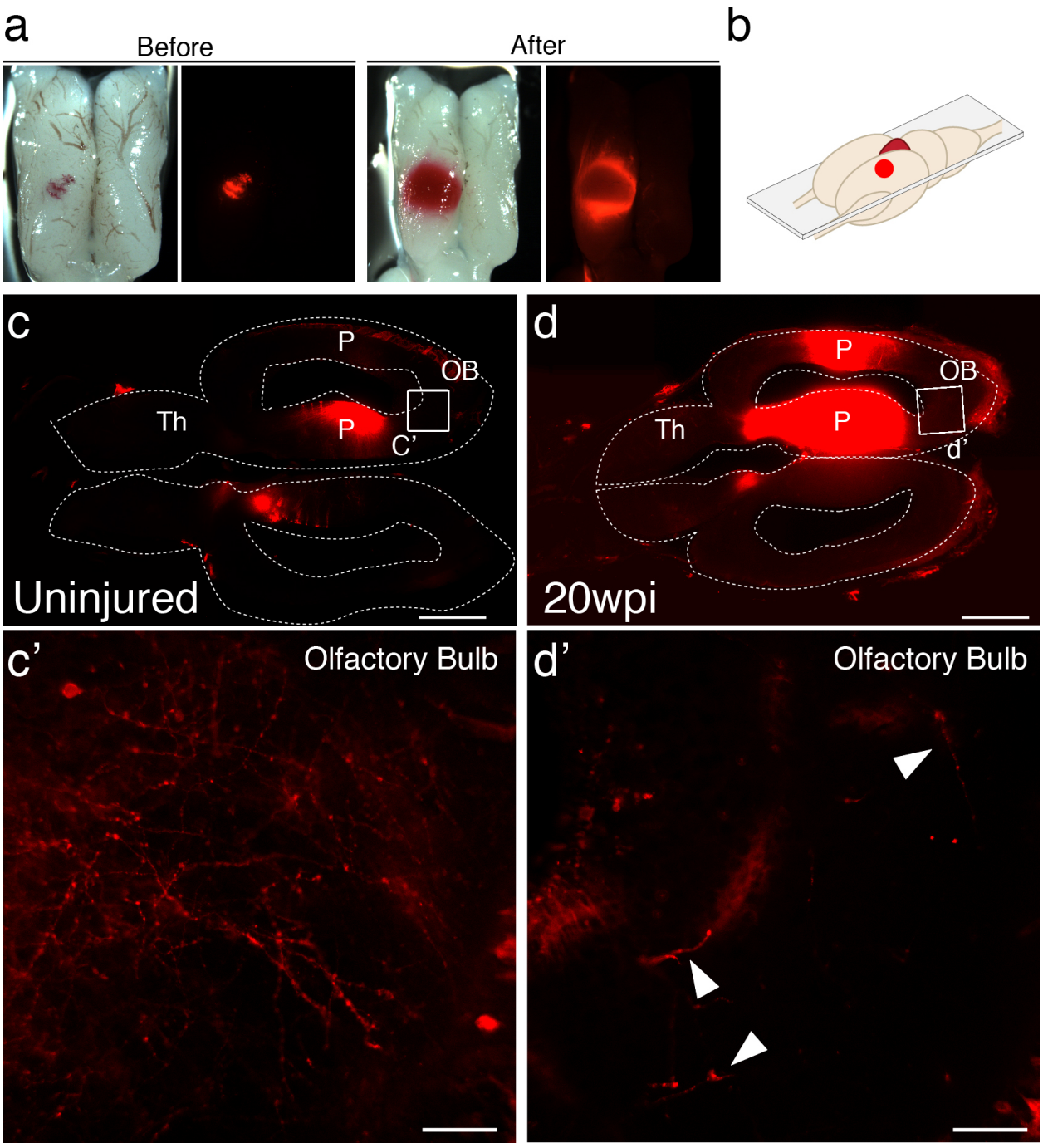

Figure 2.18: The neuronal topography of the lateral pallium is not disorganized.

(a) Representative immunohistochemistry images of the lateral pallium from contralateral, injured (11wpi), and sham brains, labeled for NeuN (top panels) and Tle4 (bottom panels). (b) Representative in situ hybridization images of *rorb* on 11wpi injured, contralateral, and uninjured lateral pallium sections. LP, Lateral Pallium; V, Ventricle. Scale Bars; 50 μm (a), 200 μm (b).

Figure 2.18 (Continued)

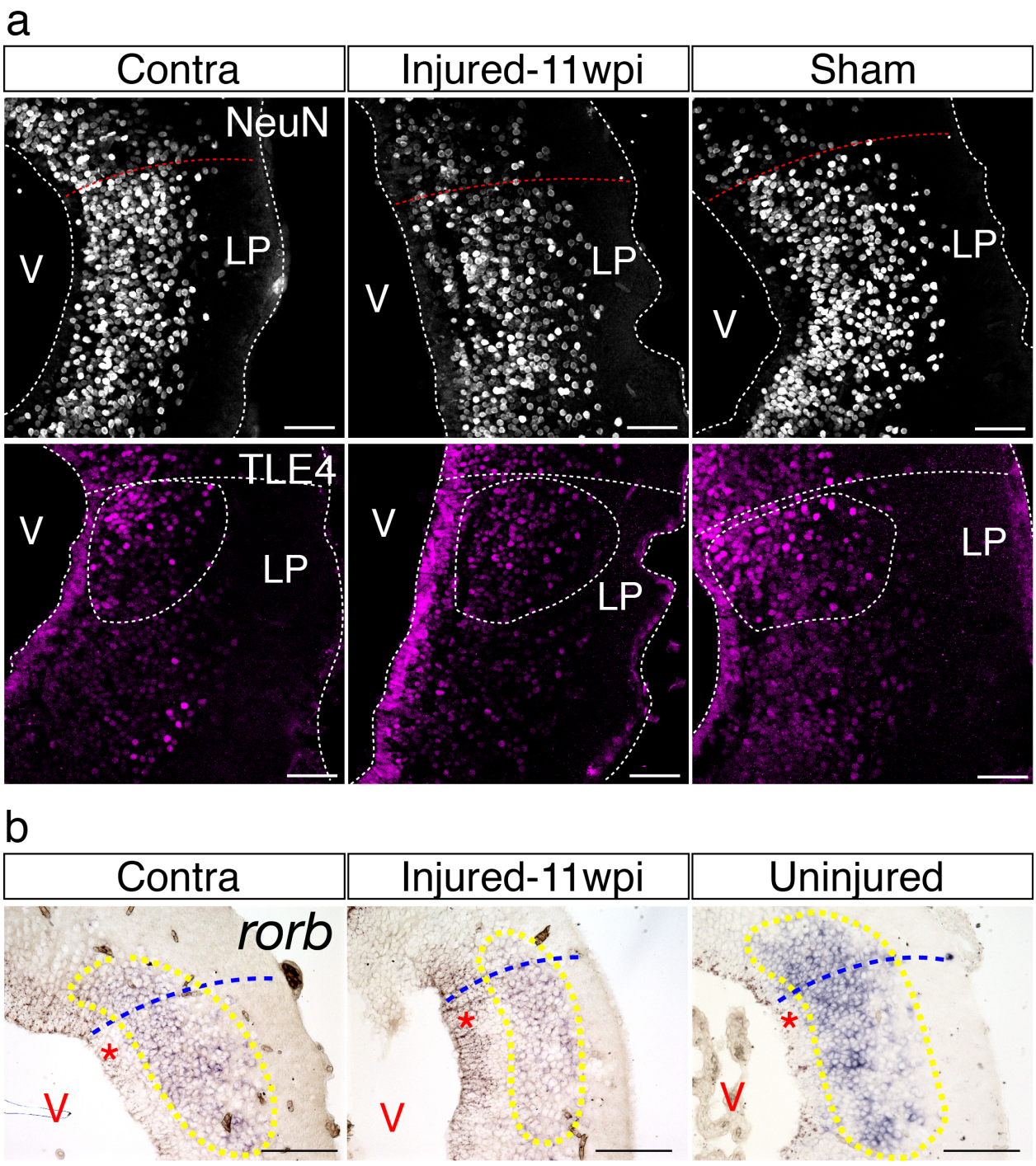

To further investigate the failure of regenerated neurons to regenerate long-distance projections, we imaged the axon bundles connecting the pallium to the olfactory bulb using diffusion tensor imaging (DTI) in both control and regenerated animals at 11wpi (n=2). In agreement with our retrograde tracing results, magnetic resonance tractography revealed distinct three-dimensional fiber tracts connecting the pallium and the olfactory bulb in the control, contralateral hemisphere. In striking contrast, we observed significant truncation of the same bundles in the regenerated hemisphere **(Figure 2.16d, arrowheads)**. These results show that regeneration of the pallium does not remake long-distance projections present in the original brain.

While it is unclear why the regenerated axons cannot project to their correct targets, it is known that, in mammals, myelin associated inhibitors of axon regeneration play a role (Baldwin and Giger, 2015). To determine whether the axolotl pallium is myelinated, a sagittal section of the axolotl brain was immunostained with MBP. To our surprise, we found that the pallium is completely unmyelinated while the axons in the anterior commissure, thalamus, optic tectum, and spinal cord were all myelinated **(Figure 2.19)**. Therefore, it is unlikely that myelin associated inhibitors are responsible for the failure of correct axonal projection in the axolotl.

To investigate whether regenerated neurons could excite physiological targets that were more closely located, we stimulated the dorsal pallium and performed extracellular field recordings in the lateral and medial pallium. We used *ex vivo* brain slices of uninjured and injured (11-15wpi) axolotls **(Figure 2.20a-b)**. We found that, in both DP-to-LP and DP-to-MP connections, the amplitude of the pre-synaptic fiber volley (a measure of the number of axons being activated by an electrical stimulus; Negative Peak 1 or NP1) was significantly reduced in the injured pallium compared to controls (DP-to-LP: Uninjured n=5 animals; Injured n=3 animals; DP-to-MP: Uninjured n=4 animals; Injured n=3 animals) **(Figure 2.20c-d)**, indicating that the activity of presynaptic axons is altered upon regeneration due to a change in number or firing properties of axons. In accordance, we also observed that the field population spike (fEPSP) of both LP and

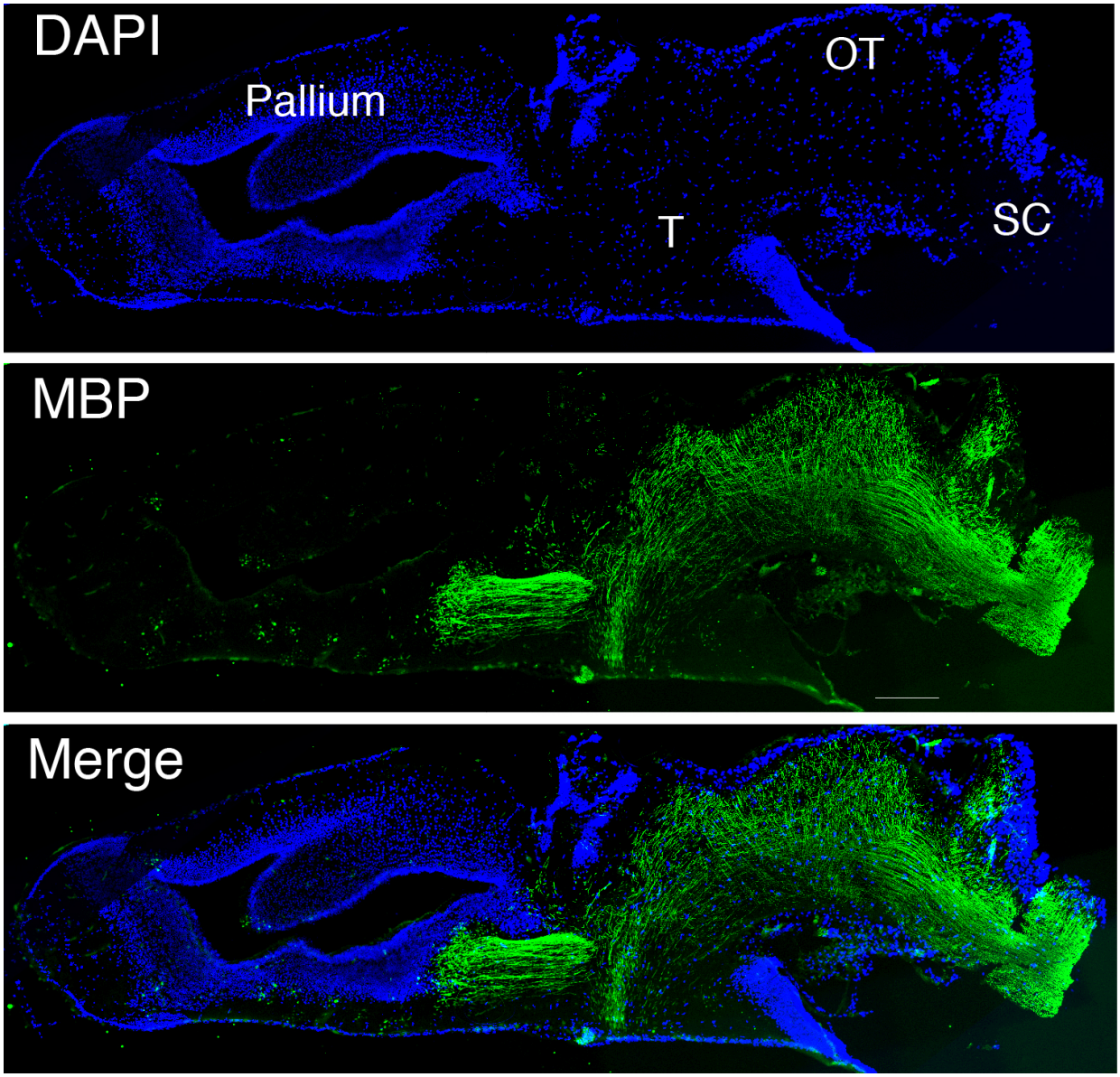

Figure 2.19 The axolotl pallium lacks myelination.

MBP staining reveals the lack of myelination in the pallium. In contrast, the fibers of the anterior commissure, thalamus, optic tectum, and spinal cord are myelinated. T, Thalamus; OT, Optic Tectum; SC, Spinal Cord.

Figure 2.20: Reduced activation of medial and lateral pallium by regenerated neurons in the dorsal pallium.

(a) Schematic of tissue preparation for slice electrophysiology. (b) Schematic of experimental details showing the location of the stimulation (DP) and the field recording (MP and LP). (c) Dorsal-lateral NP1 and field pop spike amplitude is decreased in injured pallium (n=15 slices; black circles) compared to control pallium (n=15 slices; white circles) as measured by extracellular field recordings. Inset, representative traces for uninjured and injured pallium recordings. (d) Dorsal-medial NP1 and field pop spike amplitude is decreased in injured pallium (n=9 slices; black circles) compared to control pallium (n=9 slices; white circles) as measured by extracellular field recordings. DP, Dorsal Pallium; LP, Lateral Pallium; MP, Medial Pallium; V, Ventricle.

All results are expressed as the mean ± SEM. ** $p<0.005$, *** $p<0.001$; Two-way ANOVA repeated measures with Bonferroni post hoc test.

Figure 2.20 (Continued)

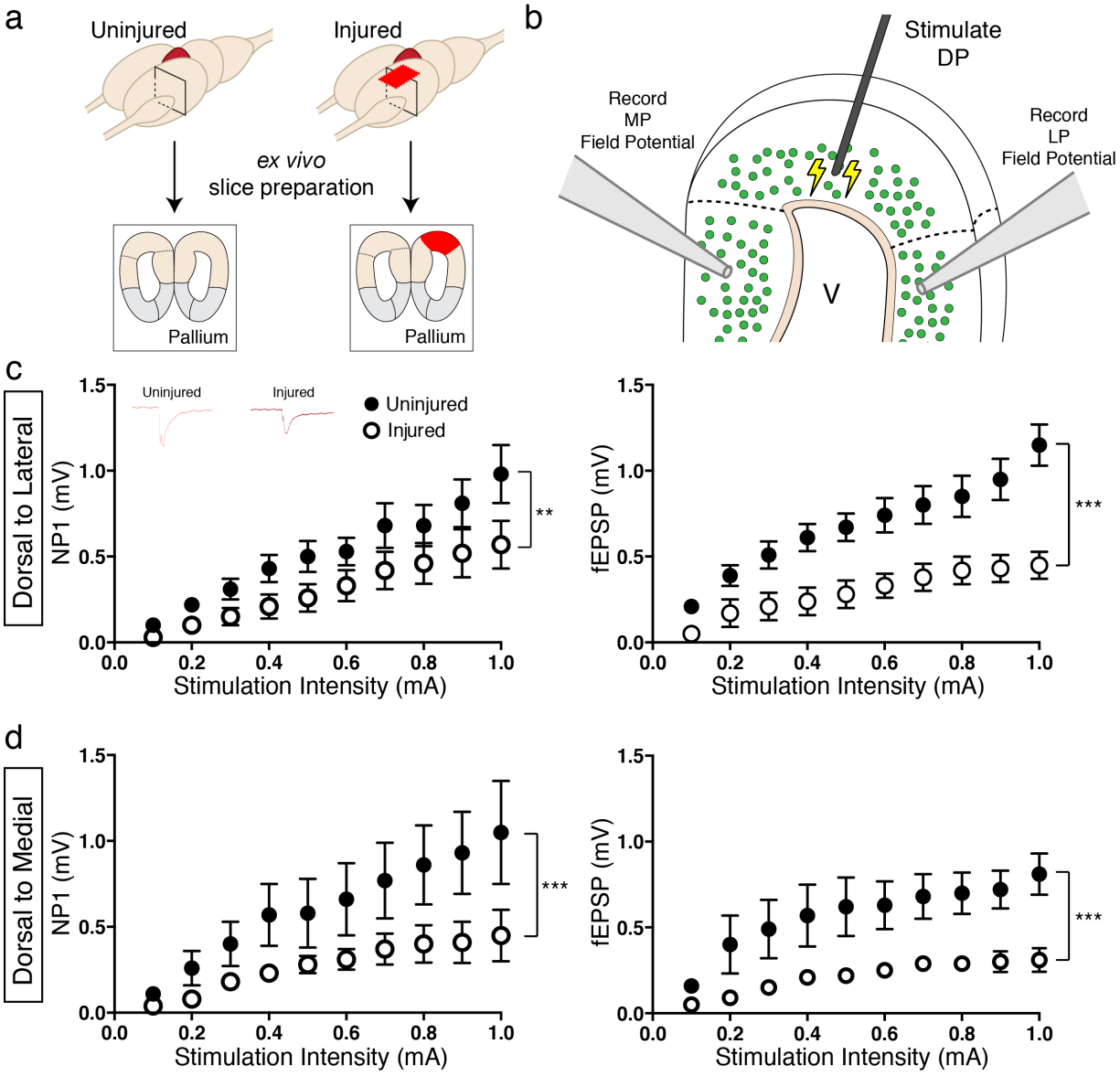

MP was significantly decreased in injured axolotls compared to controls upon dorsal pallium stimulation **(Figure 2.20c-d)**, indicating that the MP and LP are not functionally activated to the same extent in the regenerated brain versus controls.

The data indicate that despite the striking ability of axolotl to regenerate a diversity of neuronal subtypes that are electrophysiologically mature and receive local afferent inputs, newborn neurons cannot rebuild long-distance circuit, as was previously assumed. This demonstrates an unknown obstacle to functional brain repair even in a highly regenerative species.

Discussion

The function of the mammalian brain relies on the processing power of an outstanding diversity of neuronal subtypes, which are integrated into distinct networks necessary for the execution of specific functions. One central goal of regenerative medicine in the CNS is therefore to rebuild not only the original heterogeneity of neurons but also their specific patterns of connectivity within the endogenous tissue.

Prior work suggested that the axolotl might be a good model to understand the mechanisms of complete CNS regeneration because of its capacity to grossly regenerate large portions of the brain when mechanically injured (Burr, 1916; Kirsche and Kirsche, 1964b; Maden et al., 2013; Winkelmann and Winkelmann, 1970). However, it remains unclear to what extent brain regeneration in the axolotl leads to reformation of functional tissue.

Here, we found that, upon a large mechanical injury to the pallium, the adult axolotl can regenerate the original neuronal diversity. Notably, newborn neurons acquire intrinsic electrophysiological properties and process afferent input in a manner that is indistinguishable from the endogenous neurons in uninjured brains. It is also interesting that this capacity is not lost after metamorphosis, challenging the theory that, in this species, regeneration is partly linked to the maintenance of a paedomorphic state in adulthood (Kirsche et al., 1965). These results

indicate that, beyond instructing the birth of new neurons, the adult axolotl brain is capable of regenerating a diversity of neurons that in turn are electrophysiologically functional, even when a large region of the brain is removed.

An outstanding question in the field of brain regeneration remains whether, beyond rebuilding cellular complexity and local connectivity, new connections to distant targets can be restored upon brain regeneration. It is similarly unknown whether tissue architecture and neuronal topography can be regenerated. We found that axolotls possess only limited capacity to rebuild original tissue architecture after large deletions of the pallium. In addition, we uncovered an unexpected limitation to the capacity of newborn neurons to extend axons to original targets in distal brain regions. It is possible that the observed limitations relate to a lack of instructive signals from the environment rather than intrinsic limitations of the regenerated neurons. For example, in order to reach the OB, newborn neurons of the pallium will have to extend axons through uninjured territory that may lack developmental ligands necessary for axon guidance to the OB.

The processes and mechanisms that initially trigger wound closure and subsequently sustain brain repair in regenerative vertebrate species are not known. Using *in vivo* MRI, we were able to observe, for the first time, the dynamic changes in tissue morphology that occur in live animals over the course of brain regeneration. We found that early steps of wound closure involve the generation of thinner processes from a stump that directionally grow towards each other before fusing. This strategy resembles that observed in the limb, in which closure of the wound by the wound epithelium after amputation is necessary for subsequent regenerative steps and may serve as a source of signals to govern downstream regenerative events (Mescher, 1976; Thornton, 1957). It is possible that, much like the limb, morphogenetic movements act as a signaling event to trigger cellular proliferation and accumulation of newborn, differentiated cells at the site of injury. In support of this possibility, we did not observe major waves of neuronal migration from regions adjacent to the injury site, and the topography of neurons in these regions remains properly organized upon regeneration. In the future, it will be interesting to determine the

cellular source of the newborn neurons. Activated ependymoglia cells are one of the major sources of injury-induced newborn neurons in the newt and zebrafish (Berg et al., 2010; Kroehne et al., 2011), and these cells may similarly be the main origin of newborn neurons in the axolotl pallium. An alternative, yet not exclusive, possibility is that reprogramming of endogenous differentiated cells may contribute to the generation of new neurons. Such reprogramming events were reported, for example, in the zebrafish retina, where Mueller glia appears capable of generating new neurons upon retinal injury (Bernardos et al., 2007; Fausett and Goldman, 2006; Ramachandran et al., 2010; Thummel et al., 2008).

Together, our findings establish the axolotl pallium as a model to further investigate how diverse populations of electrophysiologically functional neurons are mechanistically regenerated. In addition, the results highlight previously unappreciated limits for what vertebrates are able to achieve when faced with the need to regenerate the most complex tissues. This should help define concrete goals and expectations for cellular replacement outcomes in the central nervous system of mammals.

Chapter 3

Identification of Brain Regeneration-Induced Gene Expression Changes

Introduction

Stroke and brain injury remain two of the leading causes of disability in the world (Coronado et al., 2011; Ovbiagele and Nguyen-Huynh, 2011). While modest axonal sprouting occurs in the neocortex in mouse and primate models of stroke and brain injury, strategies to induce neurogenesis in the neocortex could also contribute to functional regeneration. However, the adult mammalian brain is severely limited in its ability to generate new neurons. In the uninjured mammalian brain, neurogenesis is restricted to two niches. Neural stem cells of the subventricular zone (SVZ) give rise to interneurons of the olfactory bulb while those in the subgranular zone differentiate into granular cells of the dentate gyrus (Bond et al., 2015). In both cases, these newborn neurons integrate into pre-existing, mature circuits, indicating that, even in the mammalian brain, adult neural circuits could incorporate new neurons. During homeostasis, it is believed that other regions of the mammalian brain do not generate new neurons.

Upon focal ischemia, limited regeneration of different cell types is observed in the striatum and the neocortex. NSCs of the SVZ exhibit increased rate of proliferation, and some neuroblasts, normally destined to the olfactory bulb, migrate towards other regions of the brain (Carlén et al., 2009; Faiz et al., 2015; Gu et al., 2000; Jiang et al., 2001; Kernie and Parent, 2010; Kreuzberg et al., 2010; Leker et al., 2007; Liu et al., 2009; Magnusson et al., 2014). Newly generated medium spiny neurons in the striatum survive long-term and form synapses with neighboring neurons (Hou et al., 2008; Yamashita et al., 2006). In contrast, most newborn neurons in the mouse neocortex fail to survive and integrate into the circuitry. The surviving cells from the SVZ that have migrated into the neocortex differentiate into astrocytes (Carlén et al., 2009; Faiz et al., 2015), and the evidence for regeneration of cortical neurons is controversial. In accordance, carbon dating of human cortical neurons from postmortem stroke-affected tissue revealed that the human neocortex does not contain new neurons upon ischemia (Huttner et al., 2014).

In murine models of traumatic brain injury to the neocortex, NSCs of the SVZ also display increased rate of proliferation (Chang et al., 2016; Chirumamilla et al., 2002; Goings et al., 2004;

Goodus et al., 2014; Ramaswamy et al., 2005; Saha et al., 2013). Much like in ischemia models, some neuroblasts from the SVZ migrate towards the injury site via chemoattracts such as SDF-1 (Goings et al., 2004; Saha et al., 2013). In the neocortex, most progenitors differentiate into glia, and it remains controversial whether mature neurons are generated in the neocortex.

These findings reveal that NSCs in the SVZ respond to injury by proliferating and differentiating, but the neuroblasts that have migrated into the neocortex do not survive nor do they generate the cortical neuronal diversity that has been lost by the injury. Molecular intervention by factors such as FGF2 and EGF has shown some success to increase proliferation rate after brain injury (Saha et al., 2012). Application of exogenous factors could drive existing NSCs to 1) differentiate into the correct neuronal populations, 2) survive long-term, and 3) integrate into the pre-existing circuitry. Finding molecular targets to enhance these properties of NSCs is challenging. One plausible method is to elucidate the molecular mechanisms underlying neurogenesis in the olfactory bulb and hippocampus, two normally neurogenic regions. Another complementary approach is to study the mechanism of brain regeneration in organisms that are naturally endowed with superior regenerative capacities such as the zebrafish and salamanders.

As described in Chapter 2, the axolotl brain is able to regenerate the correct neuronal populations, which mature into electrophysiologically functional neurons and receive afferent inputs (Amamoto et al., 2016). However, the molecular mechanism of this regenerative process is unknown. Previously, transcriptional analysis of the telencephalon and midbrain ventricular cells in the zebrafish and newt, respectively, has identified key genes and signaling pathways that are critical for neurogenesis in regenerative species (Berg et al., 2010; Berg et al., 2011; Kizil et al., 2012a; Kizil et al., 2012c; Kyritsis et al., 2012). For example, *gata3* is upregulated in the radial glia cells in the zebrafish telencephalon upon stab injury, and knockdown of *gata3* leads to reduced proliferation and subsequent neurogenesis (Kizil et al., 2012c). In the newt, inhibition of Sonic Hedgehog signaling by cyclopamine significantly reduces the number of regenerating midbrain dopaminergic neurons upon specific ablation of dopaminergic neurons (Berg et al.,

2010). These pioneering studies laid the groundwork to start understanding the molecular mechanism of brain regeneration.

Here, we sought to determine which genes are up- and downregulated during the regenerating process in the previously-defined axolotl injury model. We dissected out the axolotl telencephalon at 1, 2, and 4wpi, and performed RNA-sequencing to identify differentially expressed genes. We found that at 1wpi, immune-related molecules were significantly upregulated. At 2 and 4wpi, we found an enrichment of genes related to cell cycle regulation and retinoic acid signaling, which are two key components of vertebrate brain development. However, because whole brains, instead of specific cell types, were collected for analysis at each time point, the data generated considerable noise. In the future, it will be necessary to develop tools to isolate specific cell types from organisms that are difficult to genetically engineer. Additionally, we asked whether the molecular players involved in one regenerative organ may play a role in the regeneration of another organ. We found that select limb regeneration markers were prominently expressed in the brain during regeneration, suggesting that some molecular mechanisms may be shared between organs.

Results

Whole-brain transcriptome during regeneration are highly similar among time points

To quantify gene expression changes during axolotl brain regeneration, we identified differentially expressed genes using RNA sequencing. As described in Chapter 2, a portion of the dorsal pallium of the left hemisphere was stereotactically excised by a microknife. We previously determined three key time points in the first four weeks: at 1wpi, the wound and blood were clearly visible, at 2wpi, the wound edges have smoothened and the blood has cleared away, and at 4wpi, the wound has closed and proliferation of ependymoglia cells have begun. The RNA was collected from all cells of the pallium and subpallium at 1, 2, and 4wpi as well as the uninjured contralateral hemisphere at 1wpi (n=3 for each time point) **(Figure 3.1)**.

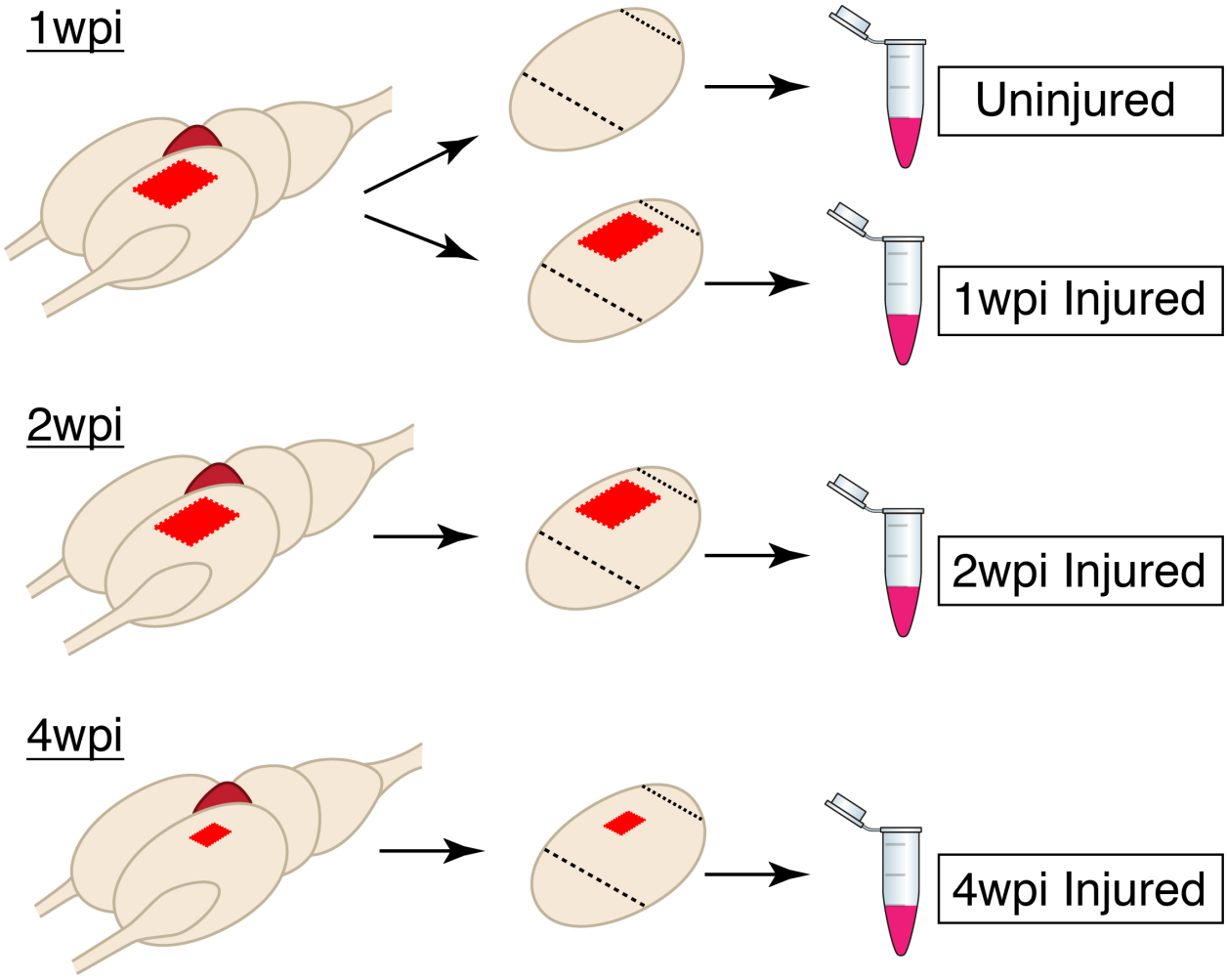

Figure 3.1: Experimental design for transcriptional profiling the axolotl brain during first four weeks of regeneration.

Fresh brains were harvested at 1, 2, and 4wpi (n=3 for each time point). For the 1wpi brains, both the contralateral and injured hemispheres were collected, and the contralateral 1wpi hemisphere was denoted as uninjured. From each hemisphere, the regions between the olfactory bulb and caudal telencephalon were extracted (as represented by the black dotted lines). The tissue was subsequently homogenized in Trizol and the RNA was extracted. wpi, weeks post injury.

We estimated the transcript counts from all samples and found high correlation between biological replicates and between conditions (average Pearson correlation between all samples = 0.86). In accordance, unbiased hierarchical clustering of all transcripts separated the 2wpi and 4wpi conditions from the uninjured and 1wpi conditions, but the distance separating each condition was minimal **(Figure 3.2)**. It is possible that the injury does not elicit a major transcriptional response. Alternatively, it is likely that only select cell types respond to the injury, such as the ependymoglia cells. By sampling the whole pallium and subpallium, we were not able to detect many of the subtle gene expression changes from these select cells.

Genes involved in immune activation, cell cycle regulation, and retinoic acid signaling are enriched in differentially expressed transcripts

Despite the high correlation between conditions, we asked whether there were differentially expressed (DE) transcripts between conditions. Out of 73,108 transcripts with more than one transcript expressed in any of the samples, 192 transcripts were differentially expressed (adjusted *p-value* <0.05). We analyzed the top 30 transcripts differentially induced during the first four weeks of brain regeneration **(Figure 3.3)**. Seven out of 30 transcripts did not share sequences with any of the protein sequences from any organism in the UniRef90 database. Interestingly, out of the 23 annotated transcripts, many have known functions in immune response and cell cycle regulation **(Figure 3.3; immune genes in red, cell cycle genes in blue)**. In particular, we observed an upregulation of *cxcl12* (also known as SDF-1), which, in the mammalian brain, is induced after brain injury and functions as a neuroblast and angioblast chemotaxis factor (Filippo et al., 2013; Kokovay et al., 2010; Robin et al., 2006; Saha et al., 2013; Stumm and Höllt, 2007; Stumm et al., 2003). We also found an upregulation of *toll-like receptor 5* (*tlr5*), which is expressed highly during cerebral ischemia in mouse models and is critical for immune cell activation (Wang et al., 2011). Of genes that are implicated in cell cycle control, we observed a downregulation of *host cell factor c1* (*hcfc1*), which has been shown to promote cell

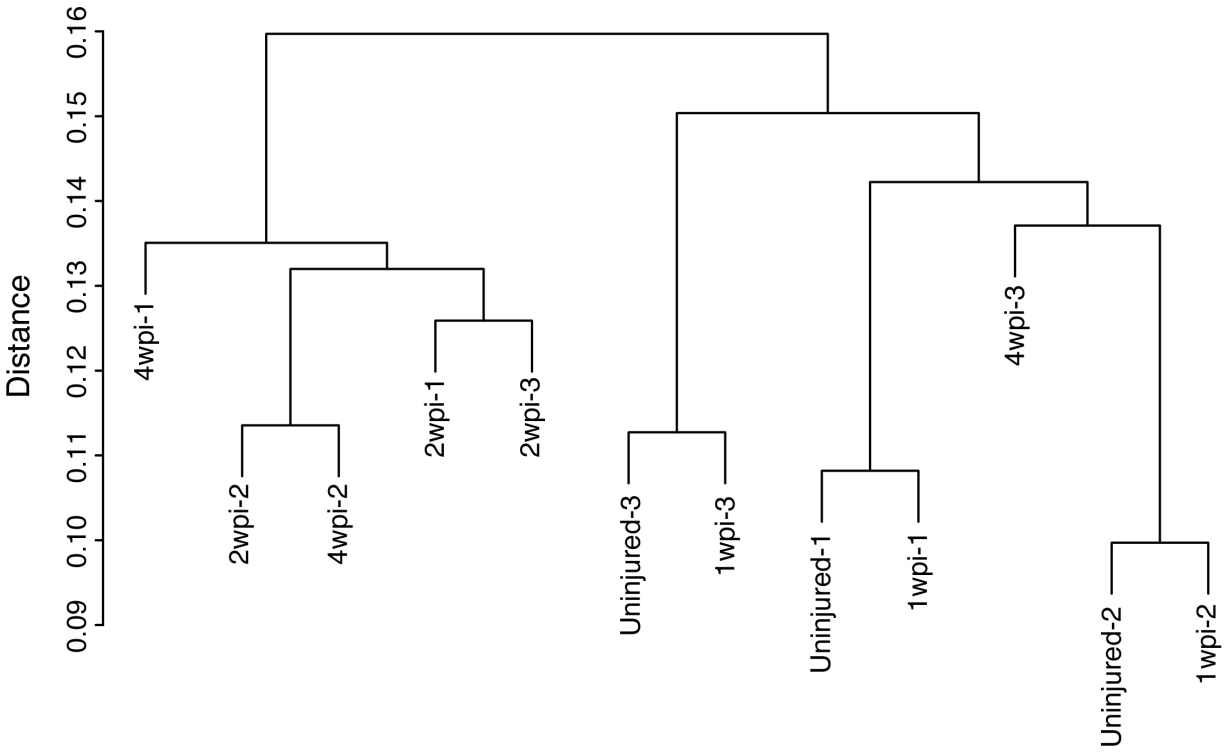

Figure 3.2: Uninjured and 1wpi cluster from 2wpi and 4wpi, but over short distance.

Unbiased hierarchical clustering revealed that 2wpi and 4wpi samples are more similar to each other than uninjured and 1wpi samples. Note the distance (as determined by 1-correlation), indicating the similarity between samples and conditions.

Figure 3.3: Top 30 differentially expressed transcripts include immune-related genes, cell cycle genes, and retinoic acid pathway genes.

192 out of 73,108 transcripts were differentially expressed between conditions. The top 30 DE transcripts are displayed. Transcripts that did not make the cutoff ($E<10^{-3}$) by BLASTX do not have an associated gene name. Four immune-related genes (*tnfsf10, colec12, cxcl12, tlr5*), four cell cycle genes (*hcfc1, nuf2a, plk1, cenpf*), and 2 retinoic acid signaling pathway genes (*aldh1a2, rai1*) were among the differentially expressed genes.

Figure 3.3 (Continued)

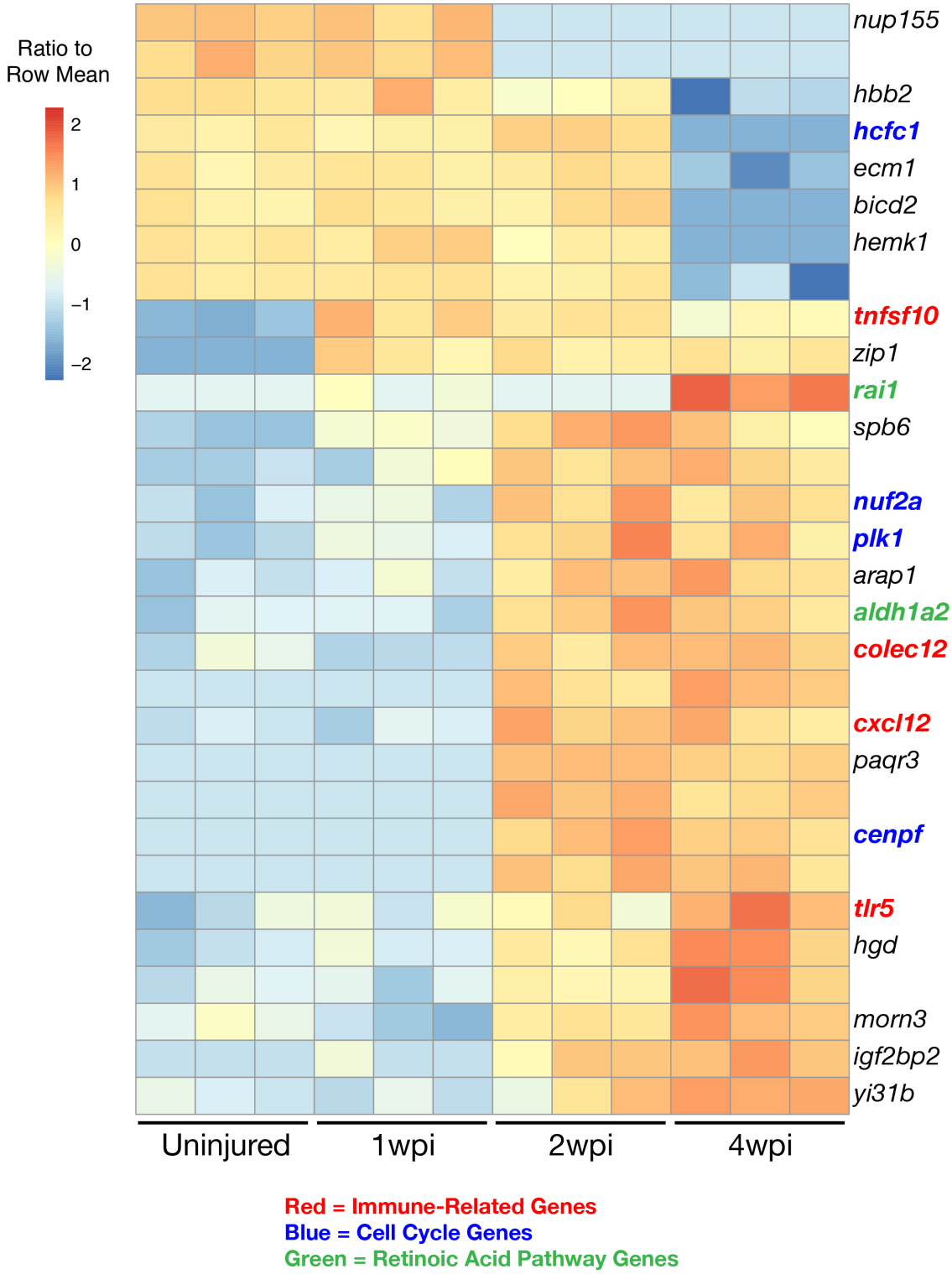

Red = Immune-Related Genes
Blue = Cell Cycle Genes
Green = Retinoic Acid Pathway Genes

cycle exit in neural stem cells *in vitro* (Huang et al., 2012). We also detected an upregulation of *centromere protein f* (*cenpf*), a well-characterized marker of G2 phase during cellular proliferation. In accordance with our histological data in Chapter 2, these results suggest that activation of immune system and cellular proliferation are two key components during the first four weeks of brain regeneration in the axolotl.

Interestingly, we also found an upregulation of *aldehyde dehydrogenase 1 family member a2* (*aldh1a2*) and *retinoic acid induced 1* (*rai1*) at 4wpi **(Figure 3.3)**. *aldh1a2* is the enzyme that catalyzes the synthesis of retinoic acid (RA) (Zhao et al., 1996), which has critical roles in neuronal differentiation and patterning (Aoto et al., 2008; Denisenko-Nehrbass et al., 2000; Maden, 2007; Wong et al., 2006). *aldh1a2* is upregulated upon spinal cord contusion in the mouse (Zhelyaznik et al., 2003), and in the peripheral nervous system, RA signaling positively regulates neurite outgrowth (Wong et al., 2006). *rai1* is a transcriptional regulator that is upregulated during RA-induced neuronal differentiation *in vitro* (Imai et al., 1995), and loss of *rai1* function leads to motor and learning deficits in mice *in vivo* (Huang et al., 2016). This result suggests a role for RA signaling during brain regeneration in the axolotl.

Limb blastema markers are expressed in the regenerating brain

Another approach to determine the key regulators of brain regeneration is to analyze the gene expression patterns between two diverse regenerating systems. The axolotl is known to regenerate the limb, tail, spinal cord, and the heart. Among these, the gene expression changes during regeneration of the limb are well characterized (Bryant et al., 2017; Campbell et al., 2011; Gorsic et al., 2008; Holman et al., 2012; Monaghan et al., 2012; Stewart et al., 2013; Wu et al., 2013), and several markers of limb blastema have been identified, some of which are necessary for proper regeneration. We sought to determine whether limb blastema markers are also expressed in the proliferating ependymoglia cells during brain regeneration. For this purpose, we performed *in situ* hybridization against three limb blastema markers that have been recently

identified, *cirbp, ptma,* and *kazald1*, in the 4wpi brain, a time point at which a pool of $BrdU^+$ proliferative cells populate the injured region (Bryant et al., 2017). Interestingly, all three genes were upregulated in the injured region compared to the contralateral, uninjured hemisphere **(Figure 3.4)**. These results suggest that some transcriptional programs may be shared between the brain and limb during regeneration.

Discussion

In the United States alone, nearly 5.3 million people live with a disability related to traumatic brain injury (TBI) (Coronado et al., 2011). To compound, stroke affects nearly 800,000 people in the United States each year (Ovbiagele and Nguyen-Huynh, 2011). Over the last couple of decades, incidence of stroke in developed nations has slightly decreased, but this decrease may be due to better understanding of vascular health. Treating the human brain after damage remains a challenge, given the limited ability for generation of new neurons at the injury site. In particular, impairment in the neocortex is truly debilitating as this is the region of the human brain that is crucial for critical thinking, sensory perception, and fine motor movement. It is also the region of the brain that exhibits no neurogenesis in the adult mammalian brain.

Among vertebrates, fish, amphibians, and reptiles exhibit neurogenesis in the pallium during homeostasis (Amamoto et al., 2016; Baumgart et al., 2012; Font et al., 1997; Font et al., 1991; Kirkham et al., 2014; Kroehne et al., 2011; Maden et al., 2013; Molowny et al., 1995; Skaggs et al., 2014). Mice, however, generate new neurons only in two regions of the brain: the olfactory bulb and hippocampus (Bond et al., 2015). In addition, carbon dating of the adult human brain has revealed a novel neurogenic niche in the striatum (Ernst et al., 2014). Nevertheless, there is no evidence to indicate that new neurons populate the neocortex in the uninjured mammalian brain. Upon injury or ischemia, neuroblasts migrate to the injury site in the cortex, but fail to survive, differentiate, and integrate in the existing cortical circuit (Arvidsson et al., 2002; Gu et al., 2000; Jiang et al., 2001; Jin et al., 2006; Kernie and Parent, 2010; Kreuzberg et al., 2010; Leker

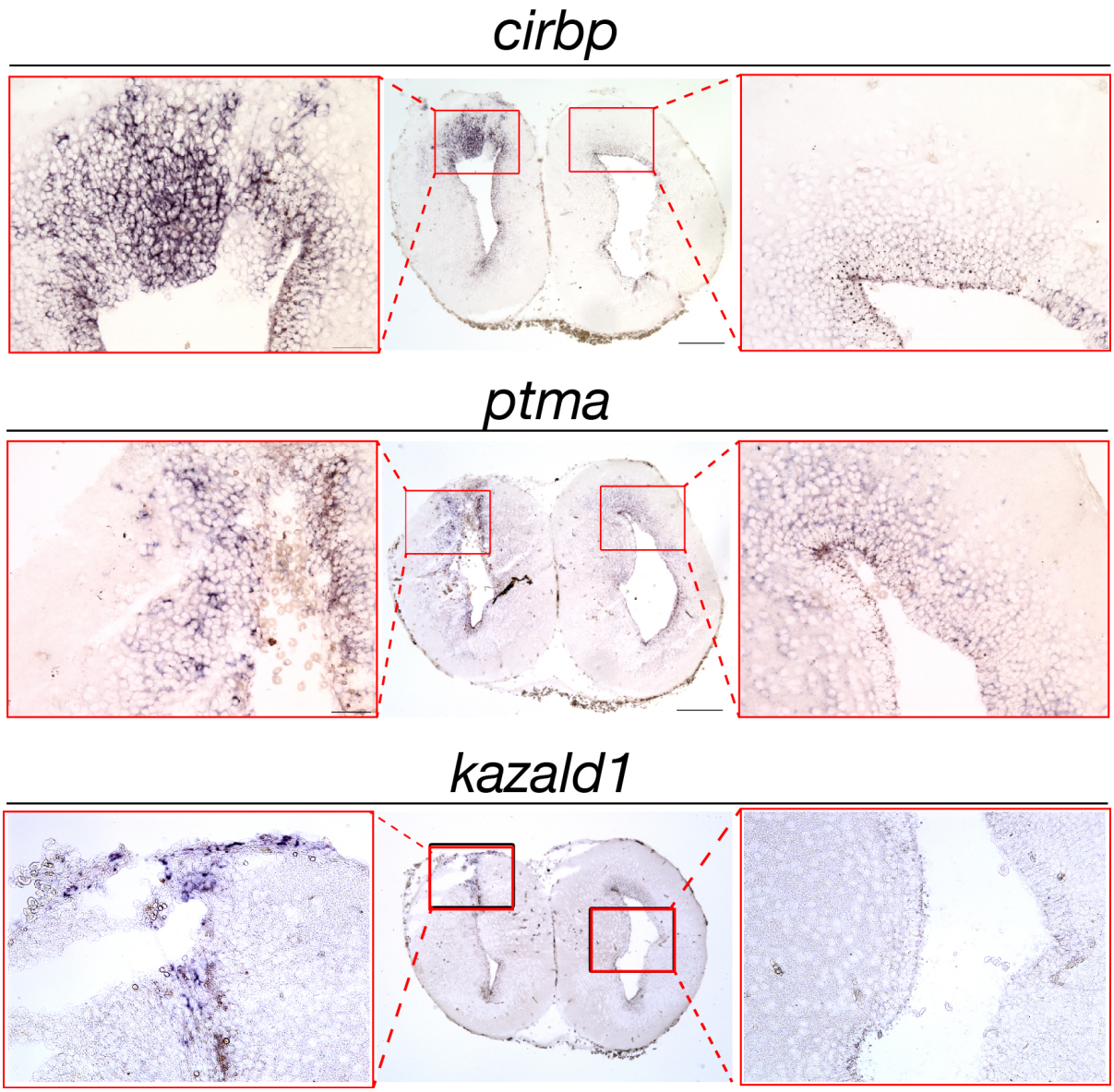

Figure 3.4: Injured dorsal pallium upregulates limb blastema markers.

Representative *in situ* hybridization of three limb blastema markers, *cirbp, ptma,* and *kazald1* on 4wpi coronal sections. At this time point, proliferation of ependymoglia cells is evident at the injury site (the left hemisphere here). Insets, high magnification images of the injured (left panel) and uninjured contralateral (right panel) dorsal pallium. All probes show specific staining at the injury site compared to the uninjured hemisphere. Scale bars; 500 μm (middle panels), 100 μm (left and right panels).

et al., 2007; Liu et al., 2009; Magnusson et al., 2014; Ohira et al., 2010). These results suggest that 1) there exists a population of neural stem cells that can be activated upon injury, and 2) these cells require exogenous factors to facilitate proper functioning within the neocortex. Identifying such key factors has proven challenging, despite the availability of excellent animal models.

Animal models of TBI and stroke represent the human conditions. As a common model of TBI, fluid percussion injury (FPI) induces a fluid pressure pulse against the dura to generate a deformation of the brain, mostly in the neocortex (Xiong et al., 2013). Controlled cortical impact (CCI) injury model uses a mechanical force against the dura to induce cortical tissue damage. To model stroke, middle cerebral artery occlusion (MCAO) is often used to create an infarct in the neocortex and striatum (Fluri et al., 2015). These models recapitulate the wide-ranging damage from TBI and stroke, affecting numerous cell types and structures. Yet, it is difficult to fully elucidate the molecular mechanisms governing neuroblast differentiation, survival, and integration when the animal models are inept at these tasks. One approach to identify the transcriptional programs that mediate each of these processes is to study regenerative non-mammalian vertebrates such as fish, amphibians, and reptiles. As discussed in Chapter 2, the axolotl can regenerate the neuronal diversity in the pallium with fidelity, and these neurons survive long-term and electrophysiologically mature. These traits make it an attractive model to delve deeper into the molecular mechanisms underlying the process of brain regeneration.

Here, transcriptional profiling at various time points (1, 2, and 4wpi) during the regenerative process revealed a small set of differentially expressed genes (192 out of 73108 transcripts). These numbers likely undermine the cell type-specific transcriptional changes because the whole tissue was profiled. In the injured mammalian brain, the cell types that react to damage are the neural stem cells, astrocytes, and immune cells, and contribution from neurons is minimal (Arvidsson et al., 2002; Carlén et al., 2009; Faiz et al., 2015; Liu et al., 2009). In the axolotl brain, considering that most of the cells in the pallium are neurons, the majority of the cells

sampled may not have exerted a major transcriptional induction. In the future, it will be important to profile the transcriptional program of specific cell populations or single cells. Despite the expanding repertoire of genetic and viral methods of cell labeling in the axolotl (Whited et al., 2012; Whited et al., 2013), these approaches are either time-consuming or limited in cell type specificity. A novel, quick technology for cell purification is necessary for organisms such as the axolotl, and our attempt to develop such a technology is described in the Appendix.

Despite the low number of DE transcripts, we discovered three sets of genes within the top 30 DE genes that were intriguing. As expected from our histological data from Chapter 2, we found an upregulation of cell cycle inducers (*nuf2a, plk1,* and *cenpf*) and a downregulation of a cell cycle inhibitor (*hcfc1*). Both *nuf2a* and *cenpf* are genes associated with the centromere (Hori et al., 2003), and *cenpf* is a well-known marker for the G2 phase of the cell cycle. Previously, we observed that wound closure precedes ependymoglia proliferation, an event that occurs between 2wpi and 4wpi. In the RNA-seq data, already at 2wpi, cell cycle regulators (*nuf2a, plk1,* and *cenpf*) are upregulated, suggesting that the molecular program for cell division is already in place at 2wpi.

Furthermore, genes associated with the immune system were upregulated during regeneration (*tlr5, cxcl12, colec12,* and *tnfsf10*). Both in the zebrafish and newt, activation of the immune system accompanies brain regeneration (Kirkham et al., 2011; Kyritsis et al., 2012). In particular, administration of an anti-inflammatory drug, dexamethasone, upon stab injury in the zebrafish pallium decreases the proliferative response by the radial glia cells (Kyritsis et al., 2012). Moreover, ablation of macrophages in the axolotl limb impairs regeneration by affecting the initial stages of blastema formation (Godwin et al., 2013). These results highlight the crucial role of the immune system during regeneration, and it is possible that in the axolotl brain, recruitment and activation of immune cells play a role during regeneration. However, in the mammalian brain, it is becoming more apparent that immune cells like microglia and immune-related molecules are crucial for proper circuit formation (Huh et al., 2000; Schafer et al., 2012; Stevens et al., 2007;

Syken et al., 2006). For example, microglia and astrocytes mediate synapse pruning in a complement-dependent and independent manner, respectively, in the developing mouse dorsal lateral geniculate nucleus (Chung et al., 2013; Schafer et al., 2012). Therefore, during brain regeneration in the axolotl, in which new neurons need to integrate into the pre-existing circuitry, immune cells and molecules may be required not just for initiation of the proliferative response, but also proper local circuit formation.

Among the induced immune-related genes, *cxcl12* (more commonly known as SDF-1) is well-characterized for its effect on neuroblast migration during development and injury (Filippo et al., 2013; Kokovay et al., 2010; Robin et al., 2006; Saha et al., 2013; Stumm and Höllt, 2007; Stumm et al., 2003). SDF-1 is a ligand that binds CXCR4, and it has been shown to regulate the migration of interneurons to the neocortex (Stumm et al., 2003). In both stroke and TBI models, SDF-1 is upregulated at the injury site and is necessary and sufficient to attract neuroblasts from the SVZ expressing CXCR4. In our axolotl brain injury model, we have shown that the majority of the newborn neurons populate the injured regions, although a small number of newborn neurons are generated at distant regions as well. These results indicate that the neurons generated from the ependymoglia cells migrate specifically towards the injury site, and upregulation of genes such as *cxcl12* may contribute to the homing ability of these newly generated neurons.

We also found a set of genes associated with retinoic acid (*aldh1a2* and *rai1*) within our top 30 DE transcripts. *aldh1a2* catalyzes the synthesis of RA (Zhao et al., 1996), which has been implicated in neuronal development and synaptic function in the mammalian brain (Maden, 2007). For example, in the developing mouse spinal cord, blocking retinoic acid signaling leads to failure of lateral motor column neuron differentiation while exogenously activating retinoic acid signaling blocks thoracic motor column neuron differentiation (Sockanathan et al., 2003). Upon injury to the mouse spinal cord or sciatic nerve, components of the retinoic acid signaling pathway are transcriptionally induced. Overexpression of retinoic acid receptor β2 in dorsal root ganglion neurons promote neurite outgrowth both *in vitro* and *in vivo* (Wong et al., 2006). In the axolotl, the

retinoic acid signaling pathway is well-studied for its role in proximodistal patterning during limb regeneration (Maden and Hind, 2003). While the function of retinoic acid signaling in the axolotl brain is not well understood currently, it is possible that this signaling pathway mediates the differentiation of neuroblasts into proper neuronal subtypes in the pallium. Alternatively, retinoic acid signaling may be required to promote axon and dendrite outgrowth and synapse formation. In accordance, *retinoic acid induced 1* (*rai1*), which is also upregulated at 4wpi, has been shown to be a transcriptional activator for genes involved in circuit assembly such as *Cdh7, Epha7,* and *Pcdh20* (Huang et al., 2016). Future studies could address the function of these differentially expressed transcripts by morpholino knockdown or *in vivo* CRISPR, both of which have been successfully applied in the axolotl (Fei et al., 2014; Flowers et al., 2014; Schnapp et al., 2005).

Development of various organs is mediated by shared signaling pathways such as the Wnt and Shh pathways. Similarly, regeneration of different organs may share transcriptional programs that promote or inhibit regeneration. The zebrafish heart and fin are two well-studied models for regeneration, and both systems upregulate *leptin b* (*lepb*) upon injury (Kang et al., 2016). Interestingly, the enhancer element of *lepb* could drive expression in both organs, but the proximal enhancer fragment is specific for the heart while the distal enhancer fragment is specific for the fin. Similarly, *gata3* expression is induced in the zebrafish brain, fin, and heart during injury to each of these organs (Kizil et al., 2012c). In both the brain and fin, *gata3* is necessary for initiation of proliferation, indicating that, for some cellular processes that are commonly shared between organs such as proliferation, similar genes and pathways may be involved. In the axolotl, the limb is the most well-characterized molecularly, and many blastema-specific genes have been identified using microarrays and RNA-seq (Bryant et al., 2017; Campbell et al., 2011; Gorsic et al., 2008; Habermann et al., 2004; Holman et al., 2012; Monaghan et al., 2012; Stewart et al., 2013; Wu et al., 2013). We found an induction of recently-identified blastema markers, *cirbp, kazald1,* and *ptma* (Bryant et al., 2017), within the injured pallium at 4wpi. While the function of these genes in the brain is unknown, they represent another set of genes that could mediate

proper brain regeneration in the axolotl. For example, *cirbp* in the axolotl limb shows an anti-apoptotic function during regeneration. Considering that one of the major differences between axolotl and mammalian brain regeneration is the survival of neuroblasts, this gene may be an ideal candidate for further testing.

The molecular mechanisms underlying various regenerative processes are beginning to be elucidated, and promising candidates could show efficacy in promoting mammalian brain regeneration in the future. For brain injuries, the prevalence of stroke and TBI remains high, and therapeutics to treat a damaged human brain may require novel approaches. While these injuries are complex, affecting hundreds of cell types, the one silver lining is the existence of functional NSCs. From mouse studies, it is becoming clear that these cells can be activated, proliferate, and migrate to the neocortex, but they fail to differentiate, survive, and integrate in the circuit. True regeneration of the human neocortex likely requires a synthetic biology approach to generate human NSCs that incorporates genetic programs engineered using principles learned from regenerative organisms. The repertoire of synthetic gene circuits and signaling pathways are rapidly expanding (Lienert et al., 2014), and they are incorporated into systems such as Chimeric Antigen Receptor T Cells (CAR-T cells), which are already in clinical trials and showing great promise to combat leukemia and glioblastoma (Brown et al., 2016; van der Stegen et al., 2015). The immune system has the intrinsic advantage that the cells are easily extracted from patients, expanded and engineered *in vitro*, and transplanted back into the patients. In the brain, a novel, safe approach to either 1) isolate, engineer *in vitro*, and graft NSCs or 2) deliver gene circuits *in vivo* is necessary.

Our results identified a handful of transcripts that are differentially expressed during the first four weeks of brain regeneration in the axolotl. While these transcripts likely represent a small subset of genes that control brain regeneration, this study could be the start to understanding the molecular mechanism governing the regeneration of neuronal diversity in the adult axolotl pallium.

Chapter 4

Discussion

The diversity of neuronal subtypes connected within a defined tissue architecture and neural network allows the adult human brain to process information in a manner that is unrivaled by any other known structure. The cellular complexity and heterogeneity of the adult human brain is only recently beginning to be defined at the molecular level (Darmanis et al., 2015; Hawrylycz et al., 2012; Kang et al., 2011; Lake et al., 2016). Despite the progress of molecular identification of cellular diversity, the function of each neuronal population and its respective circuitry remains largely unknown. However, disruption of brain structure, connectivity, and neuronal composition is often associated with behavioral deficits, as observed in models of neurodevelopmental, neuropsychiatric, and neurodegenerative diseases as well as brain injuries. For example, degeneration of upper motor neurons and the corticospinal tract in the human neocortex is partially responsible for the motor deficits seen in patients with Amyotrophic Lateral Sclerosis (Mitchell and Borasio, 2007). Therefore, it is likely that restoration of cognitive function in response to injury or disease requires the rebuilding of the correct tissue architecture and connectivity as well as regeneration of the diversity of mature neurons. To discover new strategies that could impart regeneration to the human brain, it is necessary to investigate a model system that could accomplish these tasks naturally.

Among vertebrates, salamanders and teleost fish possess unmatched brain regenerative capacities as larvae and adults (Tanaka and Ferretti, 2009). However, it was not known whether the brain regenerates with fidelity in terms of neuronal diversity, electrophysiological properties, cellular topography, and functional connectivity, all likely requirements for functional regeneration. Here, I used the axolotl pallium as the system to answer these questions. I found that the exact diversity of neurons regenerates in the dorsal pallium, and these neurons integrate into the local circuitry and acquire mature electrophysiological properties. Surprisingly, the tissue architecture remained disorganized even after prolonged period of regeneration, and the local and long-distance circuit failed to rebuild to the extent of the original uninjured tissue (Amamoto et al.,

2016). These results underscore the distinct difference in difficulty between generating new neurons locally at the injured site and integrating the new tissue into the pre-existing brain.

Neuronal regeneration in the adult pallium has been described in many organisms, including the zebrafish, salamanders, and lizards among vertebrates (Amamoto et al., 2016; Baumgart et al., 2012; Font et al., 1997; Font et al., 1991; Kirkham et al., 2014; Kroehne et al., 2011; Maden et al., 2013; Molowny et al., 1995; Skaggs et al., 2014). The cellular processes accompanying neuronal regeneration including proliferation, differentiation, and integration could be performed locally, within the regenerated tissue. The majority of the cells within the new tissue is newly generated, which may facilitate the interaction between different cell types. Accordingly, I found that increased proliferation and neurogenesis is largely restricted to the injury site. Moreover, the regenerated neurons receive afferent inputs and fire action potentials with comparable frequency and amplitude to those of pre-existing neurons. These processes may be controlled by cell-intrinsic mechanisms that do not require contributions from brain regions outside of the injury site.

In contrast, for proper brain regeneration, the neurons within the regenerated tissue need to integrate with other parts of the brain, which were created during embryonic development. The heterochrony between the new and old tissue may inhibit aspects of brain regeneration that involve external contributions. For example, in the mammalian brain, axons project to their targets based on the interaction between receptors and extrinsic axon guidance cues secreted by other cell types within the axonal tract (Chilton, 2006). After development, these extrinsic cues maintain expression at low levels, but the distribution is significantly altered as adults (Harel and Strittmatter, 2006), which could inhibit proper axon guidance for regenerated or transplanted neurons. In the axolotl telencephalon, I found that the long-distance connections from a specific neuronal subtype in the pallium are not restored even after 42 weeks of regeneration (Amamoto et al., 2016). In the future, it will be of great interest to determine whether the impairment in axon guidance is due to intrinsic or extrinsic factors. It may be possible to parse between these two

possibilities by transplanting the regenerated adult neurons into the dorsal pallium of a neonatal axolotl and seeing whether the adult neurons could project to the correct target in a more permissive environment.

The data highlight previously unappreciated limits for what vertebrates are able to achieve when faced with the need to regenerate the most complex tissues. It also poses a series of questions on whether true integration of entire potions of newly generated brain into pre-existing networks is possible outside of development, and whether the addition of new tissue results in functional regeneration. It is tempting to speculate whether the newly regenerated neuronal diversity can serve similar functional roles despite being housed within different tissue architecture. Innovation of behavioral assays to test the function of the regenerated portions of the pallium is much needed to begin to answer this fundamental question. This work is in its infancy, due to the difficulty of designing behavioral paradigms that test for pallial function in an organism where responses to different sensory stimuli have not yet been investigated, and the circuits involved are not mapped onto the pallium. In addition, precise behavioral assays will be likely required, given that removal of part of the pallium, much like the mammalian cerebral cortex, does not result in overtly abnormal behavior because of compensatory effects by remaining circuits. Upon regeneration of the midbrain dopaminergic neurons in the adult newt, the animal regained locomotive ability when stimulated with amphetamine (Parish et al., 2007). This behavioral recovery is also dependent on proliferation, suggesting that it is not completely mediated by synaptic plasticity. It will be interesting to see whether regenerated dopaminergic neurons are able to project to their long-distance targets. There may be an inherent difference in the environment of the newt midbrain and the axolotl pallium in permissiveness for axon guidance. Alternatively, ablation of specific neurons without affecting the overall structure like in the study by Parish et al. may promote a more complete axon regeneration compared to damage to the whole tissue.

Given the age of the new tissue and its newborn neurons in the regenerated axolotl brain, it is possible that they will adopt a new function within the brain, based on experience upon neurogenesis. Experience-dependent transcription, synapse formation, and pruning are highly active in an immature circuit of a neonatal mouse (Chung et al., 2013; Greer and Greenberg, 2008; Holtmaat and Svoboda, 2009; Schafer et al., 2012), and the new tissue within the axolotl dorsal pallium may resemble a developing brain. Because the process of circuitry formation is partly based on activity and experience, it is unlikely that axolotl brain regeneration will recreate the same exact circuitry as previously. Accordingly, I also found that the neuronal topography is altered upon regeneration, which would make it more difficult for regeneration of the pre-existing circuitry. On the other hand, it is also unlikely that the regenerated tissue will have no function, given the high energetic cost of regeneration (Bely and Nyberg, 2010). Therefore, I speculate that the new circuitry is sculpted based on the direct experience at the time of neurogenesis and will acquire a new function.

This work demonstrates the ability for the axolotl brain to regenerate the exact neuronal populations lost from injury. The mechanism by which the ependymoglia cells respond to loss of specific neuronal subtypes is an open question. Broadly, at least two possible mechanisms could mediate this process: 1) homogeneous pool of ependymoglia cells respond to the lack of feedback signals from the injured neuronal populations and repopulate the specific neuronal subtypes by differentiation, or 2) heterogeneous subtypes of ependymoglia cells respond to the lack of feedback signals from the injured neuronal populations and only the specific ependymoglia cells for the lost neuronal subtypes proliferate and subsequently differentiate. While the mechanism of pallial neuron development is not studied in the axolotl, clues could be drawn from mouse cortical development. In the developing mouse neocortex, the diversity of cortical projection neurons is generated from progenitors in a sequential manner, and the birthdate determines the fate of neuronal subtypes (Molyneaux et al., 2007; Shen et al., 2006). Although some heterogeneity might exist within the progenitor pool (Franco et al., 2012), birth order still remains a major

determinant of neuronal fate in this system. In the neurogenic axolotl pallium, it will be interesting to determine the cellular fate of specific ependymoglia by sparse labeling via viral or electroporation approaches. From this experiment, if ependymoglia from specific regions (e.g. medial pallium) only give rise to neurons of specific neuronal subtype, this could inform how regeneration of neuronal diversity is orchestrated. To further investigate the heterogeneity of the proliferating ependymoglia cells during regeneration, it is possible to apply single-cell RNA sequencing, which has become more cost-effective and high throughput in the recent years (Klein et al., 2015; Macosko et al., 2015; Shekhar et al., 2016). The molecular information for neuronal fate may already be coded in the cluster of proliferative ependymoglia cells prior to differentiation at 4wpi. In the planarian, specific removal of eye tissue does not induce eye progenitor proliferation (LoCascio et al., 2017). Instead, the rate of cell death in the new eye tissue decreases, which ultimately leads to regeneration of a correctly-sized eye. Conversely, when a large wound such as a head amputation is made, progenitor proliferation is triggered, suggesting that there are at least two modes of injury-induced regeneration. In the axolotl brain, we found that our injury paradigm that removes a large portion of the dorsal pallium induces a significant increase in proliferation both at the injury site and in distant regions of the forebrain, and this injury may be more similar to the large wound injury in planarian. On the other hand, specific ablation of specific neuronal subtypes by genetic or chemical means could induce a different mode of regeneration where homeostatic-level of proliferation, coupled with decreased cell death, is adequate for regeneration of specific neuronal subtypes. Understanding the mechanisms by which neuronal diversity is regenerated in the axolotl could inform how to apply regenerative medicine to patients suffering from brain injury.

The cellular processes and mechanisms that initially trigger wound closure and subsequently sustain brain repair in regenerative vertebrate species are not known. Using *in vivo* MRI, we were able to observe, for the first time, the dynamic changes in tissue morphology that occur in live animals over the course of brain regeneration. We found that early steps of wound

closure involve the generation of thinner processes from a stump that directionally grow towards each other before fusing. This strategy resembles that observed in the limb, in which closure of the wound by the wound epithelium after amputation is necessary for subsequent regenerative steps and may serve as a source of signals to govern downstream regenerative events (Mescher, 1976; Thornton, 1957). An outstanding question that remains is whether proliferation is necessary for wound closure and whether wound closure is necessary for proliferation. The former question could be addressed by experimentally inhibiting proliferation of ependymoglia cells by chemicals such as AraC, which has been shown to work in newts (Parish et al., 2007). The latter question, however, is difficult considering there are no established methods to mechanically obstruct the wound edges from closing. Despite the technical difficulty, answering this question could be the first step towards identifying signaling molecules that regulate the initial proliferative stage.

Our findings in Chapter 2 establish the axolotl pallium as a model to further investigate how diverse populations of electrophysiologically functional neurons are mechanistically regenerated. Understanding the molecular mechanisms that govern each step of the regenerative process in the axolotl brain could inform the missing molecular components that could enable cortical neurogenesis in humans upon injury.

In the United States alone, traumatic brain injury (TBI) and stroke affect 1.7 million and 800,000 people annually, respectively (Coronado et al., 2011; Ovbiagele and Nguyen-Huynh, 2011). Treating the human brain after damage remains a challenge, given the limited ability for generation of new neurons at the injury site. Upon injury or ischemia, neuroblasts migrate to the injury site in the cortex, but fail to survive, differentiate, or integrate into the existing cortical circuit (Carlén et al., 2009; Faiz et al., 2015). These results suggest that 1) there exists a population of neural stem cells that can be activated upon injury, and 2) these cells require exogenous factors to facilitate proper functioning within the neocortex. Identifying such key factors has proven challenging, despite the availability of excellent animal models (Fluri et al., 2015; Xiong et al., 2013). Therefore, a new approach is necessary. A complementary method would be to identify

factors that regulate cortical neurogenesis and functional circuit formation using regenerative model systems such as the axolotl and apply the knowledge to a mammalian system.

In Chapter 3, I analyzed the transcriptional profile of the first four weeks of brain regeneration in the axolotl, during which wound closure, immune activation, and proliferation occur at the injury site. This analysis revealed a small set of differentially expressed genes (192 out of 73108 transcripts). These numbers likely undermine the cell type-specific transcriptional changes because the whole tissue was profiled. In the injured mammalian brain, the cell types that react to damage are the neural stem cells, astrocytes, and immune cells, and contribution from neurons is minimal (Saha et al., 2012). In the axolotl brain, however, considering that most of the cells in the pallium are neurons, the majority of the cells sampled may not have exerted a major transcriptional induction. In the future, it will be important to profile the transcriptional program of specific cell populations or single cells (using a method like the one described in the Appendix).

Nonetheless, I found that certain sets of genes were differentially expressed during regeneration. I found an upregulation of cell cycle inducers (*nuf2a, plk1,* and *cenpf*) and a downregulation of a cell cycle inhibitor (*hcfc1*), which was expected from our histology data in Chapter 2. I also discovered that genes associated with the immune system were upregulated during regeneration (*tlr5, cxcl12, colec12,* and *tnfsf10*). Interestingly, within our top 30 DE transcripts, I found a set of genes associated with retinoic acid (*aldh1a2* and *rai1*), which play an extensive role during mammalian brain development (Maden, 2007). In this study, I did not determine whether these genes play a role during regeneration, and it will take further investigation to answer this question. Despite the lack of a sequenced genome, the axolotl is amenable to various gain-of-function and loss-of-function tools including *in vivo* electroporation and morpholino knockdown (Fei et al., 2014; Flowers et al., 2014; Kuo et al., 2015; Sugiura et al., 2016; Whited et al., 2012; Whited et al., 2013). Therefore, molecular interrogation of regeneration

mechanism could identify necessary components of brain regeneration that could be used for translational medicine.

A question in the field of regenerative biology is how to apply the knowledge to regenerative medicine for human patients. The molecular mechanisms underlying various regenerative processes are beginning to be elucidated, and promising candidates for mammalian regeneration could show efficacy in the future. For brain injuries, the prevalence of stroke and TBI remains high, and therapeutics to treat a damaged human brain may require novel approaches. While these injuries are complex, affecting hundreds of cell types, the one silver lining is the existence of functional NSCs. From mouse studies, it is becoming clear that these cells can be activated, proliferate, and migrate to the neocortex, but they fail to differentiate, survive, and integrate in the circuit (Arvidsson et al., 2002; Carlén et al., 2009; Chang et al., 2016; Chirumamilla et al., 2002; Faiz et al., 2015; Goings et al., 2004; Gu et al., 2000; Jiang et al., 2001; Kernie and Parent, 2010; Kreuzberg et al., 2010; Leker et al., 2007; Liu et al., 2009; Magnusson et al., 2014; Ohira et al., 2010). True regeneration of the human neocortex likely requires a synthetic biology approach to generate human NSCs that incorporates genetic programs engineered using principles learned from regenerative organisms.

The repertoire of synthetic gene circuits and signaling pathways are rapidly expanding (Lienert et al., 2014), and they are incorporated into systems such as Chimeric Antigen Receptor T Cells (CAR-T cells), which are already in clinical trials and showing great promise to combat leukemia and glioblastoma (Brown et al., 2016; van der Stegen et al., 2015). The immune system has the intrinsic advantage that the cells are easily extracted from patients, expanded and engineered *in vitro*, and transplanted back into the patients. In the brain, a novel, safe approach to either 1) isolate, engineer *in vitro*, and graft back NSCs or 2) deliver gene circuits *in vivo* to NSCs is necessary. In order to incorporate large gene circuits with multiple coding regions and both upstream and downstream regulatory elements, new technologies like Human Artificial Chromosome (HAC) might be necessary. As it currently stands, a HAC is a non-integrating vector

that can carry large genomic loci and also replicate to daughter cells, making it an ideal gene delivery vector (Kazuki and Oshimura, 2011). In the future, we may be able to engineer regeneration-specific gene circuits with user-defined rheostats into endogenous NSCs in human patients, which would enable the generation of cortical neurons lost in disease and injury.

To gain a deeper understanding of the molecular mechanism of brain regeneration, a more efficient approach to probe the transcriptional change is necessary. Quantitative transcriptional analysis of specific cell types remains a challenge in organisms that are not genetically tractable, given the lack of promoters and genetic manipulation. In the Appendix, I describe a new method to purify specific neuronal subtypes from unlabeled brain samples for downstream whole-genome transcriptional analysis. Building upon other technologies (Hrvatin et al., 2014; Molyneaux et al., 2015; Pan et al., 2011; Pechhold et al., 2009; Yamada et al., 2010), my approach is suited for both fresh or frozen brain samples. Recently, single-cell RNA-seq studies have identified neuronal and non-neuronal class-specific signature genes, such as those for adult human cortical neurons (Darmanis et al., 2015; Lake et al., 2016). My technology will invariably rely on the identification of such signature genes from single-cell data and availability of reliable antibodies. Conversely, single-cell RNA-seq may rely on technology like this for deeper sequencing depth of one or two user-defined neuronal subtypes. With such technologies, identification of regeneration-specific genes in the axolotl brain will be facilitated, and we will be able to start understanding the molecular mechanisms governing brain regeneration in organisms like the axolotl.

Materials and Methods

Animals

Wildtype axolotls (*Ambystoma mexicanum*) were obtained from the Ambystoma Genetic Stock Center (University of Kentucky, Lexington, KY) and were housed in standard conditions at 16°C in Holtfreter's solution. Adult animals, 15-18 cm in length, were used for all experiments. Anesthesia was achieved by immersion in 0.03% ethyl-p-aminobenzoate (benzocaine; Sigma-Aldrich, St. Louis, MO) or 0.1% ethyl 3-aminobenzoate methanesulfonate **(**tricaine; Sigma-Aldrich). All animal experiments performed were approved by the Harvard University IACUC and were in accordance with institutional and federal guidelines.

Injury

To access the telencephalon of anesthetized axolotls, two rectangular scalp skin flaps followed by cranial flaps were created dorsally with spring scissors. Incisions outlining a 0.8 mm X 1 mm rectangular injury site were made in the left dorsal pallium with a microknife (Fine Science Tools, Foster City, CA) secured onto a micromanipulator. The caudal-medial corner of the rectangular injury site is defined as 1 mm lateral from and 2 mm rostral from the choroid plexus. The injury site tissue was removed using No.5 forceps. After the injury, the cranial flaps were replaced, and the skins flaps were secured with non-absorbable silk sutures (Myco Medical, Cary, NC). In sham injury, the telencephalon was similarly exposed but the dorsal pallium was left intact.

BrdU/EdU labeling

250 µl (8 mg/ml in PBS) of BrdU (Sigma-Aldrich) or EdU (Thermo Fisher Scientific, Waltham, MA) was injected intraperitoneally. For animals sacrificed at 4wpi, BrdU/EdU was injected three times a week while for animals sacrificed at 11wpi, BrdU/EdU was injected once at 3, 4, and 5wpi due to the toxic effect of more frequent regimens of BrdU/EdU administration. BrdU incorporation was

analyzed by immunohistochemical staining (see below). EdU incorporation was detected with the Click-it EdU Alexa Fluor 488 Imaging Kit (Thermo Fisher Scientific).

Immunohistochemistry, in situ hybridization, and Nissl staining

Uninjured brains were dissected and fixed overnight in 4% paraformaldehyde (PFA) at 4°C. Injured and sham-injured brains were fixed overnight with the cranium attached, dissected from the cranium, and re-fixed overnight in 4% PFA at 4°C. The extra fixation step is necessary to preserve the morphological integrity of the injured tissue. After fixation, the brains were equilibrated in 30% sucrose solution at 4°C, embedded in OCT (Sakura Finetek, Torrance, CA), and cryosectioned coronally at 30 µm thickness. 10 series (120 sections) were collected from each brain onto Vistavision microscope slides (VWR, Radnor, PA) and stored at -80°C. For BrdU detection, sections were incubated in 2M HCl for 20 minutes at 37°C, before incubation in blocking buffer (0.3% BSA, 8% serum, 0.3% Triton X-100) for 2 hours at room temperature (RT). Sections were incubated overnight at 4°C in primary antibodies, which were diluted in blocking buffer. Primary antibodies used in this study were as follows: rat anti-CTIP2 antibody 1:100 (Abcam, Cambridge, MA), mouse anti-SATB2 1:50 (Abcam), rabbit anti-TLE4 1:3000 (gift of Stefano Stifani), rabbit anti-CALB2 1:300 (Swant, Marly, Switzerland), rat anti-BrdU 1:300 (Accurate Chemical, Westbury, NY), mouse anti-BrdU 1:300 (BD Biosciences, San Jose, CA), mouse anti-NeuN 1:300 (Millipore, Billerica, MA), rabbit anti-Hu-C/D 1:300 (Genetex, Irvine, CA), rabbit anti-PH3 1:300 (Millipore), rabbit anti-Sox2 1:100 (Abcam), mouse anti-GFAP 1:300 (Sigma-Aldrich), mouse anti-Tubb3 1:300 (Covance, Princeton, NJ). Sections were incubated in appropriate secondary antibodies from the Molecular Probes Alexa Fluor series (Thermo Fisher Scientific) at 1:750 dilutions for 2 hours at RT. After washing, sections were incubated in DAPI 1:50,000 (Thermo Fisher Scientific) for 10 minutes at RT. Sections were coverslipped with Fluoromount-G (SouthernBiotech, Birmingham, AL) before imaging. Tissue sections were imaged using a Nikon 90i fluorescence microscope equipped with a Retiga Exi camera (Q-Imaging, Surrey, Canada)

and analyzed with Volocity image analysis software v4.0.1 (PerkinElmer, Waltham, MA). Confocal images were acquired with Zeiss LSM 700 confocal microscope and analyzed with the ZEN Black software.

In situ hybridization was performed as described previously (Lodato et al., 2014). Riboprobes were generated as previously described(Arlotta et al., 2005). Riboprobes for *in situ* hybridization were generated from axolotl cDNA using the following primers:

fezf2, F: AAAGCGACAGCAAACTCAGC R: gtttcctttctggtggaagc;

ctip2, F: CCGTTCAGTCTTTTGCGAAT R: TAGCTGCCTTCCATCAATCC;

tle4, F: AACAAACAGGCGGAAATTGT R: CTCTAAAGCTTGCCGATGGA;

rorb, F: GAAATTTGGCAGGATGTCCA R: ACGTCTCCAGGTGGGATTTA;

er81, F: ATGACCAGCAAGTGCCtttt R: aggtttgaCTGCtGGCATTG;

sst, F: CAGACAAGCAAGCAGCAGAG R: TCTGTGGGAACTGCAGAGTG;

calb2, F: GGTCGAGTGCCGAGTTTATG R: TTCACCCTCTCCCCAAATAA;

gad2, F: GCGAGCAAAGGGTACAGAAG R: GGCAATACATTTTTCCTTCAAAA

Nissl staining was performed as previously described (Macklis, 1993).

All primary data from immunohistochemistry and *in situ* hybridization experiments were repeated at least three times and analyzed by one investigator, then confirmed by a second, independent investigator who was blinded to experimental conditions.

Cell quantification and statistical analysis

For quantification of proliferating cells and newborn neurons, anatomically matched sections were processed to detect BrdU/PH3 or BrdU/NeuN, respectively. For quantification of the disorganization index, boxes of 400 μm in width and spanning the thickness of the pallium were superimposed at matched locations on each section and divided into three equally sized bins. For quantification of Retrobead^{+} cells, anatomically matched sections were processed to detect Retrobead^{+}/DAPI^{+} cells. All counts were performed by an investigator who was blinded to the

condition. Unpaired, two-tailed t-test, one-way ANOVA, or two-way ANOVA was used for statistical analysis.

Induction of metamorphosis

Adult axolotls of 15-18cm in length were induced to undergo metamorphosis as described previously(Page and Voss, 2009). The animals were treated with L-thyroxine (50nM, Sigma-Aldrich) for 6 months while kept in 50% water, 50% land habitat. Upon complete gill absorption and exhibition of land walking capabilities, they were transferred to a peat moss habitat and switched to a cricket diet. No surgery was performed before animals were able to feed independently.

Retrograde Tracing

For retrograde tracing, Retrobeads (Lumafluor, Durham, NC) were injected (69 nl/injection, 3 injections per site) into regions of interest in the adult axolotl brain *in vivo*. One week after injection, animals were sacrificed and the brains were processed as described above.

Whole-cell patch clamp recordings

The dorsal pallium and individual neurons were visualized and identified with a microscope equipped with Nomarski optics and infrared illumination (BX-51WI, Olympus, Shinjuku, Japan). Whole-cell patch clamp recordings were obtained from axolotl pallium of injured and uninjured animals using recording pipettes (Glass type 8250, King Precision Glass, Claremont, CA) pulled in a horizontal pipette puller (P-87, Sutter Instruments, Novato, CA) to a resistance of 3–4 MΩ, and filled with internal solution containing (in mM): 117.0 K-gluconate, 13.0 KCl, 1.0, MgCl2, 0.07 CaCl2, 0.1 EGTA, 10.0 HEPES, 2.0 Na-ATP, 0.4 Na-GTP, and 0.3% biocytin, pH adjusted to 7.3 with KOH and osmolarity adjusted to 298–300 mOsm with 15mM K_2SO4.

For data acquisition and analysis, a Multiclamp 700B amplifier (Molecular Devices Corporation, Sunnyvale, CA) and digidata 1440A were used to acquire whole cell signals. The signals were acquired at 20 KHz and filter at 2KHz. Conventional characterization of neurons was made in voltage and current clamp configurations. Access resistances were continuously monitored and experiments with changes over 20% were aborted. Analyses were performed using Origin (version 8.6, Microcal, Malvern, UK) and MiniAnalysis (Synaptosoft, Decatur, GA).

Extracellular Field Recording

Ex vivo 300 µm thick slices were prepared by sectioning uninjured and injured (11-15wpi) brains on the vibratome. The extracellular field recording was performed as described(Peça et al., 2011). Briefly, a slice was placed into recording chamber (Warner Instruments, Hamden, CT) and constantly perfused with oxygenated aCSF at room temperature at a speed of 2.0 ml/min. A platinum iridium concentric bipolar electrode (FHC) was positioned on the dorsal pallium to stimulate the neurons either in uninjured control or injured slice. A borosilicate glass recording electrodes filled with 2M NaCl was placed onto the lateral or medial pallium approximately 600 µm away from the stimulating electrode. Dorsal-lateral or dorsal-medial field population spikes were elicited by delivery step depolarization (0.15 ms duration with 0.1 mA intensity at a frequency of 0.1 Hz). Stable baseline response of pop spike for at least 5 min from individual slice was ensured before moving to input-output assay. Input-output curves were determined for both the negative peak 1 (NP1; fiber volley) and pop spike amplitude by delivery of three consecutive stimulations from 0 to 1 mA with 0.1 mA increments. Recordings were performed at room temperature and data were sampled using pCLAMP 10 software (Molecular Devices).

Calcium Imaging

Ex vivo 300 µm thick slices were prepared by sectioning uninjured and injured (11-15wpi) brains. Staining of the slices in Fluo-4 (Thermo Fisher Scientific) was performed in accordance to

protocol(Dawitz et al., 2011). Slices were imaged on Zeiss Cell Observer for 10 minutes with a frame rate of 3 Hz. The resulting movie was analyzed using the FluoroSNAPP software(Patel et al., 2015).

In vivo Magnetic Resonance Imaging

Animals for imaging were anesthetized by immersion in 0.1% tricaine (Western Chemical, Ferndale, WA). Once anesthesia was achieved, animals were transferred to an MRI-compatible bed where anesthesia was maintained by partial immersion in tricaine with exposed skin covered by a damp towel.

Animals were imaged using a 9.4T horizontal bore animal imaging system (Biospec 94/20, Bruker Corporation, Billerica, MA). A circular, 20 mm receive-only surface coil was placed over the head. The animals were then situated with their heads near the isocenter of the magnet within an 84 mm quadrature transmit/receive volume coil. T_2-weighted images were acquired using a RARE (rapid acquisition with relaxation enhancement) sequence(Hennig et al., 1986). All images had RARE factor 8 and echo time TE=33 ms, and a sufficient number of slices were acquired to cover the entire brain. Sagittal images were acquired with repetition time TR=2181 ms, 1 mm slice thickness, 158 μm × 188 μm in-plane resolution, and 1 signal average. Axial images were acquired with TR=2000 ms, 500 μm slice thickness, 150 μm × 150 μm in-plane resolution, and 16 signal averages. Coronal images were acquired with TR=3817 ms, 500 μm slice thickness, 158 μm × 188 μm in-plane resolution, and 4 signal averages.

3D surface rendering of the MRI images were created using OsiriX(Rosset et al., 2004). Regions of interest (ROI) were manually drawn on consecutive coronal T_2-weighted images to outline the contours of the brain. The pixel values within and outside of the ROIs were changed to 65,000 and -3024, respectively. 3D surface rendering was performed with these settings: highest resolution, 100 iterations, and 1000 pixel values. The sizes of the injury were determined by

manually drawing ROIs for regions that are lacking continuous closure of the ventricle. The volumes of the ROIs were calculated using the Compute Volume algorithm.

Ex vivo Diffusion Tensor Imaging

The brains of anesthetized axolotls were extracted and fixed in 4% PFA containing 1 mM gadolinium (Gd-DTPA) MRI contrast agent to reduce the T1 relaxation time while ensuring that enough T_2-weighted signal remained. For MR image acquisition, the brains were placed in formalin. Brains were scanned on a 9.4T Bruker Biospec MR system. The pulse sequence used for image acquisition was a 3D diffusion-weighted spin-echo echo-planar imaging sequence, TR=330 msec, TE=31.23 msec, number of segments 4, with an imaging matrix of 232 × 96 × 96 pixels. Spatial resolution was 50 × 50 × 50 μm. Sixty diffusion-weighted measurements and one non-diffusion weighted (b=0) measurement were acquired, corresponding to a cubic lattice in Q-space at b = 12,000 sec/mm^2 with δ = 12.0 msec, Δ = 24.2 msec, with 8 averages. The total acquisition time was 17 hours and 11 minutes for each imaging session.

Diffusion Toolkit and TrackVis (http://trackvis.org) were used to reconstruct and visualize tractography pathways. Trajectories were propagated by consistently pursuing the orientation vector of least curvature. The color-coding of tractography pathways is based on a standard RGB code, applied to the vector between the end-points of each fiber (red: left-right, green: dorsal-ventral, and blue: anterior-posterior directions). We terminated tracking when the angle between two consecutive orientation vectors was greater than the given threshold (60°) for each specimen. ROIs were placed at the injury site and anatomically matched region in the contralateral hemisphere. Representative 3D fiber tracts that pass through the ROIs and a single coronal plane are shown.

Axolotl Brain Regeneration RNA extraction and library preparation

At 3 time points (1wpi, 2wpi, and 4wpi), injured axolotls were euthanized as described above. The olfactory bulb from the injured hemisphere was removed, and the rest of the telencephalon was collected into Trizol (Thermo Fisher Scientific). The tissue was homogenized and RNA was extracted according to the Trizol protocol. Strand-specific RNA-seq library was generated and sequenced on HiSeq 2000.

Axolotl RNA-seq data processing

A comprehensive transcriptome was generated by combining the transcriptome from this study and the complete transcriptome from a recently published data (Bryant et al., 2017) using CD-HIT-EST-2D (Fu et al., 2012). Transcript abundance was estimated using Kallisto (Bray et al., 2016). The resulting matrix of read counts were imported into R by tximport (Soneson et al., 2015) and analyzed for differential expression by DESeq2 (Love et al., 2014).

Frozen Human Bran Sample

Frozen Brodmann Area 4 (Primary Motor Cortex) samples of Patient 3529 and 3589 were obtained from Human Brain and Spinal Fluid Resource Center at University of California, Los Angeles through the NIH NeuroBioBank. Patient 3529 is a 58-year-old male with no clinical brain diagnosis and the postmortem interval was 9 hours. Patient 3589 is a 53-year-old male with no clinical brain diagnosis and the postmortem interval was 15 hours. This IRB protocol (IRB16-2037) was determined to be not human subjects research by the Harvard University-Area Committee on the Use of Human Subjects.

Nuclei Isolation, Immunolabeling, and FACS

Nuclei were prepared as described previously (Krishnaswami et al., 2016), with slight modifications. Thawed tissue was minced and incubated in 1% PFA for 5 minutes. Nuclei were

prepared by Dounce homogenizing in 0.1% Triton X-100 homogenization buffer (250 mM sucrose, 25 mM KCl, 5 mM $MgCl_2$, 10mM Tris buffer, pH 8.0, 1 μM DTT, 1x Protease Inhibitor (Promega), Hoechst 33342 10 ng ml^{-1}, 0.1% Triton X-100, 40 μL ml^{-1} RNasin Plus (Promega)). Sample was then overlaid on top of 20% sucrose bed and spun at 500xg for 12 minutes at 4°C. The pellet was resuspended in 4% PFA with 40 uL ml^{-1} RNasin Plus and incubated for 15 minutes on ice. The sample was spun at 2000xg for 5 minutes at 4°C. The sample was then resuspended in blocking buffer (0.5% BSA in nuclease-free PBS, 25 μL ml^{-1} RNasin Plus) and incubated for 15 minutes. Sample was spun and the pellet was resuspended and incubated in primary antibody (1:50 SATB2 antibody (Abcam), 1:100 BCL11B antibody (Abcam) in blocking buffer) for 30 minutes at 4°C. After washing 1x with blocking buffer, the sample was incubated in secondary antibody (1:750 AlexaFluor goat anti-rat 488, 1:750 AlexaFluor goat anti-mouse 647). After 1x wash, the sample was passed through a 35μm filter (Corning) and overlaid on top of a 20% sucrose bed and spun at 1000xg for 10 minutes at 4°C. The pellet was resuspended in blocking buffer and passed through a filter before proceeding to FACS. 2N Nuclei were determined by Hoechst histogram, and $SATB2^{LO}BCL11B^{HI}$ and $SATB2^{HI}BCL11B^{LO}$ populations were sorted into blocking buffer.

RNA isolation and library preparation

RNA was extracted using the RecoverAll Total Nuclear Isolation Kit (Thermo Fisher Scientific). Crosslinking was reversed by Digestion Buffer and Protease mixture (100 μL buffer and 4 μL protease) for 3 hours at 50°C. RNA-seq library was generated using the SMART-seq Ultra Low Input RNA kit (Clontech) and Nextera XT DNA Library Prep Kit (Illumina) according to protocol. The libraries were sequenced on a HiSeq 2500.

RNA-seq data processing

RNA-seq reads were clipped and mapped onto the mouse genome (mm10) or human genome (hg38) using STAR (Dobin et al., 2013). Sample parameters used were as follows:

STAR --genomeDir ./STAR_mm10 --runThreadN 6 --readFilesCommand zcat --readFilesIn /1_HYTWMBCXX.1.CTCTCTAC_AGAGTAGA.unmapped.1.fastq.gz,2_HYTWMBCXX.2.CTCTCTAC_AGAGTAGA.unmapped.1.fastq.gz 1_HYTWMBCXX.1.CTCTCTAC_AGAGTAGA.unmapped.2.fastq.gz,2_HYTWMBCXX.2.CTCTCTAC_AGAGTAGA.unmapped.2.fastq.gz --outFileNamePrefix ./STAR_out/1 outSAMtype BAM SortedByCoordinate --outSAMunmapped Within --outSAMattributes Standard --clip3pAdapterSeq CTCTCTAC --quantMode TranscriptomeSAM GeneCounts

Read counts were generated by HT-seq (Anders et al., 2015). Sample parameters used were as follows:

htseq-count -s no ./STAR_out/1Aligned.out.sam genes.gtf > ./1_results.txt

The resulting matrix of read counts were analyzed for differential expression by DESeq2 (Love et al., 2014).

Appendix

Transcriptional Profile of Specific Neuronal Subtypes in Human Frozen Postmortem Brain

Introduction

The cellular heterogeneity in the central nervous system (CNS) is unrivaled. For example, the mouse neocortex contains various cell types, and among them are the numerous classes of neurons that have been defined by their molecular, electrophysiological, morphological, and topographical traits (Lodato and Arlotta, 2015). The diversity of neuronal subtypes most likely contributes to the complex functionality of the mammalian brain. However, it was not until recently that different cell types of the mammalian CNS have begun to be defined at the molecular level (Arlotta et al., 2005; Darmanis et al., 2015; Lake et al., 2016; Lein et al., 2004; Molyneaux et al., 2015; Tasic et al., 2016; Zeisel et al., 2015). Transcriptional profiling at the population and single-cell level has begun to elucidate the signature genes that combinatorially identify each class of neurons. Deep understanding of the molecular players within specific cell types has promoted the elucidation of mechanisms in brain development and disease.

Despite these efforts, quantitative transcriptional analysis of specific cell types remains a challenge in organisms that are not genetically tractable. In particular, the adult human brain is likely to contain an unparalleled number of cell types, and yet, there is little known about cell type-specific traits at the molecular level, especially in disease states. While human post-mortem brain tissue samples are readily available through brain banks across the country, including those with neurological disorders, these samples are either permanently fixed or flash frozen, making conventional RNA sequencing technologies difficult to implement (Evers et al., 2011). Nonetheless, there exists a great need for transcriptional profile of specific cell types in the human brain, especially in the context of disease. For example, patients with Amyotropic Lateral Sclerosis (ALS) suffer from progressive degeneration of spinal motor neurons and corticospinal motor neurons (CSMN) in the neocortex, and other cell types in the brain are largely spared (Mitchell and Borasio, 2007). To start understanding the transcriptional changes that accompany CSMN dysfunction, it is critical to purify and analyze the specific neuronal population from the primary

motor cortex. Tissue-level transcriptional analysis of the motor cortex has previously uncovered some overt transcriptional changes in ALS (Lederer et al., 2007; Wang et al., 2006); however, cell type-specific gene expression of CSMN in patients with ALS is lacking. Therefore, it was our goal to develop a new technology to quantify the gene expression of specific neuronal subtypes from frozen, post-mortem adult human brain.

The molecular picture of these diverse cell types in the human brain is beginning to be elucidated by single-cell RNA sequencing technologies. Several groups have successfully isolated single cells or nuclei from postmortem fresh or frozen human brain samples for downstream RNA sequencing (Darmanis et al., 2015; Krishnaswami et al., 2016; Lake et al., 2016). However, current single-cell technology suffers from low capture rate, and quantitative analysis of low-abundant transcripts remains challenging (Liu and Trapnell, 2016). Additionally, sampling the whole tissue for rare populations such as specific neuronal subtypes could be costly and time consuming. Another method has combined immunolabeling and laser capture microdissection to isolate specific cell types and their cellular RNA content (Cantuti-Castelvetri et al., 2007; Elstner et al., 2011; Fend et al., 1999; Jiang et al., 2005; Perrin et al., 2005; Simunovic et al., 2009; Tagliafierro et al., 2016). However, this approach is low-throughput. We sought to create a novel technology that 1) is high-throughput, 2) isolates specific, user-defined cell types from the adult human frozen brain without genetic labeling, and 3) preserves RNA quality.

Here, we describe a novel technology that combines nuclear isolation, immunolabeling, FACS purification, and RNA sequencing to obtain the gene expression profile of two classes of projection neurons from mouse and human neocortex. We concentrated our efforts to the nuclear RNA because adult neurons are fragile and the nuclear RNA has been shown to represent >87% of total RNA (Barthelson et al., 2007; Grindberg et al., 2013). Moreover, nuclei isolation does not rely on enzymatic dissociation, which alters gene expression (Grindberg et al., 2013). As a proof-of-concept, we isolated the nuclei of CorticoFugal Projection Neurons (CFuPN), which project from the neocortex to outside of the neocortex and Callosal Projection Neurons (CPN), which

project from one cortical hemisphere to the other hemisphere, from flash-frozen, P30 and adult mouse brains (Molyneaux et al., 2007). Previously defined molecular markers for these two projection neurons were differentially expressed between populations at both time points, indicating that the technology could be applied to frozen tissues to isolate nuclear RNA from specific cell types. We also demonstrated the feasibility of applying this technology to the frozen postmortem human brain by purifying putative CFuPN and CPN. In the future, this technology could broaden our knowledge of the molecular mechanisms underlying diseases of the central nervous system using widely-available human brain samples.

Results

FACS purification of immunolabeled nuclei from frozen brain samples

To purify specific neuronal populations from the frozen mouse neocortex, we modified a previously-published protocol that uses intracellular antibody staining to isolate specific cell types (Hrvatin et al., 2014; Molyneaux et al., 2015; Pan et al., 2011; Pechhold et al., 2009; Yamada et al., 2010). A modification was necessary because adult neurons, and likely frozen adult neurons, are extremely fragile. Here, we developed a protocol to purify antibody-labeled nuclei from frozen samples without enzymatic dissociation **(Figure 4.1a)**. From the flash-frozen neocortex of P30 mice, we sought to isolate two populations of projections neurons, CFuPN and CPN. BCL11B (also known as CTIP2) is expressed by CFuPN in layer 5b and 6. SATB2 is expressed by CPN in all layers (Molyneaux et al., 2007) **(Figure 4.1b)**. Although BCL11B and SATB2 expression are mutually exclusive in embryonic and early postnatal mouse neocortex, a small population of layer 5 neurons expressed both markers at P30 and adult **(Figure 4.1b, Layer 5 inset).** Upon extraction, nuclei were immunolabeled with antibodies against BCL11B and SATB2 and FACS purified into three populations: $SATB2^{LO}BCL11B^{HI}$ (P3), $SATB2^{LO}BCL11B^{MID}$ (P4), $SATB2^{HI}BCL11B^{LO}$ (P5) (n=2 for each population) **(Figure 4.1c)**. For downstream analyses, we

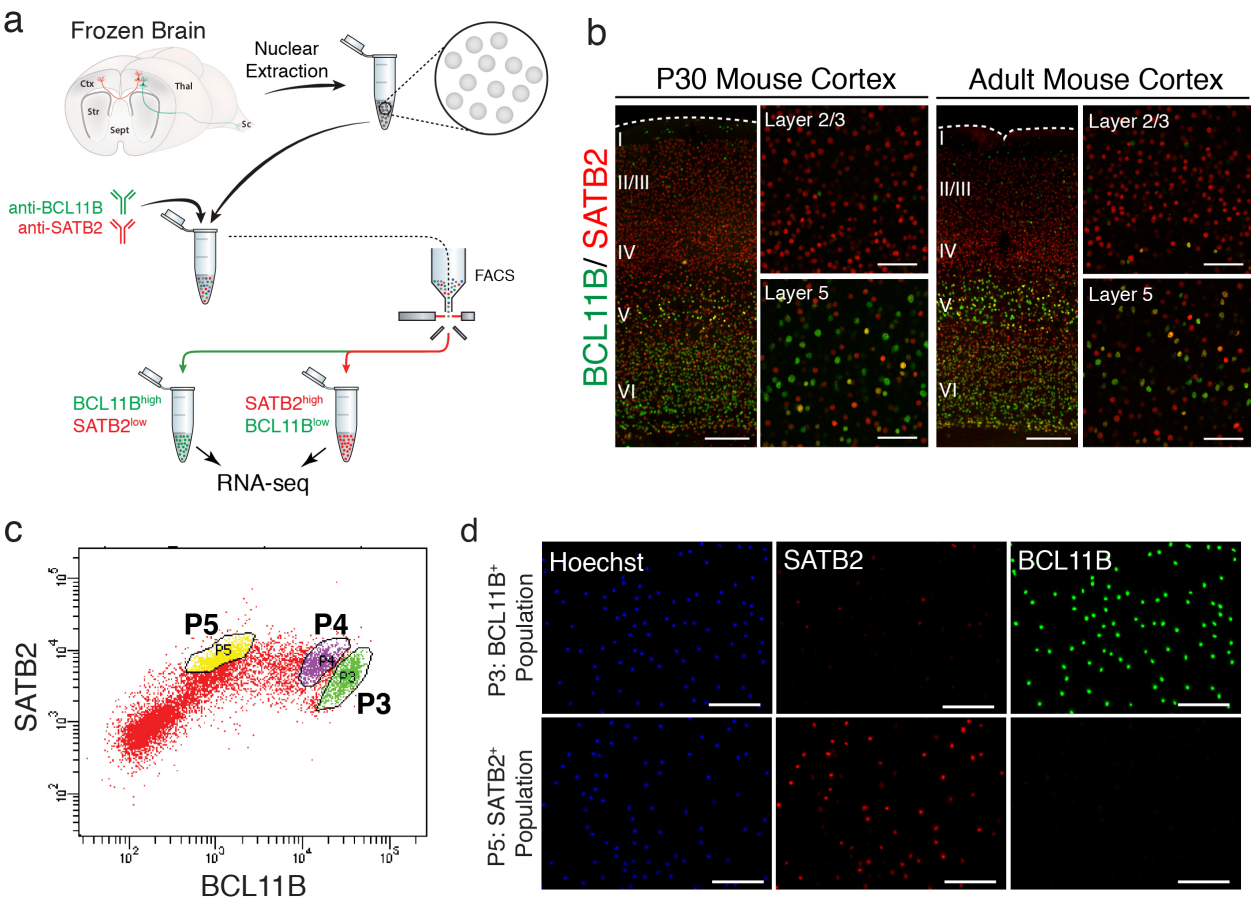

Figure 4.1: Nuclei from specific neuronal populations can be purified from P30 mouse neocortex.

(a) Schematic representation of the experimental setup. 2 neuronal populations, CPN (in red) and CFuPN (in green) are targeted for purification. Unlabeled nuclei from the frozen P30 mouse brain are extracted and immunolabeled with antibodies against BCL11B and SATB2. Nuclei are then FACS purified into 2 populations. (b) Representative images of P30 and adult mouse neocortex immunostained with BCL11B and SATB2. Layer 2/3 contains predominantly $SATB2^{+}$ CPN while Layer 5 contains $BCL11B^{+}$ CFuPN. (c) Representative FACS plot of neuronal populations immunolabeled with SATB2 (y-axis) and BCL11B (x-axis) showing clear separation. (d) Purified populations display correctly immunolabeled nuclei after FACS. Scale bars; 200 µm (b, left panels), 100 µm (b, right panels), 100 µm (d).

decided to focus on P3 and P5 populations, which likely represent CFuPN and CPN, respectively. As expected, immunolabeled nuclei were isolated into pure populations **(Figure 4.1d)**. On average, we collected 55,215 $SATB2^{LO}BCL11B^{HI}$ nuclei (n=2, henceforth $SATB2^{+}$) and 102,016 $SATB2^{HI}BCL11B^{LO}$ nuclei (n=2, henceforth $BCL11B^{+}$). These results indicate that this modified protocol could extract intact nuclei that are immunolabeled with user-defined intranuclear antibodies.

User-defined neuronal populations can be isolated and molecularly analyzed by transcriptional profiling

To determine whether we purified the correct neuronal populations, we analyzed the transcriptional profile of presumptive CFuPN and CPN populations. From purified nuclei, we extracted RNA with RNA Integrity Number ranging from 5.7 to 6.4, despite fixation and reverse crosslinking, as described previously (Molyneaux et al., 2015). SMART-Seq RNA-seq libraries were generated and sequenced on HiSeq 2500. Sequencing reads were aligned to the mm10 mouse genome using STAR, read counts were generated using HTseq, and differentially expressed genes were analyzed using DESeq2 (see Materials and Methods). Distribution of normalized read counts was virtually identical between samples **(Figure 4.2a)**. Unbiased hierarchical clustering showed that the samples of the same population from different animals clustered together (average Pearson correlation between samples within population: 0.98) **(Figure 4.2b)**. Subsequently, the two populations were analyzed for differential expression (DE), and the frequency distribution of all *p*-values showed an even distribution of null *p*-values **(Figure 4.2c)**. Between populations, we found 1583 differentially expressed genes (adjusted *p*-value < 0.05) out of 19,505 genes **(Figure 4.2d, red indicates significance)**.

We found an enrichment of known CPN and Layer 4 (L4) markers (e.g. *Cux2, Unc5d,* and *Rorb*) in the $SATB2^{+}$ population among the top 50 DE genes. Conversely, we found an enrichment of CFuPN markers (e.g. *Fezf2, Foxp2,* and *Crym*) in the $BCL11B^{+}$ population **(Figure 4.3; CPN/L4**

Figure 4.2: P30 Mouse Cortex RNA-seq data analysis quality control.

(a) Distribution of normalized read counts was virtually identical between samples. (b) Unbiased hierarchical clustering showed that the samples of the same population from different animals clustered together (average Pearson correlation between samples within population: 0.98). (c) The frequency distribution of all *p*-values showed an even distribution of null *p*-values. (d) MA plot of fold change vs. expression level. We found 1583 differentially expressed genes (adjusted *p*-value < 0.05, red dots) out of 19,505 genes.

Figure 4.2 (Continued)

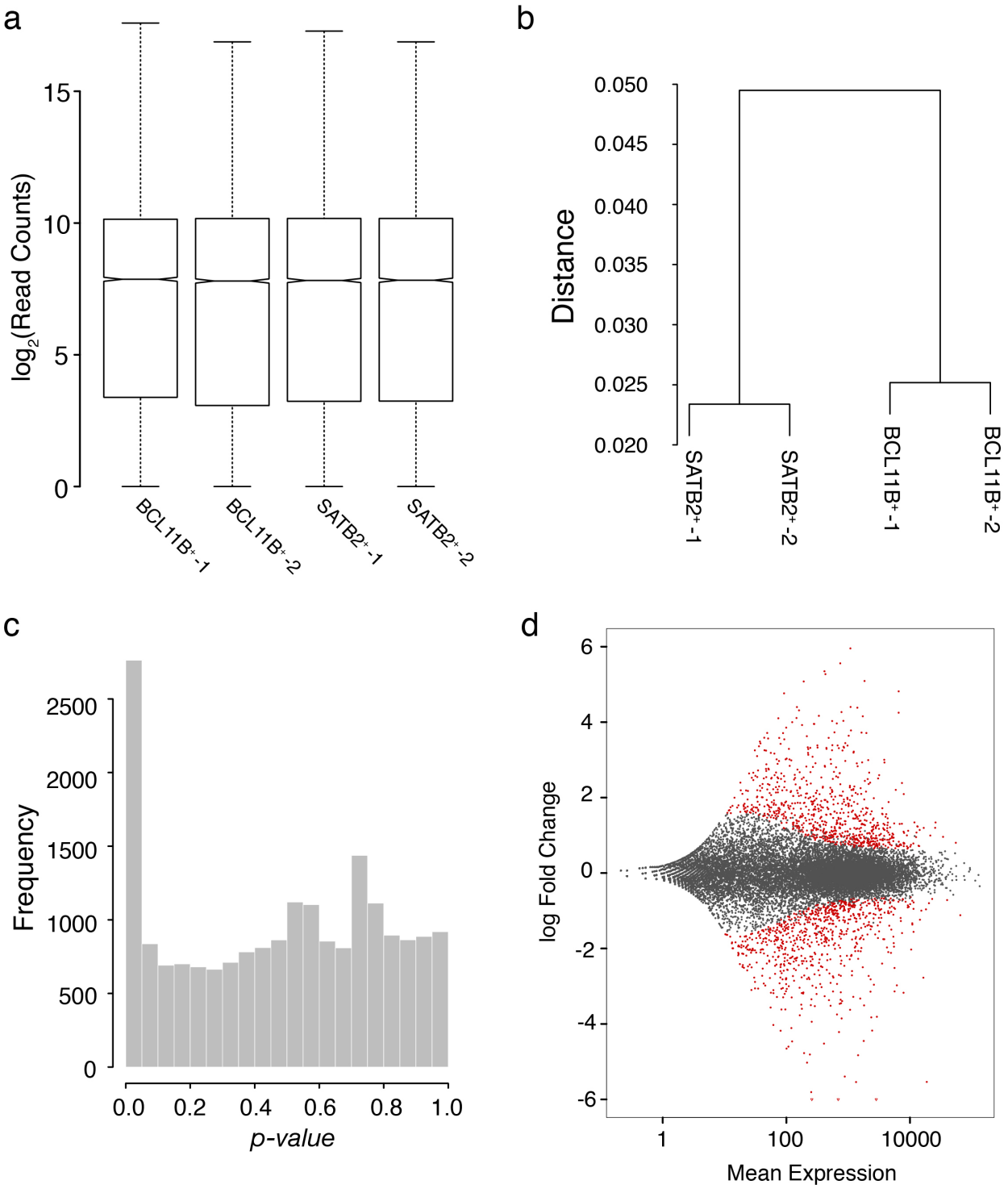

Figure 4.3: Top 50 differentially expressed genes between P30 CFuPN and CPN nuclei include known markers of these neuronal populations.

Heatmap of the top 50 differentially expressed genes between CFuPN and CPN nuclei. CPN markers (in blue) such as *Cux2, Ddit4l,* and *Plxnd1* are enriched in SATB2^{+} population. CFuPN markers (in red) such as *Crym, Fezf2,* and *Foxp2* are enriched in BCL11B^{+} population. BCL11B also labels a sparse population of interneurons, and some interneuron markers (in green) are enriched in this population as well.

Figure 4.3 (Continued)

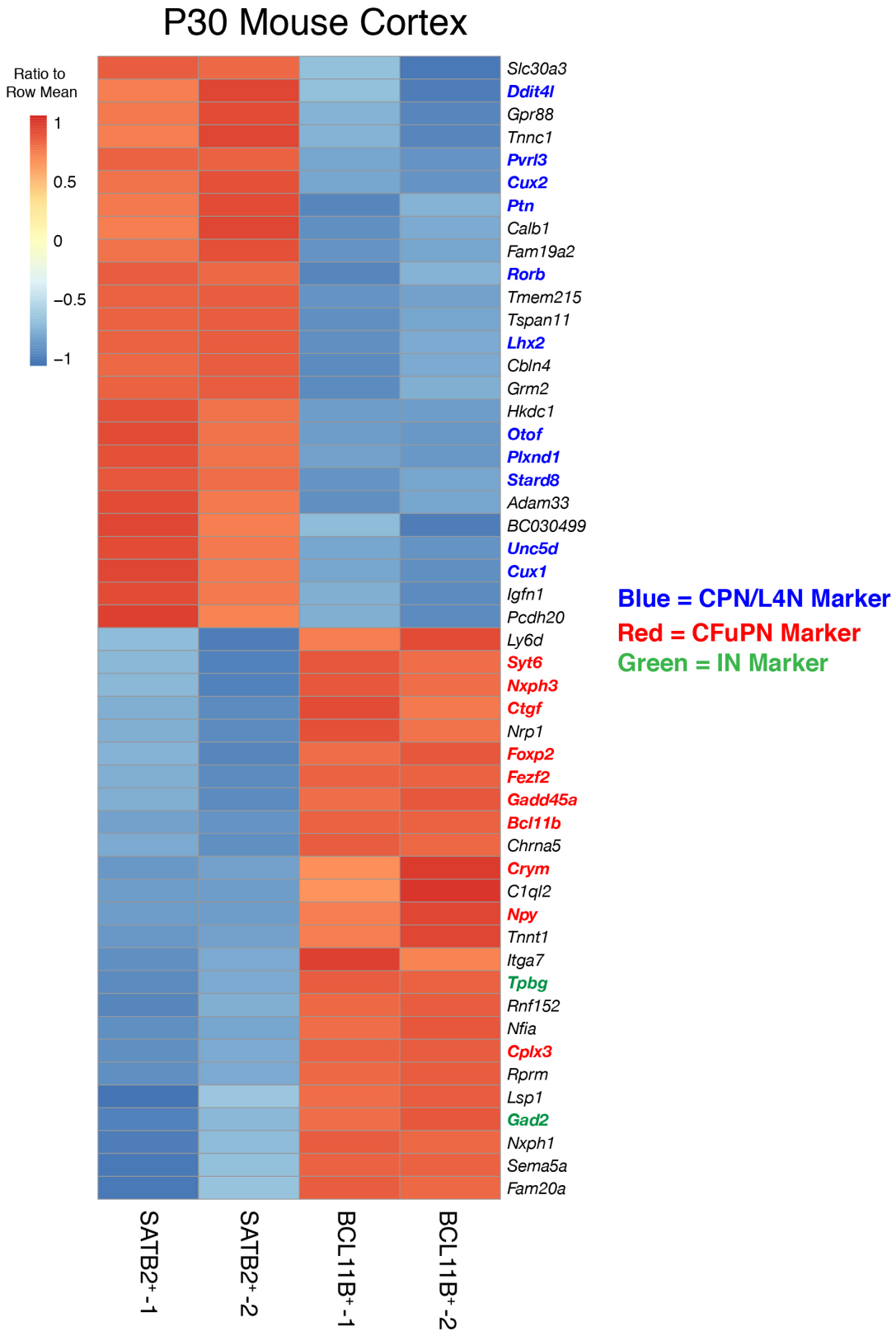

markers in blue, CFuPN markers in red). At older ages, BCL11B also labels some interneurons in the neocortex (Nikouei et al., 2016). Therefore, we found an enrichment of some interneuron markers in the BCL11B$^+$ population (*gad2* and *Tpbg*) **(Figure 4.3, in green)**. To validate the differentially expressed genes, we chose four genes (*Ddit4l, Unc5d, Kcnn2,* and *Rprm*) for further analysis. Using RNAscope double fluorescent *in situ* hybridization, we localized the expression of these genes in specific neuronal populations. We found that *Ddit4l* and *Unc5d* were expressed in layers 2-4 and they colocalized with *Satb2* **(Figure 4.4)**. Additionally, *Kcnn2* and *Rprm* were expressed in layer 5 and 6, respectively, and they were specifically localized to *Bcl11b*$^+$ neurons **(Figure 4.4)**. These results indicate that this novel technique can purify CFuPN and CPN nuclei from a fresh frozen mouse neocortex for downstream quantitative RNA-seq analysis of pure neuronal populations.

Specific neuronal subtypes from the frozen adult neocortex can be purified and analyzed

To determine whether this technology is applicable to frozen adult mouse brains, we purified the same populations (BCL11B$^+$ and SATB2$^+$) from the neocortex of 1+ year old mice. On average, we collected 33,142 BCL11B$^+$ nuclei (n=2) and 50,179 SATB2$^+$ nuclei (n=2), which were comparable in number to P30 samples. The sequencing reads were analyzed as previously described, and the quality control parameters were virtually identical to the P30 samples **(Figure 4.5)**. Even from the adult neocortex, we found an enrichment of CPN/L4 markers in the SATB2$^+$ population among the Top50 DE genes. CFuPN genes and interneuron genes were enriched in the BCL11B$^+$ population **(Figure 4.6)**. These results indicate the feasibility of applying this technique to frozen adult mammalian brains to purify and transcriptionally profile specific populations of cells.

Putative cortical projection neurons can be isolated from frozen postmortem human brain samples

Figure 4.4: Transcripts enriched in either neuronal population by RNA-seq are expressed in the correct population as assessed by RNAscope.

(a) RNA-seq dataset showed higher normalized counts of *Ddit4l* in the SATB2$^+$ population (left panel). Double fluorescence *in situ* hybridization using RNAscope showed localization of *Ddit4l* in the upper layers (middle panel). Higher magnification of layer 2/3 shows expression of *Ddit4l* in *Satb2$^+$cells.* (b) Same analysis as (a) for *Unc5d*. (c) RNA-seq dataset showed higher normalized counts of *Kcnn2* in the BCL11B$^+$ population (left panel). Double fluorescence *in situ* hybridization using RNAscope showed localization of *Kcnn2* in the layer 5 (middle panel). Higher magnification of layer 5 shows expression of *Kcnn2* in *Bcl11b$^+$cells.* (d) Same analysis as (c) for *Rprm* in layer 6. Scale bars; 200 μm (a-d, middle panels), 100 μm (a-d, right panels),

Figure 4.4 (Continued)

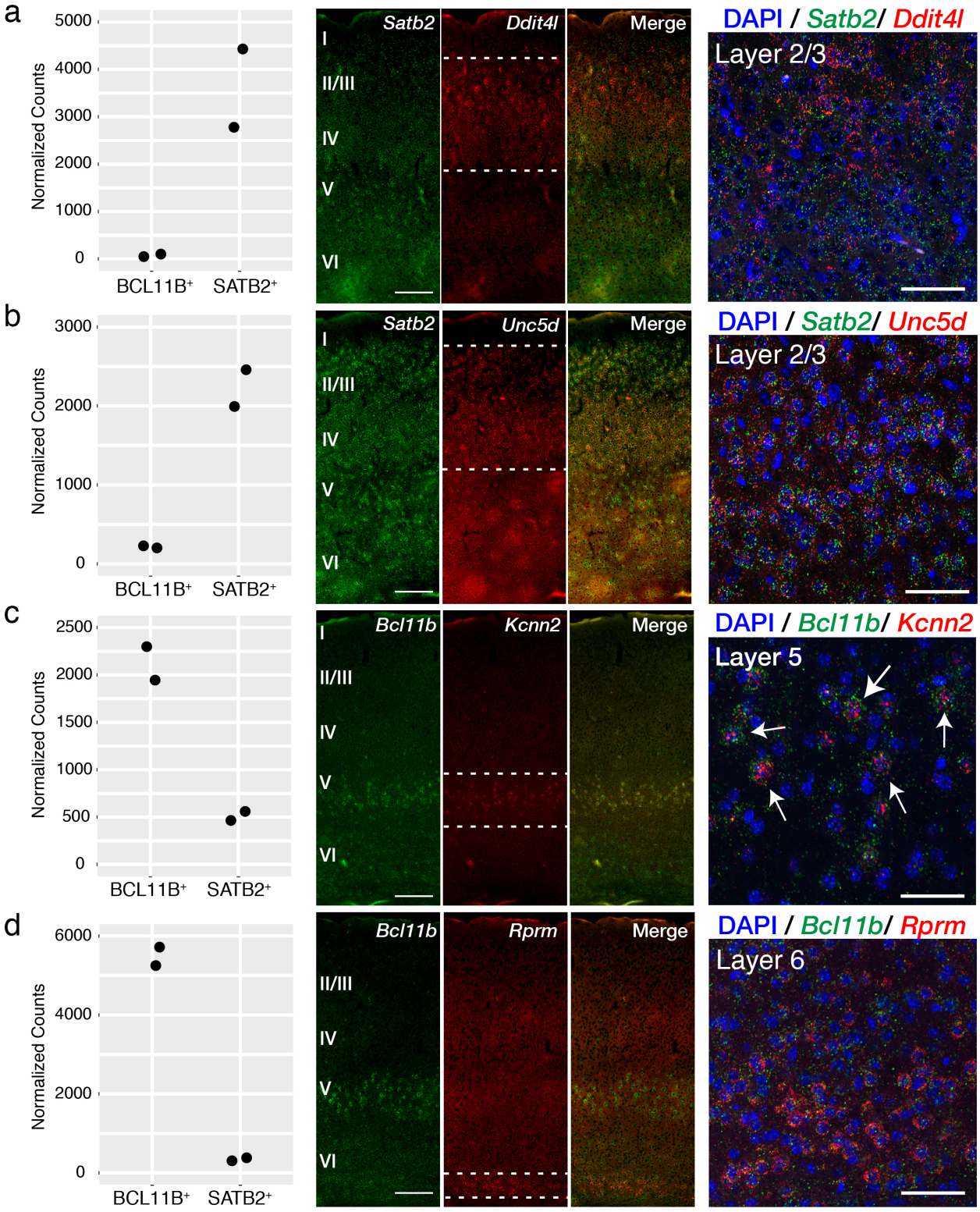

Figure 4.5: RNA-seq data analysis quality control for adult mouse cortex.

(a) Distribution of normalized read counts was virtually identical between samples. (b) Unbiased hierarchical clustering showed that the samples of the same population from different animals clustered together. (c) The frequency distribution of all *p*-values showed an even distribution of null *p*-values. (d) MA plot of fold change vs. expression level.

Figure 4.5 (Continued)

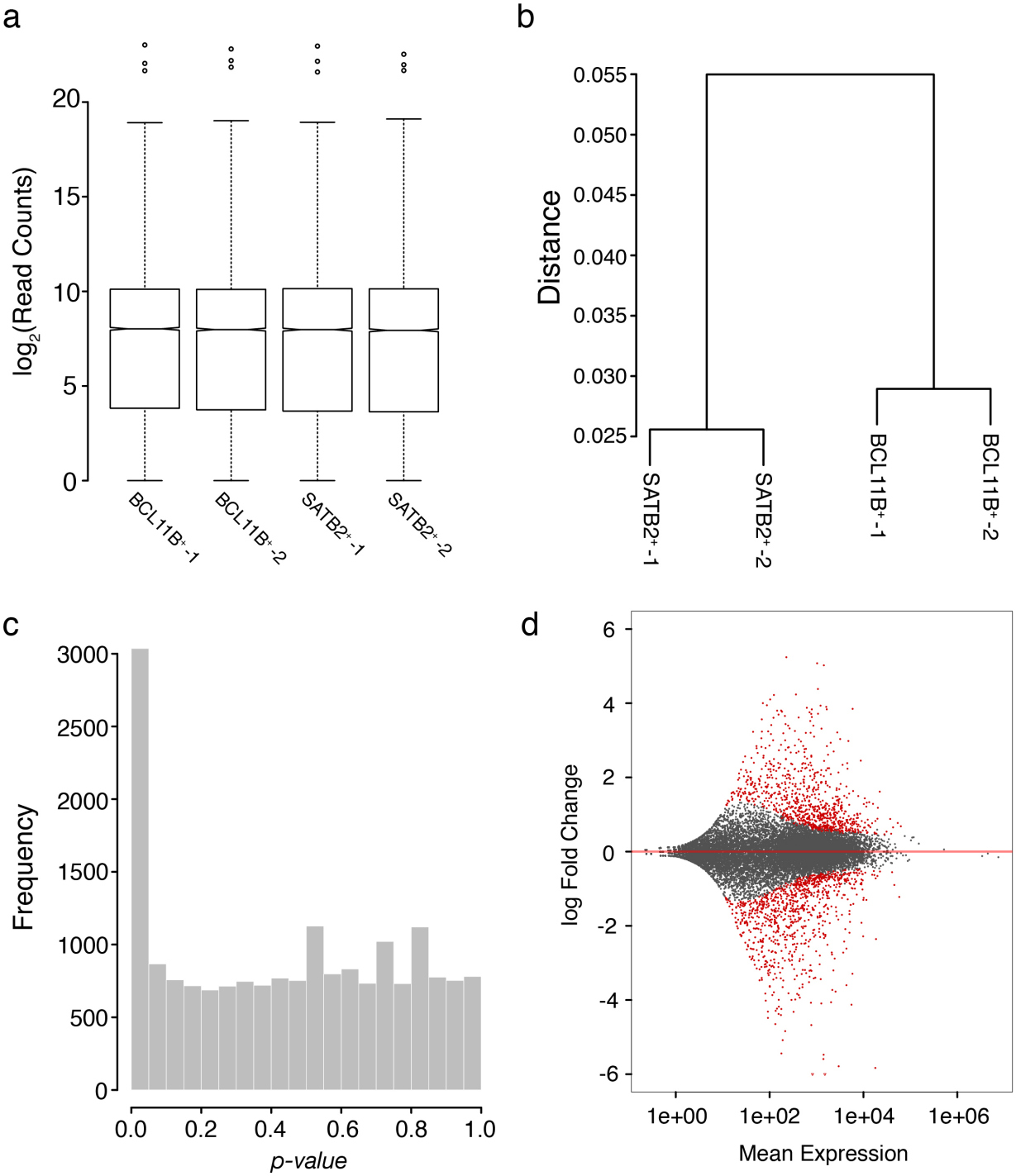

Figure 4.6: Top 50 differentially expressed genes between adult CFuPN and CPN nuclei include known markers of these neuronal populations.

Heatmap of the top 50 differentially expressed genes between CFuPN and CPN nuclei. CPN markers (in blue) such as *Cux2, Unc5d,* and *Plxnd1* are enriched in SATB2^{+} population. CFuPN markers (in red) such as *Tle4, Fezf2,* and *Foxp2* are enriched in BCL11B^{+} population. BCL11B also labels a sparse population of interneurons, and some interneuron markers (in green) are enriched in this population as well.

Figure 4.6 (Continued)

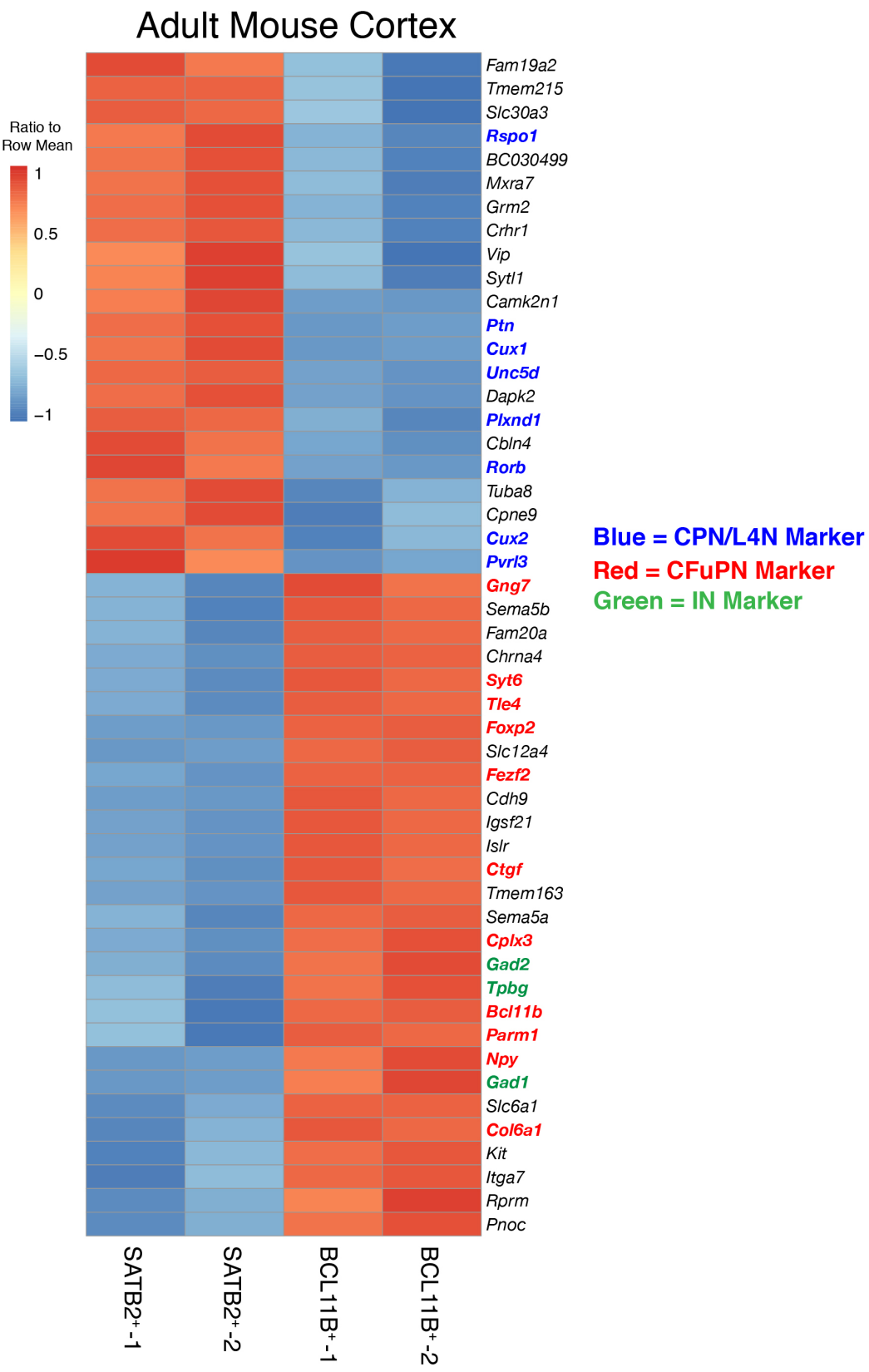

To determine whether this protocol is applicable to the frozen postmortem human brain samples, we obtained two frozen brain samples (Brodmann Area 4, primary motor cortex) from postmortem patients (for description of the samples, see Materials and Methods). We used the same protocol as before **(Figure 4.7a)**, and FACS purified $SATB2^{LO}BCL11B^{HI}$ and $SATB2^{HI}BCL11B^{LO}$ nuclei **(Figure 4.7b)**. Purified populations were observed, as expected, indicating that nuclear isolation of specific neuronal subtypes from frozen postmortem human brain tissue is feasible using this technique.

From deep sequencing of these two populations, we found known markers of cortical projection neurons enriched within the $SATB2^{+}$ population **(Figure 4.8).** In the adult human brain, it is not known if SATB2 specifically labels callosal projection neurons. From previous single-cell RNA-seq studies on the adult human brain, SATB2 has been shown to be expressed in all cortical projection neurons (Darmanis et al., 2015; Lake et al., 2016). Therefore, it may be necessary to find more specific markers of putative CPN in the adult human brain. Nonetheless, these results indicate that it is possible to specifically purify projection neurons from the frozen postmortem human brain tissue without genetic labeling.

Discussion

Technologies to enable transcriptional analysis of the human brain are rapidly expanding. At the population level, distinct regions of the fetal and adult human brain have been sampled for gene expression analysis (Bossers et al., 2009; Dangond et al., 2004; Dumitriu et al., 2012; Hauser et al., 2005; Hawrylycz et al., 2012; Kang et al., 2011; Lederer et al., 2007; Miller et al., 2006; Moran et al., 2006; Offen et al., 2009; Papapetropoulos et al., 2006; Wang et al., 2006). These pioneering studies have shed light on molecular mechanisms of human brain development and diseases. Despite progress, these tissue-level approaches cannot account for cellular heterogeneity of the human brain, an organ unrivaled in complexity. In human brain disorders, histological studies have underscored the cell type specificity of cellular dysfunction and

Figure 4.7: Nuclei from specific neuronal populations can be purified from frozen adult postmortem human neocortex.

(a) Schematic representation of the experimental setup. 2 neuronal populations, putative CPN and CFuPN are targeted for purification. Unlabeled nuclei from the frozen postmortem adult human brain are extracted and immunolabeled with antibodies against BCL11B and SATB2 to label these two neuronal populations. Nuclei are then FACS purified into 2 populations. (b) Representative FACS plot of neuronal populations immunolabeled with SATB2 (y-axis) and BCL11B (x-axis) showing clear separation. (c) Purified populations display correctly immunolabeled nuclei after FACS. Scale bars; 100 μm (c).

Figure 4.7 (Continued)

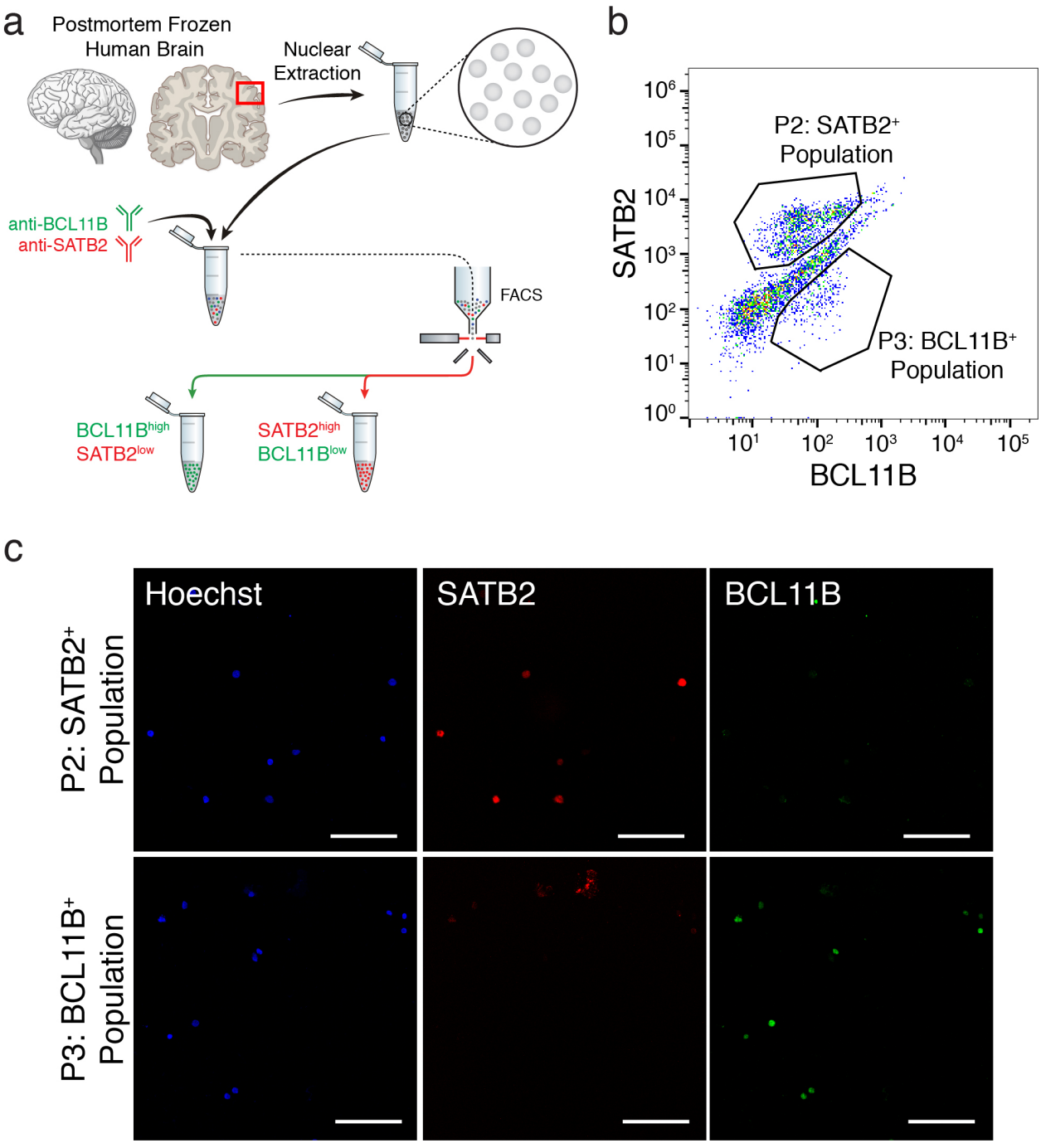

Figure 4.8: Top 50 differentially expressed genes between adult human cortical BCL11B$^+$ and SATB2$^+$ nuclei include known markers of projection neurons in the SATB2$^+$ population.

Heatmap of the top 50 differentially expressed genes between adult human cortical BCL11B$^+$ and SATB2$^+$ nuclei. Cortical Projection Neuron/CPN markers (in red) such as *Ldb2, Rorb,* and *Neurod2* are enriched in SATB2$^+$ population.

Figure 4.8 (Continued)

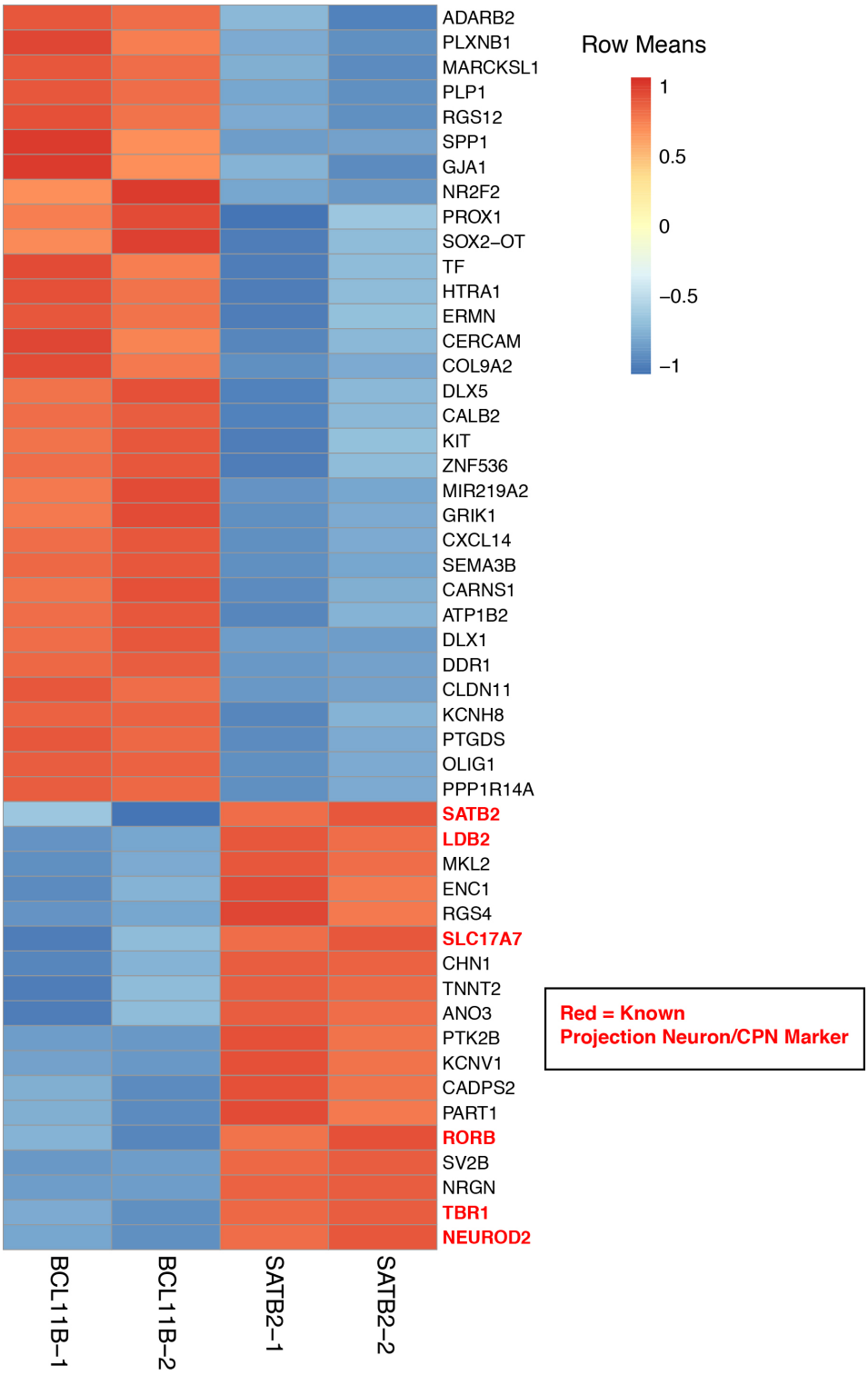

degeneration. For example, patients with Amyotropic Lateral Sclerosis (ALS) suffer from progressive degeneration of spinal motor neurons and corticospinal motor neurons (CSMN) in the neocortex (Mitchell and Borasio, 2007). To understand the transcriptional changes that accompany CSMN dysfunction, it is critical to purify and analyze this specific neuronal population from the primary motor cortex.

Recent development in single-cell RNA-seq technology has enabled unbiased sampling of all cell types from a human brain tissue sample (Darmanis et al., 2015; Krishnaswami et al., 2016; Lake et al., 2016). Aside from the inherent challenges with single-cell RNA-seq (Liu and Trapnell, 2016), it is impractical to assess the gene expression changes in all cell types if one is interested in a select neuronal subtypes. Therefore, bulk RNA-seq of purified neuronal populations is a complementary approach to quantify gene expression in specific cell types. Here, we developed a new method to quantify gene expression in pure neuronal populations from a frozen postmortem human brain without the need for genetic labeling.

With this technology, we can start to interrogate the transcriptional changes that accompany specific neuronal subtypes in the adult human brain. Counting only those from the NIH brain bank, over 16,000 postmortem samples are available, and many of them are available as flash frozen samples. The main challenge with using this technique or single-nuclei RNA-seq for gaining mechanistic insight into a nervous system disorder is determining which disease can benefit from a postmortem transcriptome data. Postmortem brains of patients with neurodevelopmental disorders such as Down Syndrome and Autism Spectrum Disorder may not exhibit the gene expression changes associated with the disease progression because of the early disease onset. On the other hand, postmortem brains of patients with neurodegenerative disorders may not contain the neuronal subtype of choice because they have already degenerated by the time of death. To understand the molecular mechanism of neurodegenerative disorders, it may require postmortem brain samples of diagnosed patients, whose manner of death was accidental, unrelated to the disease.

Taken together, this technology could enable transcriptional profiling of specific neuronal subtypes in the adult mouse brain and postmortem human brain without a need for genetic labeling. Identification of different cell types and molecular markers will rely on single-cell technologies, and this complementary method will allow users to define one subpopulation of interest and gain quantitative transcriptional analysis with deep bulk sequencing.

References

Alcamo, E.A., Chirivella, L., Dautzenberg, M., Dobreva, G., Fariñas, I., Grosschedl, R., and McConnell, S.K. (2008). Satb2 regulates callosal projection neuron identity in the developing cerebral cortex. Neuron *57*, 364-377.

Alunni, A., Krecsmarik, M., Bosco, A., Galant, S., Pan, L., Moens, C.B., and Bally-Cuif, L. (2013). Notch3 signaling gates cell cycle entry and limits neural stem cell amplification in the adult pallium. Development (Cambridge, England) *140*, 3335-3347.

Amamoto, R., and Arlotta, P. (2014). Development-inspired reprogramming of the mammalian central nervous system. Science (New York, NY) *343*, 1239882.

Amamoto, R., Huerta, V.G., Takahashi, E., Dai, G., Grant, A.K., Fu, Z., and Arlotta, P. (2016). Adult axolotls can regenerate original neuronal diversity in response to brain injury. eLife *5*.

Anders, S., Pyl, P.T., and Huber, W. (2015). HTSeq--a Python framework to work with high-throughput sequencing data. Bioinformatics (Oxford, England) *31*, 166-169.

Aoto, J., Nam, C.I., Poon, M.M., Ting, P., and Chen, L. (2008). Synaptic signaling by all-trans retinoic acid in homeostatic synaptic plasticity. Neuron *60*, 308-320.

Arlotta, P., Molyneaux, B.J., Chen, J., Inoue, J., Kominami, R., and Macklis, J.D. (2005). Neuronal subtype-specific genes that control corticospinal motor neuron development in vivo. Neuron *45*, 207-221.

Arvidsson, A., Collin, T., Kirik, D., Kokaia, Z., and Lindvall, O. (2002). Neuronal replacement from endogenous precursors in the adult brain after stroke. Nature medicine *8*, 963-970.

Ayari, B., Hachimi, K.H., Yanicostas, C., Landoulsi, A., and Soussi-Yanicostas, N. (2010). Prokineticin 2 Expression Is Associated with Neural Repair of Injured Adult Zebrafish Telencephalon. Journal of Neurotrauma *27*, 959-972.

Baldwin, K.T., and Giger, R.J. (2015). Insights into the physiological role of CNS regeneration inhibitors. Frontiers in molecular neuroscience *8*, 23.

Barbosa, J.S., Sanchez-Gonzalez, R., Di Giaimo, R., Baumgart, E.V., Theis, F.J., Götz, M., and Ninkovic, J. (2015). Neurodevelopment. Live imaging of adult neural stem cell behavior in the intact and injured zebrafish brain. Science (New York, NY) *348*, 789-793.

Barthelson, R.A., Lambert, G.M., Vanier, C., Lynch, R.M., and Galbraith, D.W. (2007). Comparison of the contributions of the nuclear and cytoplasmic compartments to global gene expression in human cells. BMC genomics *8*, 340.

Bartolini, G., Ciceri, G., and Marín, O. (2013). Integration of GABAergic interneurons into cortical cell assemblies: lessons from embryos and adults. Neuron *79*, 849-864.

Baumgart, E.V., Barbosa, J.S., Bally-cuif, L., and Götz, M. (2012). Stab wound injury of the zebrafish telencephalon: a model for comparative analysis of reactive gliosis. Glia *60*, 343-357.

Bely, A.E., and Nyberg, K.G. (2010). Evolution of animal regeneration: re-emergence of a field. Trends in ecology & evolution *25*, 161-170.

Berg, D.A., Kirkham, M., Beljajeva, A., Knapp, D., Habermann, B., Ryge, J., Tanaka, E.M., and Simon, A. (2010). Efficient regeneration by activation of neurogenesis in homeostatically quiescent regions of the adult vertebrate brain. Development (Cambridge, England) *137*, 4127-4134.

Berg, D.A., Kirkham, M., Wang, H., Frisén, J., and Simon, A. (2011). Dopamine controls neurogenesis in the adult salamander midbrain in homeostasis and during regeneration of dopamine neurons. Cell stem cell *8*, 426-433.

Bernardos, R.L., Barthel, L.K., Meyers, J.R., and Raymond, P.A. (2007). Late-stage neuronal progenitors in the retina are radial Müller glia that function as retinal stem cells. The Journal of neuroscience : the official journal of the Society for Neuroscience *27*, 7028-7040.

Berninger, B., Costa, M.R., Koch, U., Schroeder, T., Sutor, B., Grothe, B., and Götz, M. (2007). Functional properties of neurons derived from in vitro reprogrammed postnatal astroglia. The Journal of neuroscience : the official journal of the Society for Neuroscience *27*, 8654-8664.

Bond, A.M., Ming, G.-L.L., and Song, H. (2015). Adult Mammalian Neural Stem Cells and Neurogenesis: Five Decades Later. Cell stem cell *17*, 385-395.

Bossers, K., Meerhoff, G., Balesar, R., van Dongen, J.W., Kruse, C.G., Swaab, D.F., and Verhaagen, J. (2009). Analysis of gene expression in Parkinson's disease: possible involvement of neurotrophic support and axon guidance in dopaminergic cell death. Brain pathology (Zurich, Switzerland) *19*, 91-107.

Bray, N.L., Pimentel, H., Melsted, P., and Pachter, L. (2016). Near-optimal probabilistic RNA-seq quantification. Nature biotechnology *34*, 525-527.

Britanova, O., de Juan Romero, C., Cheung, A., Kwan, K.Y., Schwark, M., Gyorgy, A., Vogel, T., Akopov, S., Mitkovski, M., Agoston, D.*, et al.* (2008). Satb2 is a postmitotic determinant for upper-layer neuron specification in the neocortex. Neuron *57*, 378-392.

Brown, C.E., Alizadeh, D., Starr, R., Weng, L., Wagner, J.R., Naranjo, A., Ostberg, J.R., Blanchard, M.S., Kilpatrick, J., Simpson, J.*, et al.* (2016). Regression of Glioblastoma after Chimeric Antigen Receptor T-Cell Therapy. The New England journal of medicine *375*, 2561-2569.

Brox, A., Puelles, L., Ferreiro, B., and Medina, L. (2003). Expression of the genes GAD67 and Distal-less-4 in the forebrain of Xenopus laevis confirms a common pattern in tetrapods. The Journal of comparative neurology *461*, 370-393.

Brox, A., Puelles, L., Ferreiro, B., and Medina, L. (2004). Expression of the genes Emx1, Tbr1, and Eomes (Tbr2) in the telencephalon of Xenopus laevis confirms the existence of a ventral pallial division in all tetrapods. The Journal of comparative neurology *474*, 562-577.

Bryant, D.M., Johnson, K., DiTommaso, T., Tickle, T., Couger, M.B., Payzin-Dogru, D., Lee, T.J., Leigh, N.D., Kuo, T.-H.H., Davis, F.G.*, et al.* (2017). A Tissue-Mapped Axolotl De Novo Transcriptome Enables Identification of Limb Regeneration Factors. Cell Rep *18*.

Buffo, A., Vosko, M.R., Ertürk, D., Hamann, G.F., Jucker, M., Rowitch, D., and Götz, M. (2005). Expression pattern of the transcription factor Olig2 in response to brain injuries: implications for neuronal repair. Proceedings of the National Academy of Sciences of the United States of America *102*, 18183-18188.

Burr, H.S. (1916). Regeneration in the brain of Amblystoma. I. The regeneration of the forebrain. Journal of Comparative Neurology *26*, 203-211.

Butler, E.G., and Ward, M.B. (1967). Reconstitution of the spinal cord after ablation in adult Triturus. Developmental biology *15*, 464-486.

Caiazzo, M., Dell'Anno, M.T., Dvoretskova, E., Lazarevic, D., Taverna, S., Leo, D., Sotnikova, T.D., Menegon, A., Roncaglia, P., Colciago, G.*, et al.* (2011). Direct generation of functional dopaminergic neurons from mouse and human fibroblasts. Nature *476*, 224-227.

Campbell, L.J., Suárez-Castillo, E.C., Ortiz-Zuazaga, H., Knapp, D., Tanaka, E.M., and Crews, C.M. (2011). Gene expression profile of the regeneration epithelium during axolotl limb regeneration. Developmental dynamics : an official publication of the American Association of Anatomists *240*, 1826-1840.

Cano-Martínez, A., Vargas-González, A., Guarner-Lans, V., Prado-Zayago, E., León-Oleda, M., and Nieto-Lima, B. (2010). Functional and structural regeneration in the axolotl heart (Ambystoma mexicanum) after partial ventricular amputation. Archivos de cardiología de México *80*, 79-86.

Cantuti-Castelvetri, I., Keller-McGandy, C., Bouzou, B., Asteris, G., Clark, T.W., Frosch, M.P., and Standaert, D.G. (2007). Effects of gender on nigral gene expression and parkinson disease. Neurobiology of disease *26*, 606-614.

Carlén, M., Meletis, K., Göritz, C., Darsalia, V., Evergren, E., Tanigaki, K., Amendola, M., Barnabé-Heider, F., Yeung, M.S., Naldini, L.*, et al.* (2009). Forebrain ependymal cells are Notch-dependent and generate neuroblasts and astrocytes after stroke. Nature neuroscience *12*, 259-267.

Chambers, S.M., Fasano, C.A., Papapetrou, E.P., Tomishima, M., Sadelain, M., and Studer, L. (2009). Highly efficient neural conversion of human ES and iPS cells by dual inhibition of SMAD signaling. Nature biotechnology *27*, 275-280.

Chang, E.H., Adorjan, I., Mundim, M.V., Sun, B., Dizon, M.L., and Szele, F.G. (2016). Traumatic Brain Injury Activation of the Adult Subventricular Zone Neurogenic Niche. Front Neurosci *10*.

Chen, B., Schaevitz, L.R., and McConnell, S.K. (2005a). Fezl regulates the differentiation and axon targeting of layer 5 subcortical projection neurons in cerebral cortex. Proceedings of the National Academy of Sciences of the United States of America *102*, 17184-17189.

Chen, C.-C.C., Winkler, C.M., Pfenning, A.R., and Jarvis, E.D. (2013). Molecular profiling of the developing avian telencephalon: regional timing and brain subdivision continuities. The Journal of comparative neurology *521*, 3666-3701.

Chen, J., Magavi, S.S., and Macklis, J.D. (2004). Neurogenesis of corticospinal motor neurons extending spinal projections in adult mice. Proceedings of the National Academy of Sciences of the United States of America *101*, 16357-16362.

Chen, J.-G.G., Rasin, M.-R.R., Kwan, K.Y., and Sestan, N. (2005b). Zfp312 is required for subcortical axonal projections and dendritic morphology of deep-layer pyramidal neurons of the cerebral cortex. Proceedings of the National Academy of Sciences of the United States of America *102*, 17792-17797.

Chilton, J.K. (2006). Molecular mechanisms of axon guidance. Developmental biology *292*, 13-24.

Chirumamilla, S., Sun, D., Bullock, M.R., and Colello, R.J. (2002). Traumatic brain injury induced cell proliferation in the adult mammalian central nervous system. J Neurotrauma *19*.

Chung, W.-S.S., Clarke, L.E., Wang, G.X., Stafford, B.K., Sher, A., Chakraborty, C., Joung, J., Foo, L.C., Thompson, A., Chen, C.*, et al.* (2013). Astrocytes mediate synapse elimination through MEGF10 and MERTK pathways. Nature *504*, 394-400.

Coronado, V.G., Xu, L., Basavaraju, S.V., McGuire, L.C., Wald, M.M., Faul, M.D., Guzman, B.R., Hemphill, J.D., for, and Centers (2011). Surveillance for traumatic brain injury-related deaths--United States, 1997-2007. Morbidity and mortality weekly report Surveillance summaries (Washington, DC : 2002) *60*, 1-32.

Dangond, F., Hwang, D., Camelo, S., Pasinelli, P., Frosch, M.P., Stephanopoulos, G., Stephanopoulos, G., Brown, R.H., and Gullans, S.R. (2004). Molecular signature of late-stage human ALS revealed by expression profiling of postmortem spinal cord gray matter. Physiological genomics *16*, 229-239.

Darmanis, S., Sloan, S.A., Zhang, Y., Enge, M., Caneda, C., Shuer, L.M., Hayden Gephart, M.G., Barres, B.A., and Quake, S.R. (2015). A survey of human brain transcriptome diversity at the single cell level. Proceedings of the National Academy of Sciences of the United States of America *112*, 7285-7290.

Dawitz, J., Kroon, T., Hjorth, J.J.J., and Meredith, R.M. (2011). Functional calcium imaging in developing cortical networks. Journal of visualized experiments *56*.

De la Rossa, A., Bellone, C., Golding, B., Vitali, I., Moss, J., Toni, N., Lüscher, C., and Jabaudon, D. (2013). In vivo reprogramming of circuit connectivity in postmitotic neocortical neurons. Nature neuroscience *16*, 193-200.

Denisenko-Nehrbass, N.I., Jarvis, E., Scharff, C., Nottebohm, F., and Mello, C.V. (2000). Site-specific retinoic acid production in the brain of adult songbirds. Neuron *27*, 359-370.

Dobin, A., Davis, C.A., Schlesinger, F., Drenkow, J., Zaleski, C., Jha, S., Batut, P., Chaisson, M., and Gingeras, T.R. (2013). STAR: ultrafast universal RNA-seq aligner. Bioinformatics (Oxford, England) *29*, 15-21.

Dray, N., Bedu, S., Vuillemin, N., Alunni, A., Coolen, M., Krecsmarik, M., Supatto, W., Beaurepaire, E., and Bally-Cuif, L. (2015). Large-scale live imaging of adult neural stem cells in their endogenous niche. Development (Cambridge, England) *142*, 3592-3600.

Dugas-Ford, J., Rowell, J.J., and Ragsdale, C.W. (2012). Cell-type homologies and the origins of the neocortex. Proceedings of the National Academy of Sciences of the United States of America *109*, 16974-16979.

Dumitriu, A., Latourelle, J.C., Hadzi, T.C., Pankratz, N., Garza, D., Miller, J.P., Vance, J.M., Foroud, T., Beach, T.G., and Myers, R.H. (2012). Gene expression profiles in Parkinson disease prefrontal cortex implicate FOXO1 and genes under its transcriptional regulation. PLoS genetics *8*.

Eiraku, M., Watanabe, K., Matsuo-Takasaki, M., Kawada, M., Yonemura, S., Matsumura, M., Wataya, T., Nishiyama, A., Muguruma, K., and Sasai, Y. (2008). Self-organized formation of polarized cortical tissues from ESCs and its active manipulation by extrinsic signals. Cell stem cell *3*, 519-532.

Elstner, M., Morris, C.M., Heim, K., Bender, A., Mehta, D., Jaros, E., Klopstock, T., Meitinger, T., Turnbull, D.M., and Prokisch, H. (2011). Expression analysis of dopaminergic neurons in Parkinson's disease and aging links transcriptional dysregulation of energy metabolism to cell death. Acta neuropathologica *122*, 75-86.

Ernst, A., Alkass, K., Bernard, S., Salehpour, M., Perl, S., Tisdale, J., Possnert, G., Druid, H., and Frisén, J. (2014). Neurogenesis in the striatum of the adult human brain. Cell *156*, 1072-1083.

Espuny-Camacho, I., Michelsen, K.A., Gall, D., Linaro, D., Hasche, A., Bonnefont, J., Bali, C., Orduz, D., Bilheu, A., Herpoel, A.*, et al.* (2013). Pyramidal neurons derived from human pluripotent stem cells integrate efficiently into mouse brain circuits in vivo. Neuron *77*, 440-456.

Evers, D.L., Fowler, C.B., Cunningham, B.R., Mason, J.T., and O'Leary, T.J. (2011). The effect of formaldehyde fixation on RNA: optimization of formaldehyde adduct removal. The Journal of molecular diagnostics : JMD *13*, 282-288.

Faiz, M., Sachewsky, N., Gascón, S., Bang, K.W., Morshead, C.M., and Nagy, A. (2015). Adult Neural Stem Cells from the Subventricular Zone Give Rise to Reactive Astrocytes in the Cortex after Stroke. Cell stem cell *17*, 624-634.

Fausett, B.V., and Goldman, D. (2006). A role for alpha1 tubulin-expressing Müller glia in regeneration of the injured zebrafish retina. The Journal of neuroscience : the official journal of the Society for Neuroscience *26*, 6303-6313.

Fei, J.-F.F., Schuez, M., Tazaki, A., Taniguchi, Y., Roensch, K., and Tanaka, E.M. (2014). CRISPR-mediated genomic deletion of Sox2 in the axolotl shows a requirement in spinal cord neural stem cell amplification during tail regeneration. Stem cell reports *3*, 444-459.

Fend, F., Emmert-Buck, M.R., Chuaqui, R., Cole, K., Lee, J., Liotta, L.A., and Raffeld, M. (1999). Immuno-LCM: Laser Capture Microdissection of Immunostained Frozen Sections for mRNA Analysis. The American Journal of Pathology *154*, 61-66.

Filippo, T.R., Galindo, L.T., Barnabe, G.F., Ariza, C.B., Mello, L.E., Juliano, M.A., Juliano, L., and Porcionatto, M.A.A. (2013). CXCL12 N-terminal end is sufficient to induce chemotaxis and proliferation of neural stem/progenitor cells. Stem cell research *11*, 913-925.

Fleisch, V.C., Fraser, B., and Allison, W.T. (2011). Investigating regeneration and functional integration of CNS neurons: lessons from zebrafish genetics and other fish species. Biochimica et biophysica acta *1812*, 364-380.

Flowers, G.P., Timberlake, A.T., McLean, K.C., Monaghan, J.R., and Crews, C.M. (2014). Highly efficient targeted mutagenesis in axolotl using Cas9 RNA-guided nuclease. Development (Cambridge, England) *141*, 2165-2171.

Fluri, F., Schuhmann, M.K., and Kleinschnitz, C. (2015). Animal models of ischemic stroke and their application in clinical research. Drug Des Devel Ther *9*, 3445-3454.

Font, E., Desfilis, E., Pérez-Cañellas, M., Alcántara, S., and García-Verdugo, J.M. (1997). 3-Acetylpyridine-induced degeneration and regeneration in the adult lizard brain: a qualitative and quantitative analysis. Brain research *754*, 245-259.

Font, E., García-Verdugo, J.M., Alcántara, S., and López-García, C. (1991). Neuron regeneration reverses 3-acetylpyridine-induced cell loss in the cerebral cortex of adult lizards. Brain research *551*, 230-235.

Franco, S.J., Gil-Sanz, C., Martinez-Garay, I., Espinosa, A., Harkins-Perry, S.R., Ramos, C., and Müller, U. (2012). Fate-restricted neural progenitors in the mammalian cerebral cortex. Science (New York, NY) *337*, 746-749.

Fu, L., Niu, B., Zhu, Z., Wu, S., and Li, W. (2012). CD-HIT: accelerated for clustering the next-generation sequencing data. Bioinformatics (Oxford, England) *28*, 3150-3152.

Ganz, J., Kaslin, J., Freudenreich, D., Machate, A., Geffarth, M., and Brand, M. (2012). Subdivisions of the adult zebrafish subpallium by molecular marker analysis. The Journal of comparative neurology *520*, 633-655.

Ganz, J., Kroehne, V., Freudenreich, D., Machate, A., Geffarth, M., Braasch, I., Kaslin, J., and Brand, M. (2014). Subdivisions of the adult zebrafish pallium based on molecular marker analysis. F1000Research *3*, 308.

Godwin, J.W., Pinto, A.R., and Rosenthal, N.A. (2013). Macrophages are required for adult salamander limb regeneration. Proceedings of the National Academy of Sciences of the United States of America *110*, 9415-9420.

Goings, G.E., Sahni, V., and Szele, F.G. (2004). Migration patterns of subventricular zone cells in adult mice change after cerebral cortex injury. Brain Res *996*.

Goodus, M.T., Guzman, A.M., Calderon, F., Jiang, Y., and Levison, S.W. (2014). Neural Stem Cells in the Immature, but Not the Mature, Subventricular Zone Respond Robustly to Traumatic Brain Injury. Dev Neurosci-basel *0*.

Gorsic, M., Majdic, G., and Komel, R. (2008). Identification of differentially expressed genes in 4-day axolotl limb blastema by suppression subtractive hybridization. Journal of physiology and biochemistry *64*, 37-50.

Greer, P.L., and Greenberg, M.E. (2008). From synapse to nucleus: calcium-dependent gene transcription in the control of synapse development and function. Neuron *59*, 846-860.

Grindberg, R.V., Yee-Greenbaum, J.L., McConnell, M.J., Novotny, M., O'Shaughnessy, A.L., Lambert, G.M., Araúzo-Bravo, M.J., Lee, J., Fishman, M., Robbins, G.E.*, et al.* (2013). RNA-sequencing from single nuclei. Proceedings of the National Academy of Sciences of the United States of America *110*, 19802-19807.

Gu, W., Brännström, T., and Wester, P. (2000). Cortical neurogenesis in adult rats after reversible photothrombotic stroke. Journal of cerebral blood flow and metabolism : official journal of the International Society of Cerebral Blood Flow and Metabolism *20*, 1166-1173.

Habermann, B., Bebin, A.-G.G., Herklotz, S., Volkmer, M., Eckelt, K., Pehlke, K., Epperlein, H.H., Schackert, H.K., Wiebe, G., and Tanaka, E.M. (2004). An Ambystoma mexicanum EST sequencing project: analysis of 17,352 expressed sequence tags from embryonic and regenerating blastema cDNA libraries. Genome biology *5*.

Harel, N.Y., and Strittmatter, S.M. (2006). Can regenerating axons recapitulate developmental guidance during recovery from spinal cord injury? Nature reviews Neuroscience *7*, 603-616.

Hauser, M.A., Li, Y.-J.J., Xu, H., Noureddine, M.A., Shao, Y.S., Gullans, S.R., Scherzer, C.R., Jensen, R.V., McLaurin, A.C., Gibson, J.R.*, et al.* (2005). Expression profiling of substantia nigra in Parkinson disease, progressive supranuclear palsy, and frontotemporal dementia with parkinsonism. Archives of neurology *62*, 917-921.

Hawrylycz, M.J., Lein, E.S., Guillozet-Bongaarts, A.L., Shen, E.H., Ng, L., Miller, J.A., van de Lagemaat, L.N., Smith, K.A., Ebbert, A., Riley, Z.L.*, et al.* (2012). An anatomically comprehensive atlas of the adult human brain transcriptome. Nature *489*, 391-399.

Heinrich, C., Blum, R., Gascón, S., Masserdotti, G., Tripathi, P., Sánchez, R., Tiedt, S., Schroeder, T., Götz, M., and Berninger, B. (2010). Directing astroglia from the cerebral cortex into subtype specific functional neurons. PLoS biology *8*.

Hennig, J., Nauerth, A., and Friedburg, H. (1986). RARE imaging: a fast imaging method for clinical MR. Magnetic Resonance in Medicine *3*, 823-833.

Herrick, C.J. (1948). The Brain of the Tiger Salamander, *Ambystoma tigrinum* (Chicago, Illinois: The University of Chicago Press).

Holman, E.C., Campbell, L.J., Hines, J., and Crews, C.M. (2012). Microarray analysis of microRNA expression during axolotl limb regeneration. PloS one *7*.

Holtmaat, A., and Svoboda, K. (2009). Experience-dependent structural synaptic plasticity in the mammalian brain. Nature reviews Neuroscience *10*, 647-658.

Hori, T., Haraguchi, T., Hiraoka, Y., Kimura, H., and Fukagawa, T. (2003). Dynamic behavior of Nuf2-Hec1 complex that localizes to the centrosome and centromere and is essential for mitotic progression in vertebrate cells. Journal of cell science *116*, 3347-3362.

Hou, S.-W.W., Wang, Y.-Q.Q., Xu, M., Shen, D.-H.H., Wang, J.-J.J., Huang, F., Yu, Z., and Sun, F.-Y.Y. (2008). Functional integration of newly generated neurons into striatum after cerebral ischemia in the adult rat brain. Stroke *39*, 2837-2844.

Hrvatin, S., Deng, F., O'Donnell, C.W., Gifford, D.K., and Melton, D.A. (2014). MARIS: method for analyzing RNA following intracellular sorting. PloS one *9*.

Huang, L., Jolly, L.A., Willis-Owen, S., Gardner, A., Kumar, R., Douglas, E., Shoubridge, C., Wieczorek, D., Tzschach, A., Cohen, M.*, et al.* (2012). A noncoding, regulatory mutation implicates HCFC1 in nonsyndromic intellectual disability. Am J Hum Genet *91*, 694-702.

Huang, W.-H.H., Guenthner, C.J., Xu, J., Nguyen, T., Schwarz, L.A., Wilkinson, A.W., Gozani, O., Chang, H.Y., Shamloo, M., and Luo, L. (2016). Molecular and Neural Functions of Rai1, the Causal Gene for Smith-Magenis Syndrome. Neuron *92*, 392-406.

Huh, G.S., Boulanger, L.M., Du, H., Riquelme, P.A., Brotz, T.M., and Shatz, C.J. (2000). Functional requirement for class I MHC in CNS development and plasticity. Science (New York, NY) *290*, 2155-2159.

Huttner, H.B., Bergmann, O., Salehpour, M., Rácz, A., Tatarishvili, J., Lindgren, E., Csonka, T., Csiba, L., Hortobágyi, T., Méhes, G.*, et al.* (2014). The age and genomic integrity of neurons after cortical stroke in humans. Nature neuroscience *17*, 801-803.

Imai, Y., Suzuki, Y., Matsui, T., Tohyama, M., Wanaka, A., and Takagi, T. (1995). Cloning of a retinoic acid-induced gene, GT1, in the embryonal carcinoma cell line P19: neuron-specific expression in the mouse brain. Brain research Molecular brain research *31*, 1-9.

Jabaudon, D., Shnider, S.J., Tischfield, D.J., Galazo, M.J., and Macklis, J.D. (2012). RORβ induces barrel-like neuronal clusters in the developing neocortex. Cerebral cortex *22*, 996-1006.

Jarvis, E.D., Yu, J., Rivas, M.V., Horita, H., Feenders, G., Whitney, O., Jarvis, S.C., Jarvis, E.R., Kubikova, L., Puck, A.E.*, et al.* (2013). Global view of the functional molecular organization of the avian cerebrum: mirror images and functional columns. The Journal of comparative neurology *521*, 3614-3665.

Jiang, W., Gu, W.G., Brännström, T., Rosqvist, R., and Wester, P. (2001). Cortical neurogenesis in adult rats after transient middle cerebral artery occlusion. Stroke *32*, 1201-1207.

Jiang, Y.-M.M., Yamamoto, M., Kobayashi, Y., Yoshihara, T., Liang, Y., Terao, S., Takeuchi, H., Ishigaki, S., Katsuno, M., Adachi, H.*, et al.* (2005). Gene expression profile of spinal motor neurons in sporadic amyotrophic lateral sclerosis. Annals of neurology *57*, 236-251.

Jin, K., Sun, Y., Xie, L., Peel, A., Mao, X.O., Batteur, S., and Greenberg, D.A. (2003). Directed migration of neuronal precursors into the ischemic cerebral cortex and striatum. Molecular and Cellular Neuroscience *24*, 171-189.

Jin, K., Wang, X., Xie, L., Mao, X.O., Zhu, W., Wang, Y., Shen, J., Mao, Y., Banwait, S., and Greenberg, D.A. (2006). Evidence for stroke-induced neurogenesis in the human brain. Proceedings of the National Academy of Sciences of the United States of America *103*, 13198-13202.

Kang, H.J., Kawasawa, Y.I., Cheng, F., Zhu, Y., Xu, X., Li, M., Sousa, A.M.M.M., Pletikos, M., Meyer, K.A., Sedmak, G.*, et al.* (2011). Spatio-temporal transcriptome of the human brain. Nature *478*, 483-489.

Kang, J., Hu, J., Karra, R., Dickson, A.L., Tornini, V.A., Nachtrab, G., Gemberling, M., Goldman, J.A., Black, B.L., and Poss, K.D. (2016). Modulation of tissue repair by regeneration enhancer elements. Nature *532*, 201-206.

Kazuki, Y., and Oshimura, M. (2011). Human artificial chromosomes for gene delivery and the development of animal models. Molecular therapy : the journal of the American Society of Gene Therapy *19*, 1591-1601.

Kernie, S.G., and Parent, J.M. (2010). Forebrain neurogenesis after focal Ischemic and traumatic brain injury. Neurobiology of disease *37*, 267-274.

Kikuchi, K., Holdway, J.E., Werdich, A.A., Anderson, R.M., Fang, Y., Egnaczyk, G.F., Evans, T., Macrae, C.A., Stainier, D.Y., and Poss, K.D. (2010). Primary contribution to zebrafish heart regeneration by gata4(+) cardiomyocytes. Nature *464*, 601-605.

Kirkham, M., Berg, D.A., and Simon, A. (2011). Microglia activation during neuroregeneration in the adult vertebrate brain. Neuroscience letters *497*, 11-16.

Kirkham, M., Hameed, L.S., Berg, D.A., Wang, H., and Simon, A. (2014). Progenitor cell dynamics in the Newt Telencephalon during homeostasis and neuronal regeneration. Stem cell reports *2*, 507-519.

Kirsche, K., and Kirsche, W. (1964a). Kompensatorische Hyperplasie und Regeneration im Endhirn von Ambystoma mexicanum nach Resektion einer Hemisphäre. Zeitschrift für mikroskopisch-anatomische Forschung *71*, 505-525.

Kirsche, K., and Kirsche, W. (1964b). Regenerative vorgänge im telencephalon von Ambystoma mexicanum. Journal für Hirnforschung *7*, 421-436.

Kirsche, K., Kirsche, W., and Richter, W. (1965). Der Einfluß der experimentell erzeugten Metamorphose auf die regenerativen Vorgange im Vorderhirn von Ambystoma mexicanum. Zeitschrift für mikroskopisch-anatomische Forschung *74*, 69-79.

Kishimoto, N., Shimizu, K., and Sawamoto, K. (2012). Neuronal regeneration in a zebrafish model of adult brain injury. Disease models & mechanisms *5*, 200-209.

Kizil, C., Dudczig, S., Kyritsis, N., Machate, A., Blaesche, J., Kroehne, V., and Brand, M. (2012a). The chemokine receptor cxcr5 regulates the regenerative neurogenesis response in the adult zebrafish brain. Neural development *7*, 27.

Kizil, C., Kaslin, J., Kroehne, V., and Brand, M. (2012b). Adult neurogenesis and brain regeneration in zebrafish. Developmental neurobiology *72*, 429-461.

Kizil, C., Kyritsis, N., Dudczig, S., Kroehne, V., Freudenreich, D., Kaslin, J., and Brand, M. (2012c). Regenerative neurogenesis from neural progenitor cells requires injury-induced expression of Gata3. Developmental cell *23*, 1230-1237.

Klein, A.M., Mazutis, L., Akartuna, I., Tallapragada, N., Veres, A., Li, V., Peshkin, L., Weitz, D.A., and Kirschner, M.W. (2015). Droplet barcoding for single-cell transcriptomics applied to embryonic stem cells. Cell *161*, 1187-1201.

Kmet, M., Guo, C., Edmondson, C., and Chen, B. (2013). Directed differentiation of human embryonic stem cells into corticofugal neurons uncovers heterogeneous Fezf2-expressing subpopulations. PloS one *8*.

Kokoros, J.J., and Northcutt, R.G. (1977). Telencephalic efferents of the tiger salamander Ambystoma tigrinum tigrinum (Green). The Journal of comparative neurology *173*, 613-628.

Kokovay, E., Goderie, S., Wang, Y., Lotz, S., Lin, G., Sun, Y., Roysam, B., Shen, Q., and Temple, S. (2010). Adult SVZ lineage cells home to and leave the vascular niche via differential responses to SDF1/CXCR4 signaling. Cell stem cell *7*, 163-173.

Kragl, M., Knapp, D., Nacu, E., Khattak, S., Maden, M., Epperlein, H.H., and Tanaka, E.M. (2009). Cells keep a memory of their tissue origin during axolotl limb regeneration. Nature *460*, 60-65.

Kreuzberg, M., Kanov, E., Timofeev, O., Schwaninger, M., Monyer, H., and Khodosevich, K. (2010). Increased subventricular zone-derived cortical neurogenesis after ischemic lesion. Experimental neurology *226*, 90-99.

Krishnaswami, S.R., Grindberg, R.V., Novotny, M., Venepally, P., Lacar, B., Bhutani, K., Linker, S.B., Pham, S., Erwin, J.A., Miller, J.A.*, et al.* (2016). Using single nuclei for RNA-seq to capture the transcriptome of postmortem neurons. Nature protocols *11*, 499-524.

Kroehne, V., Freudenreich, D., Hans, S., Kaslin, J., and Brand, M. (2011). Regeneration of the adult zebrafish brain from neurogenic radial glia-type progenitors. Development (Cambridge, England) *138*, 4831-4841.

Kuo, T.-H.H., Kowalko, J.E., DiTommaso, T., Nyambi, M., Montoro, D.T., Essner, J.J., and Whited, J.L. (2015). TALEN-mediated gene editing of the thrombospondin-1 locus in axolotl. Regeneration (Oxford, England) *2*, 37-43.

Kyritsis, N., Kizil, C., Zocher, S., Kroehne, V., Kaslin, J., Freudenreich, D., Iltzsche, A., and Brand, M. (2012). Acute inflammation initiates the regenerative response in the adult zebrafish brain. Science (New York, NY) *338*, 1353-1356.

Lake, B.B., Ai, R., Kaeser, G.E., Salathia, N.S., Yung, Y.C., Liu, R., Wildberg, A., Gao, D., Fung, H.-L.L., Chen, S.*, et al.* (2016). Neuronal subtypes and diversity revealed by single-nucleus RNA sequencing of the human brain. Science (New York, NY) *352*, 1586-1590.

Lederer, C.W., Torrisi, A., Pantelidou, M., Santama, N., and Cavallaro, S. (2007). Pathways and genes differentially expressed in the motor cortex of patients with sporadic amyotrophic lateral sclerosis. BMC genomics *8*, 26.

Lein, E.S., Zhao, X., and Gage, F.H. (2004). Defining a molecular atlas of the hippocampus using DNA microarrays and high-throughput in situ hybridization. The Journal of neuroscience : the official journal of the Society for Neuroscience *24*, 3879-3889.

Leker, R.R., Soldner, F., Velasco, I., Gavin, D.K., Androutsellis-Theotokis, A., and McKay, R.D. (2007). Long-lasting regeneration after ischemia in the cerebral cortex. Stroke *38*, 153-161.

Lienert, F., Lohmueller, J.J., Garg, A., and Silver, P.A. (2014). Synthetic biology in mammalian cells: next generation research tools and therapeutics. Nature reviews Molecular cell biology *15*, 95-107.

Liu, F., You, Y., Li, X., Ma, T., Nie, Y., Wei, B., Li, T., Lin, H., and Yang, Z. (2009). Brain injury does not alter the intrinsic differentiation potential of adult neuroblasts. The Journal of neuroscience : the official journal of the Society for Neuroscience *29*, 5075-5087.

Liu, J., Liu, B., Zhang, X., Yu, B., Guan, W., Wang, K., Yang, Y., Gong, Y., Wu, X., Yanagawa, Y.*, et al.* (2014). Calretinin-positive L5a pyramidal neurons in the development of the paralemniscal pathway in the barrel cortex. Molecular brain *7*.

Liu, S., and Trapnell, C. (2016). Single-cell transcriptome sequencing: recent advances and remaining challenges. F1000Research *5*.

Lo, D.C., Allen, F., and Brockes, J.P. (1993). Reversal of muscle differentiation during urodele limb regeneration. Proceedings of the National Academy of Sciences of the United States of America *90*, 7230-7234.

LoCascio, S.A., Lapan, S.W., and Reddien, P.W. (2017). Eye Absence Does Not Regulate Planarian Stem Cells during Eye Regeneration. Developmental cell *40*, 381-391000.

Lodato, S., and Arlotta, P. (2015). Generating neuronal diversity in the mammalian cerebral cortex. Annual review of cell and developmental biology *31*, 699-720.

Lodato, S., Molyneaux, B.J., Zuccaro, E., Goff, L.A., Chen, H.-H.H., Yuan, W., Meleski, A., Takahashi, E., Mahony, S., Rinn, J.L.*, et al.* (2014). Gene co-regulation by Fezf2 selects neurotransmitter identity and connectivity of corticospinal neurons. Nature neuroscience *17*, 1046-1054.

Love, M.I., Huber, W., and Anders, S. (2014). Moderated estimation of fold change and dispersion for RNA-seq data with DESeq2. Genome biology *15*, 550.

Macklis, J.D. (1993). Transplanted neocortical neurons migrate selectively into regions of neuronal degeneration produced by chromophore-targeted laser photolysis. The Journal of neuroscience *13*, 3848-3863.

Macosko, E.Z., Basu, A., Satija, R., Nemesh, J., Shekhar, K., Goldman, M., Tirosh, I., Bialas, A.R., Kamitaki, N., Martersteck, E.M.*, et al.* (2015). Highly Parallel Genome-wide Expression Profiling of Individual Cells Using Nanoliter Droplets. Cell *161*, 1202-1214.

Maden, M. (2007). Retinoic acid in the development, regeneration and maintenance of the nervous system. Nature reviews Neuroscience *8*, 755-765.

Maden, M., and Hind, M. (2003). Retinoic acid, a regeneration-inducing molecule. Developmental dynamics : an official publication of the American Association of Anatomists *226*, 237-244.

Maden, M., Manwell, L.A., and Ormerod, B.K. (2013). Proliferation zones in the axolotl brain and regeneration of the telencephalon. Neural development *8*, 1.

Magavi, S.S., Leavitt, B.R., and Macklis, J.D. (2000). Induction of neurogenesis in the neocortex of adult mice. Nature *405*, 951-955.

Magnusson, J.P., Göritz, C., Tatarishvili, J., Dias, D.O., Smith, E.M., Lindvall, O., Kokaia, Z., and Frisén, J. (2014). A latent neurogenic program in astrocytes regulated by Notch signaling in the mouse. Science (New York, NY) *346*, 237-241.

Maroof, A.M., Keros, S., Tyson, J.A., Ying, S.-W.W., Ganat, Y.M., Merkle, F.T., Liu, B., Goulburn, A., Stanley, E.G., Elefanty, A.G.*, et al.* (2013). Directed differentiation and functional maturation of cortical interneurons from human embryonic stem cells. Cell stem cell *12*, 559-572.

März, M., Schmidt, R., Rastegar, S., and Strähle, U. (2011). Regenerative response following stab injury in the adult zebrafish telencephalon. Developmental dynamics : an official publication of the American Association of Anatomists *240*, 2221-2231.

Mescher, A.L. (1976). Effects on adult newt limb regeneration of partial and complete skin flaps over the amputation surface. The Journal of experimental zoology *195*, 117-128.

Miller, R.M., Kiser, G.L., Kaysser-Kranich, T.M., Lockner, R.J., Palaniappan, C., and Federoff, H.J. (2006). Robust dysregulation of gene expression in substantia nigra and striatum in Parkinson's disease. Neurobiology of disease *21*, 305-313.

Ming, G.-L.L., and Song, H. (2011). Adult neurogenesis in the mammalian brain: significant answers and significant questions. Neuron *70*, 687-702.

Mitchell, J.D., and Borasio, G.D. (2007). Amyotrophic lateral sclerosis. Lancet (London, England) *369*, 2031-2041.

Molnár, Z. (2011). Evolution of cerebral cortical development. Brain, behavior and evolution *78*, 94-107.

Molowny, A., Nacher, J., and Lopez-Garcia, C. (1995). Reactive neurogenesis during regeneration of the lesioned medial cerebral cortex of lizards. Neuroscience *68*, 823-836.

Molyneaux, B.J., Arlotta, P., Hirata, T., Hibi, M., and Macklis, J.D. (2005). Fezl is required for the birth and specification of corticospinal motor neurons. Neuron *47*, 817-831.

Molyneaux, B.J., Arlotta, P., Menezes, J.R., and Macklis, J.D. (2007). Neuronal subtype specification in the cerebral cortex. Nature reviews Neuroscience *8*, 427-437.

Molyneaux, B.J., Goff, L.A., Brettler, A.C., Chen, H.-H.H., Brown, J.R., Hrvatin, S., Rinn, J.L., and Arlotta, P. (2015). DeCoN: genome-wide analysis of in vivo transcriptional dynamics during pyramidal neuron fate selection in neocortex. Neuron *85*, 275-288.

Monaghan, J.R., Athippozhy, A., Seifert, A.W., Putta, S., Stromberg, A.J., Maden, M., Gardiner, D.M., and Voss, S.R. (2012). Gene expression patterns specific to the regenerating limb of the Mexican axolotl. Biology open *1*, 937-948.

Montana, C.L., Kolesnikov, A.V., Shen, S.Q., Myers, C.A., Kefalov, V.J., and Corbo, J.C. (2013). Reprogramming of adult rod photoreceptors prevents retinal degeneration. Proceedings of the National Academy of Sciences of the United States of America *110*, 1732-1737.

Moran, L.B., Duke, D.C., Deprez, M., Dexter, D.T., Pearce, R.K., and Graeber, M.B. (2006). Whole genome expression profiling of the medial and lateral substantia nigra in Parkinson's disease. Neurogenetics *7*, 1-11.

Moreno, N., Bachy, I., Rétaux, S., and González, A. (2004). LIM-homeodomain genes as developmental and adult genetic markers of Xenopus forebrain functional subdivisions. The Journal of comparative neurology *472*, 52-72.

Moreno, N., and González, A. (2007). Regionalization of the telencephalon in urodele amphibians and its bearing on the identification of the amygdaloid complex. Frontiers in neuroanatomy *1*, 1.

Nam, H.-s.S., and Benezra, R. (2009). High levels of Id1 expression define B1 type adult neural stem cells. Cell stem cell *5*, 515-526.

Neary, T.J. (1990). The Pallium of Anuran Amphibians. In Comparative Structure and Evolution of Cerebral Cortex, Part I, A.P. Edward G. Jones, ed. (New York, NY: Springer US), pp. 107-138.

Nikouei, K., Muñoz-Manchado, A.B., and Hjerling-Leffler, J. (2016). BCL11B/CTIP2 is highly expressed in GABAergic interneurons of the mouse somatosensory cortex. Journal of chemical neuroanatomy *71*, 1-5.

Niu, W., Zang, T., Zou, Y., Fang, S., Smith, D.K., Bachoo, R., and Zhang, C.-L.L. (2013). In vivo reprogramming of astrocytes to neuroblasts in the adult brain. Nature cell biology *15*, 1164-1175.

Northcutt, R.G. (2008). Forebrain evolution in bony fishes. Brain research bulletin *75*, 191-205.

Northcutt, R.G., and Kicliter, E. (1980). Organization of the amphibian telencephalon. In Comparative neurology of the telencephalon, S.O.E. Ebbesson, ed. (New York, NY: Plenum), pp. 203-255.

Offen, D., Barhum, Y., Melamed, E., Embacher, N., Schindler, C., and Ransmayr, G. (2009). Spinal cord mRNA profile in patients with ALS: comparison with transgenic mice expressing the human SOD-1 mutant. Journal of molecular neuroscience : MN *38*, 85-93.

Ohira, K., Furuta, T., Hioki, H., Nakamura, K.C., Kuramoto, E., Tanaka, Y., Funatsu, N., Shimizu, K., Oishi, T., Hayashi, M.*, et al.* (2010). Ischemia-induced neurogenesis of neocortical layer 1 progenitor cells. Nature neuroscience *13*, 173-179.

Okamoto, M., Ohsawa, H., Hayashi, T., Owaribe, K., and Tsonis, P.A. (2007). Regeneration of retinotectal projections after optic tectum removal in adult newts. Molecular vision *13*, 2112-2118.

Ovbiagele, B., and Nguyen-Huynh, M.N. (2011). Stroke epidemiology: advancing our understanding of disease mechanism and therapy. Neurotherapeutics : the journal of the American Society for Experimental NeuroTherapeutics *8*, 319-329.

Page, R.B., and Voss, S.R. (2009). Induction of metamorphosis in axolotls (Ambystoma mexicanum). Cold Spring Harbor protocols *4*.

Pagliuca, F.W., Millman, J.R., Gürtler, M., Segel, M., Van Dervort, A., Ryu, J.H., Peterson, Q.P., Greiner, D., and Melton, D.A. (2014). Generation of functional human pancreatic β cells in vitro. Cell *159*, 428-439.

Pan, Y., Ouyang, Z., Wong, W.H., and Baker, J.C. (2011). A new FACS approach isolates hESC derived endoderm using transcription factors. PloS one *6*.

Papapetropoulos, S., Ffrench-Mullen, J., McCorquodale, D., Qin, Y., Pablo, J., and Mash, D.C. (2006). Multiregional gene expression profiling identifies MRPS6 as a possible candidate gene for Parkinson's disease. Gene expression *13*, 205-215.

Parish, C.L., Beljajeva, A., Arenas, E., and Simon, A. (2007). Midbrain dopaminergic neurogenesis and behavioural recovery in a salamander lesion-induced regeneration model. Development (Cambridge, England) *134*, 2881-2887.

Patel, T.P., Man, K., Firestein, B.L., and Meaney, D.F. (2015). Automated quantification of neuronal networks and single-cell calcium dynamics using calcium imaging. Journal of neuroscience methods *243*, 26-38.

Peça, J., Feliciano, C., Ting, J.T., Wang, W., Wells, M.F., Venkatraman, T.N., Lascola, C.D., Fu, Z., and Feng, G. (2011). Shank3 mutant mice display autistic-like behaviours and striatal dysfunction. Nature *472*, 437-442.

Pechhold, S., Stouffer, M., Walker, G., Martel, R., Seligmann, B., Hang, Y., Stein, R., Harlan, D.M., and Pechhold, K. (2009). Transcriptional analysis of intracytoplasmically stained, FACS-purified cells by high-throughput, quantitative nuclease protection. Nature biotechnology *27*, 1038-1042.

Perrin, F.E., Boisset, G., Docquier, M., Schaad, O., Descombes, P., and Kato, A.C. (2005). No widespread induction of cell death genes occurs in pure motoneurons in an amyotrophic lateral sclerosis mouse model. Human molecular genetics *14*, 3309-3320.

Piatt, J. (1955a). Regeneration of the spinal cord in the salamander. Journal of Experimental Zoology.

Piatt, J. (1955b). Regeneration of the spinal cord in the salamander. Journal of Experimental Zoology *129*, 177-207.

Pierfelice, T., Alberi, L., and Gaiano, N. (2011). Notch in the vertebrate nervous system: an old dog with new tricks. Neuron *69*, 840-855.

Poss, K.D., Wilson, L.G., and Keating, M.T. (2002). Heart regeneration in zebrafish. Science (New York, NY) *298*, 2188-2190.

Puelles, L., Kuwana, E., Puelles, E., Bulfone, A., Shimamura, K., Keleher, J., Smiga, S., and Rubenstein, J.L. (2000). Pallial and subpallial derivatives in the embryonic chick and mouse telencephalon, traced by the expression of the genes Dlx-2, Emx-1, Nkx-2.1, Pax-6, and Tbr-1. The Journal of comparative neurology *424*, 409-438.

Ramachandran, R., Reifler, A., Parent, J.M., and Goldman, D. (2010). Conditional gene expression and lineage tracing of tuba1a expressing cells during zebrafish development and retina regeneration. The Journal of comparative neurology *518*, 4196-4212.

Ramaswamy, S., Goings, G.E., Soderstrom, K.E., Szele, F.G., and Kozlowski, D.A. (2005). Cellular proliferation and migration following a controlled cortical impact in the mouse. Brain Res *1053*.

Rao, N., Jhamb, D., Milner, D.J., Li, B., Song, F., Wang, M., Voss, S.R., Palakal, M., King, M.W., Saranjami, B.*, et al.* (2009). Proteomic analysis of blastema formation in regenerating axolotl limbs. BMC biology *7*, 83.

Rezania, A., Bruin, J.E., Arora, P., Rubin, A., Batushansky, I., Asadi, A., O'Dwyer, S., Quiskamp, N., Mojibian, M., Albrecht, T.*, et al.* (2014). Reversal of diabetes with insulin-producing cells derived in vitro from human pluripotent stem cells. Nature biotechnology *32*, 1121-1133.

Robin, A.M., Zhang, Z.G., Wang, L., Zhang, R.L., Katakowski, M., Zhang, L., Wang, Y., Zhang, C., and Chopp, M. (2006). Stromal cell-derived factor 1alpha mediates neural progenitor cell motility after focal cerebral ischemia. Journal of cerebral blood flow and metabolism : official journal of the International Society of Cerebral Blood Flow and Metabolism *26*, 125-134.

Rodriguez Viales, R., Diotel, N., Ferg, M., Armant, O., Eich, J., Alunni, A., März, M., Bally-Cuif, L., Rastegar, S., and Strähle, U. (2015). The helix-loop-helix protein id1 controls stem cell proliferation during regenerative neurogenesis in the adult zebrafish telencephalon. Stem cells (Dayton, Ohio) *33*, 892-903.

Rosset, A., Spadola, L., and Ratib, O. (2004). OsiriX: an open-source software for navigating in multidimensional DICOM images. Journal of digital imaging *17*, 205-216.

Rouaux, C., and Arlotta, P. (2013). Direct lineage reprogramming of post-mitotic callosal neurons into corticofugal neurons in vivo. Nature cell biology *15*, 214-221.

Rubiano, A.M.M., Carney, N., Chesnut, R., and Puyana, J.C. (2015). Global neurotrauma research challenges and opportunities. Nature *527*.

Saha, B., Jaber, M., and Gaillard, A. (2012). Potentials of endogenous neural stem cells in cortical repair. Front Cell Neurosci *6*.

Saha, B., Peron, S., Murray, K., Jaber, M., and Gaillard, A. (2013). Cortical lesion stimulates adult subventricular zone neural progenitor cell proliferation and migration to the site of injury. Stem Cell Res *11*.

Schafer, D.P., Lehrman, E.K., Kautzman, A.G., Koyama, R., Mardinly, A.R., Yamasaki, R., Ransohoff, R.M., Greenberg, M.E., Barres, B.A., and Stevens, B. (2012). Microglia sculpt postnatal neural circuits in an activity and complement-dependent manner. Neuron *74*, 691-705.

Schnapp, E., Tanaka, E.M., and Tamaka, E.M. (2005). Quantitative evaluation of morpholino-mediated protein knockdown of GFP, MSX1, and PAX7 during tail regeneration in Ambystoma mexicanum. Developmental dynamics : an official publication of the American Association of Anatomists *232*, 162-170.

Shekhar, K., Lapan, S.W., Whitney, I.E., Tran, N.M., Macosko, E.Z., Kowalczyk, M., Adiconis, X., Levin, J.Z., Nemesh, J., Goldman, M.*, et al.* (2016). Comprehensive Classification of Retinal Bipolar Neurons by Single-Cell Transcriptomics. Cell *166*, 1308.

Shen, Q., Wang, Y., Dimos, J.T., Fasano, C.A., Phoenix, T.N., Lemischka, I.R., Ivanova, N.B., Stifani, S., Morrisey, E.E., and Temple, S. (2006). The timing of cortical neurogenesis is encoded within lineages of individual progenitor cells. Nature neuroscience *9*, 743-751.

Shi, Y., Kirwan, P., Smith, J., Robinson, H.P., and Livesey, F.J. (2012). Human cerebral cortex development from pluripotent stem cells to functional excitatory synapses. Nature neuroscience *15*, 477.

Simunovic, F., Yi, M., Wang, Y., Macey, L., Brown, L.T., Krichevsky, A.M., Andersen, S.L., Stephens, R.M., Benes, F.M., and Sonntag, K.C. (2009). Gene expression profiling of substantia nigra dopamine neurons: further insights into Parkinson's disease pathology. Brain : a journal of neurology *132*, 1795-1809.

Skaggs, K., Goldman, D., and Parent, J.M. (2014). Excitotoxic brain injury in adult zebrafish stimulates neurogenesis and long-distance neuronal integration. Glia *62*, 2061-2079.

Sockanathan, S., Perlmann, T., and Jessell, T.M. (2003). Retinoid receptor signaling in postmitotic motor neurons regulates rostrocaudal positional identity and axonal projection pattern. Neuron *40*, 97-111.

Son, E.Y., Ichida, J.K., Wainger, B.J., Toma, J.S., Rafuse, V.F., Woolf, C.J., and Eggan, K. (2011). Conversion of mouse and human fibroblasts into functional spinal motor neurons. Cell stem cell *9*, 205-218.

Soneson, C., Love, M.I., and Robinson, M.D. (2015). Differential analyses for RNA-seq: transcript-level estimates improve gene-level inferences. F1000Research *4*, 1521.

Song, J., Christian, K.M., Ming, G.-l.L., and Song, H. (2012). Modification of hippocampal circuitry by adult neurogenesis. Developmental neurobiology *72*, 1032-1043.

Stevens, B., Allen, N.J., Vazquez, L.E., Howell, G.R., Christopherson, K.S., Nouri, N., Micheva, K.D., Mehalow, A.K., Huberman, A.D., Stafford, B.*, et al.* (2007). The classical complement cascade mediates CNS synapse elimination. Cell *131*, 1164-1178.

Stewart, R., Rascón, C.A., Tian, S., Nie, J., Barry, C., Chu, L.-F.F., Ardalani, H., Wagner, R.J., Probasco, M.D., Bolin, J.M.*, et al.* (2013). Comparative RNA-seq analysis in the unsequenced axolotl: the oncogene burst highlights early gene expression in the blastema. PLoS computational biology *9*.

Stumm, R., and Höllt, V. (2007). CXC chemokine receptor 4 regulates neuronal migration and axonal pathfinding in the developing nervous system: implications for neuronal regeneration in the adult brain. Journal of molecular endocrinology *38*, 377-382.

Stumm, R.K., Zhou, C., Ara, T., Lazarini, F., Dubois-Dalcq, M., Nagasawa, T., Höllt, V., and Schulz, S. (2003). CXCR4 regulates interneuron migration in the developing neocortex. The Journal of neuroscience : the official journal of the Society for Neuroscience *23*, 5123-5130.

Sugiura, T., Wang, H., Barsacchi, R., Simon, A., and Tanaka, E.M. (2016). MARCKS-like protein is an initiating molecule in axolotl appendage regeneration. Nature *531*, 237-240.

Suzuki, I.K., Kawasaki, T., Gojobori, T., and Hirata, T. (2012). The temporal sequence of the mammalian neocortical neurogenetic program drives mediolateral pattern in the chick pallium. Developmental cell *22*, 863-870.

Syken, J., Grandpre, T., Kanold, P.O., and Shatz, C.J. (2006). PirB restricts ocular-dominance plasticity in visual cortex. Science (New York, NY) *313*, 1795-1800.

Tagliafierro, L., Bonawitz, K., Glenn, O.C., and Chiba-Falek, O. (2016). Gene Expression Analysis of Neurons and Astrocytes Isolated by Laser Capture Microdissection from Frozen Human Brain Tissues. Frontiers in molecular neuroscience *9*, 72.

Takahashi, K., Tanabe, K., Ohnuki, M., Narita, M., Ichisaka, T., Tomoda, K., and Yamanaka, S. (2007). Induction of pluripotent stem cells from adult human fibroblasts by defined factors. Cell *131*, 861-872.

Tanaka, E.M., and Ferretti, P. (2009). Considering the evolution of regeneration in the central nervous system. Nature reviews Neuroscience *10*, 713-723.

Tasic, B., Menon, V., Nguyen, T.N., Kim, T.K., Jarsky, T., Yao, Z., Levi, B., Gray, L.T., Sorensen, S.A., Dolbeare, T.*, et al.* (2016). Adult mouse cortical cell taxonomy revealed by single cell transcriptomics. Nature neuroscience *19*, 335-346.

Thomson, J.A., Itskovitz-Eldor, J., Shapiro, S.S., Waknitz, M.A., Swiergiel, J.J., Marshall, V.S., and Jones, J.M. (1998). Embryonic stem cell lines derived from human blastocysts. Science (New York, NY) *282*, 1145-1147.

Thornton, C.S. (1957). The effect of apical cap removal on limb regeneration in Amblystoma larvae. The Journal of experimental zoology *134*, 357-381.

Thummel, R., Kassen, S.C., Montgomery, J.E., Enright, J.M., and Hyde, D.R. (2008). Inhibition of Müller glial cell division blocks regeneration of the light-damaged zebrafish retina. Developmental neurobiology *68*, 392-408.

Torper, O., Pfisterer, U., Wolf, D.A., Pereira, M., Lau, S., Jakobsson, J., Björklund, A., Grealish, S., and Parmar, M. (2013). Generation of induced neurons via direct conversion in vivo. Proceedings of the National Academy of Sciences of the United States of America *110*, 7038-7043.

van der Stegen, S.J., Hamieh, M., and Sadelain, M. (2015). The pharmacology of second-generation chimeric antigen receptors. Nature reviews Drug discovery *14*, 499-509.

Vierbuchen, T., Ostermeier, A., Pang, Z.P., Kokubu, Y., Südhof, T.C., and Wernig, M. (2010). Direct conversion of fibroblasts to functional neurons by defined factors. Nature *463*, 1035-1041.

Wang, X.-S.S., Simmons, Z., Liu, W., Boyer, P.J., and Connor, J.R. (2006). Differential expression of genes in amyotrophic lateral sclerosis revealed by profiling the post mortem cortex. Amyotrophic lateral sclerosis : official publication of the World Federation of Neurology Research Group on Motor Neuron Diseases *7*, 201-210.

Wang, Y.-C.C., Lin, S., and Yang, Q.-W.W. (2011). Toll-like receptors in cerebral ischemic inflammatory injury. J Neuroinflammation *8*.

Westhoff, G., and Roth, G. (2002). Morphology and projection pattern of medial and dorsal pallial neurons in the frog Discoglossus pictus and the salamander Plethodon jordani. The Journal of comparative neurology *445*, 97-121.

Whited, J.L., Lehoczky, J.A., and Tabin, C.J. (2012). Inducible genetic system for the axolotl. Proceedings of the National Academy of Sciences of the United States of America *109*, 13662-13667.

Whited, J.L., Tsai, S.L., Beier, K.T., White, J.N., Piekarski, N., Hanken, J., Cepko, C.L., and Tabin, C.J. (2013). Pseudotyped retroviruses for infecting axolotl in vivo and in vitro. Development (Cambridge, England) *140*, 1137-1146.

Winkelmann, E., and Winkelmann, A. (1970). Experimentelle Untersuchungen zur Regeneration des Telencephalon von Ambystoma mexicanum nach Resektion beider Hemisphären. Zeitschrift für mikroskopisch-anatomische Forschung *82*, 149-171.

Wong, L.-F.F., Yip, P.K., Battaglia, A., Grist, J., Corcoran, J., Maden, M., Azzouz, M., Kingsman, S.M., Kingsman, A.J., Mazarakis, N.D.*, et al.* (2006). Retinoic acid receptor beta2 promotes functional regeneration of sensory axons in the spinal cord. Nature neuroscience *9*, 243-250.

Wu, C.-H.H., Tsai, M.-H.H., Ho, C.-C.C., Chen, C.-Y.Y., and Lee, H.-S.S. (2013). De novo transcriptome sequencing of axolotl blastema for identification of differentially expressed genes during limb regeneration. BMC genomics *14*, 434.

Xiong, Y., Mahmood, A., and Chopp, M. (2013). Animal models of traumatic brain injury. Nat Rev Neurosci *14*, 128-142.

Yamada, H., Maruo, R., Watanabe, M., Hidaka, Y., Iwatani, Y., and Takano, T. (2010). Messenger RNA quantification after fluorescence activated cell sorting using intracellular antigens. Biochemical and Biophysical Research Communications *397*, 425-428.

Yamashita, T., Ninomiya, M., Hernández Acosta, P., García-Verdugo, J.M., Sunabori, T., Sakaguchi, M., Adachi, K., Kojima, T., Hirota, Y., Kawase, T.*, et al.* (2006). Subventricular zone-derived neuroblasts migrate and differentiate into mature neurons in the post-stroke adult striatum. The Journal of neuroscience : the official journal of the Society for Neuroscience *26*, 6627-6636.

Ye, Z., Mostajo-Radji, M.A., Brown, J.R., Rouaux, C., Tomassy, G.S., Hensch, T.K., and Arlotta, P. (2015). Instructing Perisomatic Inhibition by Direct Lineage Reprogramming of Neocortical Projection Neurons. Neuron *88*, 475-483.

Yoneshima, H., Yamasaki, S., Voelker, C.C., Molnár, Z., Christophe, E., Audinat, E., Takemoto, M., Nishiwaki, M., Tsuji, S., Fujita, I.*, et al.* (2006). Er81 is expressed in a subpopulation of layer 5 neurons in rodent and primate neocortices. Neuroscience *137*, 401-412.

Zeisel, A., Muñoz-Manchado, A.B., Codeluppi, S., Lönnerberg, P., La Manno, G., Juréus, A., Marques, S., Munguba, H., He, L., Betsholtz, C.*, et al.* (2015). Brain structure. Cell types in the mouse cortex and hippocampus revealed by single-cell RNA-seq. Science (New York, NY) *347*, 1138-1142.

Zhang, J., Ji, F., Liu, Y., Lei, X., Li, H., Ji, G., Yuan, Z., and Jiao, J. (2014). Ezh2 regulates adult hippocampal neurogenesis and memory. The Journal of neuroscience : the official journal of the Society for Neuroscience *34*, 5184-5199.

Zhao, D., McCaffery, P., Ivins, K.J., Neve, R.L., Hogan, P., Chin, W.W., and Dräger, U.C. (1996). Molecular identification of a major retinoic-acid-synthesizing enzyme, a retinaldehyde-specific dehydrogenase. European journal of biochemistry *240*, 15-22.

Zhelyaznik, N., Schrage, K., McCaffery, P., and Mey, J. (2003). Activation of retinoic acid signalling after sciatic nerve injury: up-regulation of cellular retinoid binding proteins. The European journal of neuroscience *18*, 1033-1040.